TelA: An agrobacterial telomere resolvase

A Thesis Submitted to the College of Graduate and Postdoctoral Studies
In Partial Fulfillment of the Requirements
For the Degree of Master of Science
In the Department of Microbiology and Immunology
University of Saskatchewan
Saskatoon

By

Siobhan L. McGrath

PERMISSION TO USE

In presenting this thesis in partial fulfillment of the requirements for a Postgraduate degree from the University of Saskatchewan, I agree that the Libraries of this University may make it freely available for inspection. I further agree that permission for copying of this thesis in any manner, in whole or in part, for scholarly purposes may be granted by the professor or professors who supervised my thesis/dissertation work or, in their absence, by the Head of the Department or the Dean of the College in which my thesis work was done. It is understood that any copying or publication or use of this thesis/dissertation or parts thereof for financial gain shall not be allowed without my written permission. It is also understood that due recognition shall be given to me and to the University of Saskatchewan in any scholarly use which may be made of any material in my thesis/dissertation.

Requests for permission to copy or to make other uses of materials in this thesis in whole or part should be addressed to:

Head of the Department of Biochemistry, Microbiology and Immunology
GA20.12, Health Sciences
107 Wiggins Road
University of Saskatchewan
Saskatoon, Saskatchewan S7N 5E5
Canada

OR

Dean
College of Graduate and Postdoctoral Studies
University of Saskatchewan
116 Thorvaldson Building, 110 Science Place
Saskatoon, Saskatchewan S7N 5C9
Canada

ABSTRACT

In contrast to the majority of prokaryotes, both the *Agrobacterium* and *Borrelia* genera have linear replicons, including both chromosomes and plasmids, which are terminated by covalently closed hairpin loops commonly referred to as hairpin telomeres. These hairpin telomeres are resolved from a dimeric replication intermediate through a process called telomere resolution. A small, diverse class of enzyme, referred to as telomere resolvases are responsible for this activity. To date, three telomere resolvases have been well-characterized including TelK from *Klebsiella* phage KO2, TelA from the *Agrobacterium* genus, and ResT from *Borrelia* species. Of these ResT is the best biochemically characterized telomere resolvase.

Previous studies have revealed that aside from the expected property of telomere resolution, ResT can anneal ssDNA and also possesses an ATP-dependent, 3'-5' unwinding activity. These results suggest ResT is a multifunctional enzyme. However, at present the *in vivo* function of these annealing and unwinding activities is unknown. In the work of Bandy *et al.* conditional expression of ResT *in vivo* showed ResT depleted cells unexpectedly ceased DNA replication and did not filament as expected, suggesting ResT could be directly or indirectly involved in DNA replication. We sought to analyze a second member of this diverse enzyme family to determine whether these unexpected activities were unique to ResT or represented a property of the enzyme family; and if these activities were identified, to create separation-of-function mutants to eventually assess their function and importance in an *in vivo* context. We selected the telomere resolvase, TelA from *Agrobacterium tumefaciens* as it is the closest to ResT in both size and sequence homology and has available partial structural data.

We have demonstrated that TelA also has the ability to promote the annealing of complementary ssDNA, and removal of the N-terminal domain of TelA produces a mutant deficient for annealing activity while still maintaining its telomere resolution capabilities. Our data suggests TelA binds ATP; however, it does not possess the ssDNA-dependent ATPase and ATP-dependent unwinding activities observed in ResT, suggesting these activities are not conserved among the telomere resolvase enzyme family. Under certain conditions, ATP can interfere with TelA's ability to perform telomere resolution and appears to reduce TelA's affinity for its replicated telomere substrate. Mutation of the active-site nucleophile of TelA (TelA Y405F), while expectedly eliminating telomere resolution, still maintains its annealing activity. Collectively, we have identified the N-terminal domain to be required for TelA's annealing

activity while the catalytic domain alone is sufficient to perform telomere resolution, representing domain separation-of-function in TelA.

ACKNOWLEDGMENTS

A special thank you to my supervisor, Dr. Kerri Kobryn, for his constant support throughout this project. It is with your levelheaded approach to science, dedication, and encouragement that I have become a more analytical and confident scientist. Your commitment to "good science" and always letting the data speak for itself are notions I intend to epitomize as I carry forward in my scientific career. I would also like to thank all past and present members of the Kobryn lab for their support and comradery. Specifically, I would like to thank Linda for her essential technical advice and for all she does to keep the lab running. Finally, I would like to thank my exceptionally lovely friends and family for their endless support and encouragement throughout this experience. My parents, Zak, Yasmina, Katie, and many others – when I was feeling overwhelmed and frustrated, excited about a result or really needed a fellow scientist (Zak and Yasmina) to empathize with, you were always there for me.

PERMISSION TO REPRODUCE

All previously published figures within this document have been reproduced with permission from the journals in which they were published.

Figure 1.1: Casjens, S. (1999). Evolution of the linear DNA replicons of the Borrelia spirochetes. Curr. Opin. Microbiol. 2: 529-534.

Figure 1.2: Chaconas, G. (2005). Hairpin telomeres and genome plasticity in Borrelia: All mixed up in the end. Mol. Microbiol. *58*, 625–635.

Figure 1.3: Kobryn, K., and Chaconas, G. (2002). ResT, a telomere resolvase encoded by the Lyme disease spirochete. Mol. Cell *9*, 195–201.

Figure 1.4: adapted from Kobryn, K., and Chaconas, G. (2014). Hairpin Telomere Resolvases. Microbiol. Spectr. *2*.

Figure 1.5: Chaconas, G. (2005). Hairpin telomeres and genome plasticity in Borrelia: All mixed up in the end. Mol. Microbiol. *58*, 625–635

Figure 1.6: Kobryn, K., and Chaconas, G. (2005). Fusion of hairpin telomeres by the B. burgdorferi telomere resolvase ResT: Implications for shaping a genome in flux. Mol. Cell *17*, 783–791

Figure 1.7: Lucyshyn, D., Huang, S.H., and Kobryn, K. (2015). Spring loading a pre-cleavage intermediate for hairpin telomere formation. Nucleic Acids Res. *43*, 6062–6074.

Figure 4.24: Huang, S.H., Cozart, M.R., Hart, M.A., and Kobryn, K. (2017). The Borrelia burgdorferitelomere resolvase, ResT, possesses ATP-dependent DNA unwinding activity. Nucleic Acids Res. *45*, 1319–1329.

TABLE OF CONTENTS **PAGE**

LIST OF TABLES **PAGE**

LIST OF FIGURES **PAGE**

LIST OF ABBREVIATIONS

BSA	Bovine serum albumin
CDD	Conserved Domain Database
DNA	deoxyribonucleic acid
DART	Domain Architecture Retrieval Tool
DSB	double-stranded break
DTT	1,4-dithiothreitol
EDC	N-(3-dimethylaminopropyl)-N'-ethylcarbodiimide hydrochloride
EDTA	Ethylenediaminetetraacetic acid
EMSA	Electrophoretic mobility shift assay
HAP	hydroxyapatite
HEPES	4-(2-hydroxyethyl)-1-piperazineethanesulfonic acid
HR	homologous recombination
HS	heparin sepharose
IDT	Integrated DNA Technologies
IPTG	Isopropyl β-D-1 thiogalatopyranoside
NHS	N-hydroxysuccinimide
OH	hydroxyl
PAGE	polyacrylamide gel electrophoresis
PNK	T4 polynucleotide kinase
RMP	recombination mediator protein
rTel	Replicated telomere
SH	Sulfhydryl
SPR	Surface Plasmon Resonance
spp.	Species
ssDNA	single-stranded DNA
SSB	single-stranded binding protein
SDS	sodium dodecyl sulfate
TAE	Tris Acetate EDTA
Tap	Terminally associated primase
TBE	Tris Borate EDTA
Ti	Tumour inducing
TP	Terminal protein

1. Introduction

1.1. Bacterial linear replicons

1.1.1. The end-replication and end-protection problems

While linear genomic elements are relatively common among eukaryotic organisms, they are decidedly less abundant amongst prokaryotes. A few select prokaryotic organisms including *Streptomyces* species (*spp*.), those from *Borrelia*, *Agrobacterium* biovar I strains, and several phages exhibit this configuration of deoxyribonucleic acid (DNA) through possession of either linear plasmids, linear chromosomes, or some combination of both. However, in maintaining a linear configuration of DNA these organisms must overcome the issue of losing genomic information over multiple rounds of DNA replication through continued shortening of the replicon – termed the end-replication problem. This hypothesis was originally described from studies of linear phage replication and proposed that during replication, lagging strand synthesis occurs in fragments and removal of the final primer leaves a 3' gap at the end of the replicon with no available 3' hydroxyl (-OH) group and thus, the termini cannot be replicated (Olovnikov, 1973). It was not until 2001, almost 30 years later, that the end-replication problem was demonstrated *in vitro* (Ohki et al., 2001). Furthermore, we must consider that even if the linear DNA is properly replicated the resulting blunt, double stranded ends are susceptible to inappropriate fusion or RecBCD degradation. This vulnerability to damage is referred to as the end-protection problem. The vast majority of eukaryotic organisms do not possess blunt-ends and instead have telomeres with 3' overhangs. With this configuration, the leading strand becomes the source of the end-replication problem (LeBel and Wellinger, 2005). Leading strand synthesis results in a blunt-ended intermediate and the 5' end of the parental strand is then resected and filled in to create a 3' overhang (Soudet et al., 2014). Eukaryotes employ telomerase to extend the ends of linear DNA molecules (Figure 1.1a, (Casjens, 1999; Lingner et al., 1995)) as well as the protein complex, shelterin, to remodel their structure for protection (De Lange, 2005). As prokaryotes do not have such enzymes, they require alternative mechanisms to circumvent the end-replication and end-protection problems.

1.1.2. Alternative solutions to the end-replication problem.

Among prokaryotes, there are examples of several varying strategies for bypassing the end-replication and end-protection problems. Both *Bacillus subtilis* phage φ29 and various

Streptomyces spp. implement the use of 5' terminally protein capped telomeres, although using differing mechanisms. This strategy consists of a terminal protein (TP) covalently attached to the 5' end of the DNA that functions as a sort of cap to both protect the ends of the linear replicon and act as a primer for DNA replication (Figure 1.1b, (Casjens, 1999)). In most cases the end termini also possess intricate secondary structure (Huang et al., 1998). The φ29 phage linear plasmid contains two origins of replication, one at each of the terminal ends of the linear replicon that are first identified by a TP-DNA polymerase complex through recognition of the parental TPs. The first nucleotide is then attached to the -OH group of the Ser^{232} residue of the primer TP by the DNA polymerase (Blanco et al., 1992; Hermoso et al., 1985). This complex then slides back one nucleotide to recover the template at the 3' terminal end of the DNA (Mendez et al., 1992) and the polymerase synthesizes a short 10 nucleotide elongation product before transitioning to DNA-primed elongation. This end-to-end mechanism removes the need for discontinuous synthesis on the lagging strand and thus, bypasses the end replication problem. Conversely, *Streptomyces* linear plasmids and chromosomes have a single internal origin of replication and implement the use of TPs by an alternative mechanism. These proteins act to fill in the missing DNA at the 3' single-stranded gaps, usually about 250-300 nucleotides in length. This process is called end-patching (Chang and Cohen, 1994). The mechanism of end-patching has yet to be fully understood although current findings indicate a requirement for accessory proteins such as the telomere associated primase (Tap) to recruit TP's to the 3' overhangs in addition to acting as a primase by adding the first 13 nucleotides to the TP (Bao and Cohen, 2003; Yang et al., 2015, 2017).

Another and by far the most simplistic solution to the end replication and the end protection problems are the use of covalently closed hairpin loops at the termini of linear replicons, referred to as hairpin telomeres (Figure 1.1c, (Casjens, 1999)). These structures can be found in the *Borrelia* (Barbour and Garon, 1987; Casjens et al., 1997; Fraser et al., 1997) and *Agrobacterium* genera (Goodner et al., 2001), *Klebsiella oxytoca* phage φKO2 (Stoppel et al., 1995), *Escherichia coli* phage N15 (Rybchin and Svarchevsky, 1999) and other phages. However, in solving the end replication problem these structures present an alternative dilemma. Among varying replication mechanisms in prokaryotes possessing these structures, all DNA replication results in daughter replicons that are covalently joined at their telomere ends and require additional processing by specialized enzymes to separate and segregate the products to

daughter cells. Among the previously mentioned prokaryotic organisms, this always appears as a strand breakage and rejoining reaction, referred to as telomere resolution (Figure 1.2). The mechanisms of linear DNA replication in organisms containing hairpin telomeres have been most extensively studied in *E. coli* phage N15 and *Borrelia burgdorferi* (Barbour and Garon, 1987; Casjens et al., 1997; Ravin, 2015; Ravin et al., 2003).

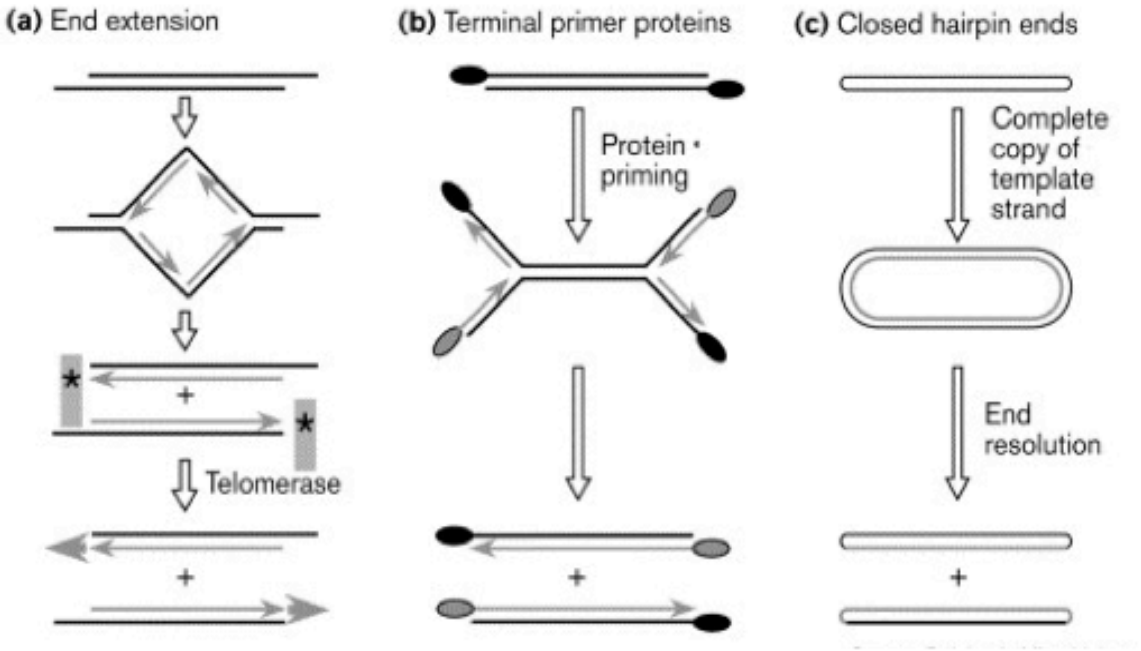

Figure 1.1 Alternative solutions to the end replication problem in linear replicons. A) Eukaryotic linear replicons are left with 3' overhangs during replication that require extension by Telomerase. Asterisks indicate areas of DNA requiring extension that were not replicated by the DNA polymerase. **B)** Terminal proteins (represented by the black and grey ovals) act as primers at the far 3' ends of the linear replicon in prokaryotes to prime DNA polymerase mediated replication. **C)** Replication of prokaryotic linear replicons with closed hairpin ends can occur through multiple mechanisms, all resulting in a replication intermediate composed of a fused dimer that is then resolved into two daughter linear replicons closed by hairpin ends. Figure reprinted with permission from (Casjens, 1999).

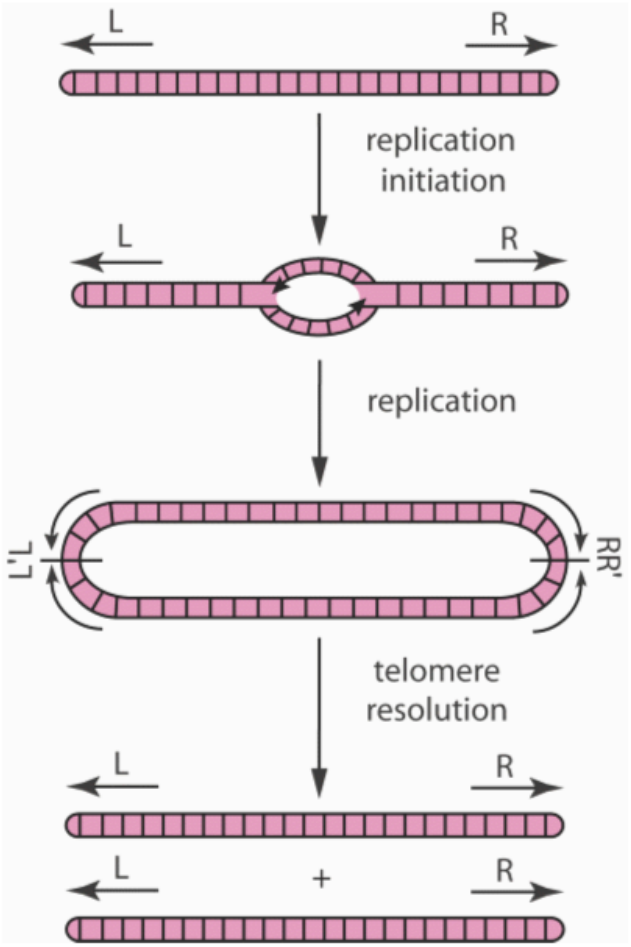

Figure 1.2 A Model of Linear DNA replication. Replication initiates at an internal origin and proceeds bidirectionally through the hairpin telomeres. The resulting replication intermediate contains the copied replicon fused into a circular dimer joined at replicated telomere junctions (denoted as L'/L and R/R') that possess inverted repeat symmetry. This dimer is then resolved into two linear replicons closed by hairpin ends through a process called telomere resolution. This figure was adapted from (Kobryn and Chaconas, 2002) and reprinted with permission from (Chaconas, 2005).

1.2. Replication of linear replicons with hairpin telomeres

1.2.1 The N15 phage paradigm

The N15 phage of *E. coli* is atypical among temperate phages in that its prophage does not integrate into the bacterial chromosome upon infection and is instead maintained as a linear plasmid. This represents an early example of linear DNA closed by covalent hairpin loops discovered in prokaryotes (Rybchin and Svarchevsky, 1999). This double-stranded DNA chromosome contains 12 base pair single-stranded cohesive ends, termed cosL and cosR in its virion, and upon infection of *E. coli* circularizes via these cohesive termini (Ravin et al., 2000; Rybchin and Svarchevsky, 1999). Instead of using this circularized DNA as a template for replication, N15 prophage DNA is then converted into a linear plasmid closed by hairpin ends through the cleavage and rejoining action of a specialized enzyme called a telomere resolvase or

protelomerase, identified as the product of phage gene *tel*N. The TelN enzyme recognizes a palindromic repeat region within the plasmid called *tel*RL and creates a staggered nick within this region. The phosphodiester bonds are then rejoined to produce a linear plasmid closed with two hairpin telomeres referred to as *tel*L and *tel*R (Deneke et al., 2000). Replication of the linear plasmid initiates at an origin located within the *rep*A gene of the plasmid and proceeds bidirectionally. Replication of the left telomere, *tel*L is completed first followed by TelN promoted telomere resolution of *tel*L/L' replicated junction, creating a Y shaped molecule. Replication of the longer right arm of the phage is subsequently completed and the *tel*R/R' junction resolved through the action of TelN to produce two linear daughter plasmids closed by hairpin telomeres. Support for this model of asymmetric linear replication and telomere resolution was confirmed through identification of the various replication intermediates by electron microscopy (Ravin et al., 2003). The minimal requirements for N15 prophage replication were experimentally determined to include: the gene product of *rep*A, a multi-domain protein that's functions include primase, helicase, and origin binding activities; the telomere resolvase, TelN; and the telomere sequence, *tel*RL (Mardanov and Ravin, 2006; Ravin et al., 2003).

During lytic replication, the head-to-head circular dimer replication intermediate is alternatively resolved into two circular monomers by the telomere resolvase, TelN, as opposed to two linear plasmids. These circular monomers are then processed in a manner reminiscent of late lytic replication in lambda phage (Ravin, 2015). It is hypothesized that this switch is the result of TelN depletion or some unknown factor that either modifies the telomere resolvase or its target site (Mardanov and Ravin, 2009). The replication of N15 prophage serves as a general model for the subsequently identified linear plasmid prophage including *K. oxytoca* phage φKO2 (Casjens et al., 2004), *Yersinia enterocolitica* phage PY54 (Hertwig et al., 2003), and others.

1.2.2. The *Borrelia* paradigm

Concurrent with the discovery of N15 prophage DNA being maintained as a linear plasmid with covalently closed hairpin ends, studies in a small number of bacterial systems revealed a unique, highly segmented genomic structure in *B. burgdorferi* including a linear chromosome and a multitude of circular and linear plasmids (Barbour and Garon, 1987; Casjens et al., 1997; Fraser et al., 1997). This constituted the first evidence of a bacterial linear

chromosome possessing hairpin telomeres, and has subsequently served as a model for linear bacterial replication. Replication of *B. burgdorferi's* linear chromosome functions with a relatively restricted set of replication proteins, relative to *E. coli*, with a simpler, single subunit replicative polymerase and no obviously encoded helicase loader (Fraser et al., 1997). *B. burgdorferi's* origin of replication (*oriC*) was identified near the center of the linear chromosome between *dna*A and *dna*N (Fraser et al., 1997; Picardeau et al., 1999). Importantly, no replication initiation was detected near the hairpin telomeres (Picardeau et al., 1999). Transcriptional directionality and the switch in polarity of the GC skew near the center of the chromosome supported the finding of a central origin (Casjens et al., 2000; Fraser et al., 1997). Additionally, these data were strengthened by the subsequent finding of an Hbb binding site near *oriC* (Kobryn et al., 2000). Hbb is an architectural protein with structural and functional similarity to a family of DNA bending proteins that aid origin DNA melting by DnaA (Mouw and Rice, 2007; Tilly et al., 1996). Replication proceeds bidirectionally, from *oriC*, through the hairpin telomeres, reflecting theta-like replication (Picardeau et al., 1999). The resulting replication intermediate is a dimer of DNA fused at replicated telomere junctions (*rTel*) containing inverted repeat symmetry. This replication model more closely resembles that depicted in Figure 1.2 than the asymmetric replication model proposed for N15 prophage. As previously discussed, the DNA dimer must then be resolved, through a two-step cleavage and rejoining reaction called telomere resolution, into two linear daughter replicons terminated by hairpin telomeres. Similar to TelN, this function is performed by the borrelial telomere resolvase, ResT, a gene product of the BBB03 locus of cp26. ResT's telomere resolution activity has been confirmed, *in vitro* (Kobryn and Chaconas, 2002) and *in vivo* (Bandy et al., 2014).

1.3. Telomere Resolvases

1.3.1. A brief overview

As previously discussed, prokaryotic organisms that use hairpin telomeres to circumvent the end replication and the end protection problems require specialized enzymes to resolve these structures following DNA replication. These specialized enzymes responsible for telomere resolution are referred to as telomere resolvases or protelomerases. However, the latter name can be misleading as these enzymes do not share any homology with the eukaryotic telomerase enzyme and the use of the "pro" prefix is typically used in reference to a precursor enzyme

(Chaconas and Kobryn, 2010). To date, telomere resolvases have been identified and characterized in seven bacterial species and three phage: *E. coli* phage N15 (Deneke et al., 2000), *K. oxytoca* phage φKO2 (Casjens et al., 2004), *Yersinia enterocolitica* phage PY54 (Hertwig et al., 2003), *A. tumefaciens* (Huang et al., 2012), the Lyme disease spirochete *B. burgdorferi* (Kobryn and Chaconas, 2002), the relapsing fever borreliae *B. hermsii*, *B. parkeri*, *B. recurrentis*, *B. turicatae*, and the avian spirochete *B. anserine* (Moriarty and Chaconas, 2009). Studies have produced crystal structures for both the agrobacterial enzyme, TelA, and the klebsiellal enzyme, TelK, (Aihara et al., 2007; Shi et al., 2013) and among the telomere resolvases, ResT from *B. burgdorferi* has been studied the most extensively at the biochemical level (Bankhead and Chaconas, 2004; Bankhead et al., 2006; Briffotaux and Kobryn, 2010; Huang and Kobryn, 2016; Huang et al., 2017; Mir et al., 2013; Tourand et al., 2009).

1.3.2. The telomere resolvase reaction mechanism and active site

Telomere resolvases constitute a new class of DNA cleavage and rejoining reaction that act on a distinct type of substrate (a replication intermediate) to produce a unique product – hairpin telomeres. These enzymes simultaneously cleave DNA 6-base pairs apart on opposite strands at the center of *rTel* junctions (previously pictured in Figure 1.2 as L/L' or R/R') to produce 6 nucleotide 5'-overhangs. These overhangs then fold back on themselves and are subsequently resealed to the DNA backbone to form covalently closed hairpins (Figure 1.3, (Huang et al., 2004a; Kobryn and Chaconas, 2002)). Although unique, these enzymes possess mechanistic similarities to both type IB topoisomerases and tyrosine recombinases, and have a tyrosine recombinase-like active site. All these enzyme classes share the similarity of proceeding as a catalytically isoenergetic two-step transesterification reaction that does not require the use of a divalent metal ion or any high energy cofactors. This is made possible through the storage of energy in the protein-DNA complex formed between the scissile phosphate and the active site nucleophile. While type IB topoisomerases act as monomers and cleave a single-strand of DNA (Shuman, 1998) and tyrosine recombinases form a tetramer to create a synaptic complex (Grindley et al., 2006), telomere resolvases are unique in that they act as a coordinated dimer to cleave two DNA strands (Aihara et al., 2007; Briffotaux and Kobryn, 2010). ResT, the borrelial telomere resolvase, was shown to require the formation of a "cross-axis" complex to facilitate

strand cleavage. This complexes formation was surprisingly stimulated by positive supercoiling (Bankhead et al., 2006).

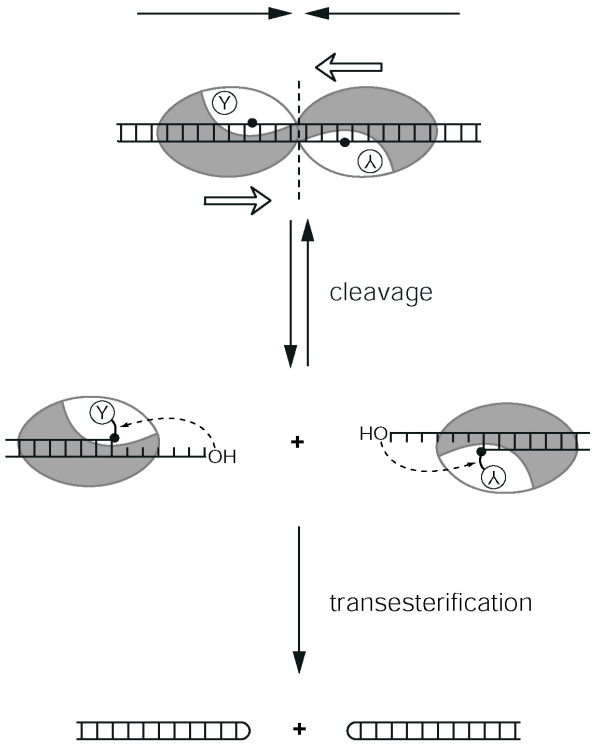

Figure 1.3. A telomere resolvase reaction mechanism. The telomere resolvase dimerizes on the replicated telomere junction (*rTel*), similarly depicted as L'/L or R/R' in Figure 1.2, containing inverted repeat symmetry (the axis of symmetry is denoted by the dashed line in the first image). The tyrosine nucleophile cleaves six base pairs apart (the scissile phosphates are denoted by black dots) on opposite strands of the DNA. This transesterification reaction results in 6 nucleotide 5'-overhangs and a phosphor-tyrosine complex. The 6 nucleotide overhangs fold back on themselves to create a hairpin conformation, and the 5'-OH acts as a nucleophile in a second transesterification reaction that reseals the DNA to the backbone and releases the tyrosine residue leaving two formed hairpin telomeres. This figure was reprinted with permission from (Kobryn and Chaconas, 2002).

An early alignment of the N15 phage telomere resolvase (TelN) against members of the integrase family revealed a weak homology to tyrosine recombinases (Rybchin and Svarchevsky, 1999). This prompted additional alignments against other telomere resolvases and studies aimed at identifying key catalytic residues required for telomere resolution (Deneke et al., 2004; Moriarty and Chaconas, 2009). Similar to tyrosine recombinases, telomere resolvases were found to possess a conserved tyrosine residue that filled the role of the active site nucleophile. A study of the borrelial telomere resolvase, ResT, used a modified DNA substrate to identify the tyrosine active site nucleophile, Y335. The scissile phosphate of the DNA was modified to a phosphorothiolate that still allows for DNA cleavage, but the liberated sulfhydryl (-SH) is a poor nucleophile and the second transesterification cannot be performed. ResT is left tethered to the DNA, allowing for identification of the active site nucleophile through tandem mass spectroscopy (Deneke et al., 2004). Additionally, ResT was shown to not tolerate mutation of its

Y335 residue (Kobryn and Chaconas, 2002). The active site nucleophiles, TelA Y405 (Huang et al., 2012) and TelK Y425 (Huang et al., 2004a) display a similar intolerance to mutation.

In addition to the active site nucleophile, telomere resolvases have an additional set of conserved catalytic residues comparable to the typical RKHRH pentad of tyrosine recombinases (Nunes-Düby et al., 1998). In tyrosine recombinases these residues play a variety of roles including general involvement in acid/base chemistry and the stabilization of the transition state (Grindley et al., 2006). Telomere resolvases generally display an RKYRH pentad of catalytic residues that can be found in both TelA and ResT (Deneke et al., 2004; Huang et al., 2012); TelK alternatively possesses a hybrid version with a lysine residue at the third position instead (Huang et al., 2004a). The study of these catalytic residues in ResT revealed that while pentad mutations could still bind DNA, they were telomere resolution incompetent (Deneke et al., 2004). Surprisingly, this excluded the last histidine residue which was shown to be dispensable for reactions with ResT and implicated it in playing a structural role instead (Chen and Rice, 2003; Deneke et al., 2004). Notably, the Y363 residue of TelA's pentad tolerates both lysine or histidine replacement (Huang et al., 2012). This reflects the pattern of both the TelK pentad and that of tyrosine recombinases. More recently, crystallizations of TelA showed TelA complexed with reaction intermediates as well as hairpin products; in one structure a mimic of the transition state with the positioning of the active site residues is shown (Figure 5. of Shi et al., 2013). While original pentad studies of ResT showed no evidence of a specific residue being implicated in protonation of the leaving group, this crystal structure indicates the third residue of the TelA pentad, Y363 is positioned to fill that role. As this protonation is less dependent on enzyme mediation, it explains the tolerance for lysine or histidine replacement at TelA Y363 and is consistent with the less defective phenotype originally observed in the equivalent ResT (Y293F) mutant (Deneke et al., 2004).

1.3.3. Domain structure

Telomere resolvases all contain a highly conserved catalytic domain, as well as variant N- and C-terminal domains that surround the central catalytic domain (Figure 1.4). While the catalytic domain is responsible for the enzyme's telomere resolution activity and contains the telomere resolution active site, the diversity of domain structure in regards to the N- and C-terminal extensions suggests alternative and potentially varying function among this enzyme

family. The borrelial enzyme, ResT, has an N-terminal domain extension with non-specific DNA binding activity (Tourand et al., 2007). While ResT's C-terminal end contains the conserved catalytic domain, it includes an additional extension on its C-terminal end that likely possesses unique properties. The klebsiellal telomere resolvase, TelK, has a unique insert on its C-terminal end referred to as the "stirrup" that is responsible for distal contacts with the DNA substrate and induces a large bend in the DNA, contributing to hairpin formation (Aihara et al., 2007). Unique to TelK, this extension does not exist in the agrobacterial enzyme, TelA. TelA instead possesses a very small C-terminal extension that contributes to dimerization contacts during telomere resolution (Figure 1.4a). However, these two enzymes display homology in a sub-domain region of their N-terminal ends, termed the N-terminal core (N-core, Figure 1.4a). Within this homologous area, TelK displays a unique insert called the muzzle that is both essential for telomere resolution and is necessary for dimerization (Aihara et al., 2007). Notably, the telomere recognition sites in ResT's C-terminal end appear to be masked by the full-length protein suggesting ResT is subject to autoinhibition by its N-terminal end (Tourand et al., 2007). As the recognition sequence of box 3 on telomeric ends (discussed later in section, 1.4.2.1) is widely abundant throughout the genome, it is not surprising that a mechanism for downregulation of ResT binding exists. It would be interesting to see if other telomere resolvases possess similar domain-based regulatory mechanisms.

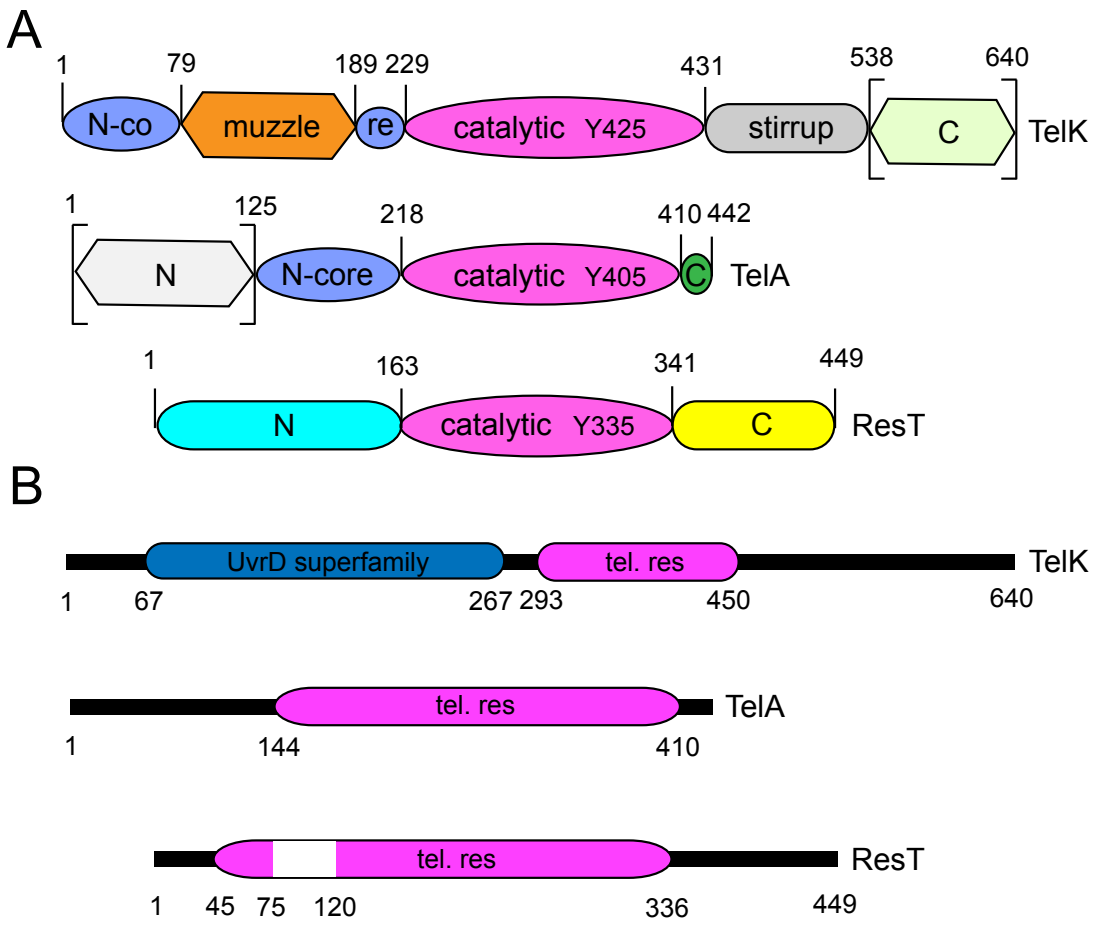

Figure 1.4. Domain diversity among characterized telomere resolvases. A) The domain architecture of three characterized telomere resolvases: TelK from *Klebsiella oxytoca* phage ϕKO2, TelA from *Agrobacterium tumefaciens*, and ResT from *Borrelia burgdorferi*. Homologous domains as identified by BLAST or through structural analysis are annotated with the same colors, while domains that share no homology among other telomere resolvases display unique coloring. Domains that have been experimentally deleted without altering telomere resolution are represented with square brackets. In all architectures the nucleophilic tyrosine is represented within the catalytic domain. **B)** Conserved domain assignments as assigned by the Conserved Domain Database (CDD) or Delta-BLAST (Boratyn et al., 2012; Marchler-Bauer et al., 2015). TelK, TelA, and ResT all contain the telomere resolvase domain (pfam 16684) as identified by the CDD. Both TelA and ResT display homology that extends beyond the catalytic domains depicted in A. ResT possesses an insert within its telomere resolvase domain not present in TelA. TelK additionally displays hits to the UvrD helicase superfamily 1 from Delta-BLAST. This figure was adapted from (Kobryn and Chaconas, 2014).

1.4 Previous characterization of telomere resolvases

1.4.1 TelA from *Agrobacterium tumefaciens*

Agrobacterium tumefaciens, the causative agent of crown gall disease in plants (Smith and Townsend, 1907), has a genome composed of both a linear and circular chromosome, and commonly carries a tumour inducing (Ti) plasmid; some strains such as the prototype C58 possess additional plasmids, for example piTC58 (Goodner et al., 1999). To date, most *A. tumefaciens* research has focused on the virulence associated with its Ti plasmid, as well as this plasmid's unique ability to export and integrate a segment of "T-DNA" into the eukaryotic genome of plants upon infection. Intuitively, this ability has been harnessed for many biotechnological applications including the production of transgenic plants (Newell, 2000). As such, little research has been put forward towards the characterization of the bacteria's linear chromosome or the agrobacterial telomere resolvase, TelA. There is a particular lack in biochemical studies performed on TelA following its original report in 2012. Along with the identification and purification of TelA, the researchers identified the enzyme's minimum target site of 26 base pairs from the native 50 base pair inverted repeat, and confirmed TelA and the minimum target sequence to be the only components necessary to perform telomere resolution, *in vitro* (Huang et al., 2012).

Following TelA's initial characterization, a series of TelA-DNA complex crystal structures were reported by Shi *et. al.* (Shi et al., 2013). Although TelK-DNA complexed crystal structures had been previously reported, they provided little insight into the role of telomere resolvases following DNA cleavage or in hairpin formation. The use of varied substrate intermediates with TelA produced co-crystal structures that suggested an active role for the enzyme in these later steps of telomere resolution. Multiple residues (Y201 and R205) appeared to stabilize an intermediate conformation by forming base stacking interactions with a nucleotide at the 6th position, flipped out in an extrahelical fashion. Furthermore, mutants of these residues displayed cleavage competency, but were unable to perform telomere resolution suggesting a role in hairpin formation (Shi et al., 2013). Notably, the previously mentioned key residues reside within the alpha helical linker of TelA at a location equivalent to the hairpin binding module of ResT (discussed in section 1.4.2.3).

1.4.2. ResT from *Borrelia burgdorferi*

1.4.2.1. Substrate promiscuity

The pathogenic bacterium, *B. burgdorferi* is unusual among prokaryotic organisms possessing hairpin telomeres in that its genome is highly segmented, being composed of a linear chromosome and a mixture of over 12 linear and 9 circular plasmids (Casjens et al., 2000). The hairpin telomeres of its linear replicons display marked sequence diversity and as such, the borrelial telomere resolvase, ResT, is uniquely required to both recognise and process a multitude of hairpin telomeres. This necessitates a level of relaxed substrate utilization for ResT not observed in other telomere resolvases. For example, the prototype *B. burgdorferi* strain B31 possesses 19 unique telomeres that have a 160-fold activity range (Tourand et al., 2009). Among these telomeres exist 5 areas of sequence homology, termed "boxes" of which the invariant box 3 is responsible for telomere recognition and does not tolerate mutation (Tourand et al., 2003). Grouping of these telomeres (Type 1, 2 or 3) is dictated by the positioning or absence of box 1. Type 2 telomeres (+3/-3) have a box 1 shifted 3 nucleotides away from the axis of symmetry and a 3 base pair deletion between box 2 and 3 as compared to Type 1 telomeres (0/0); Type 3 telomeres do not contain a box 1 sequence ((Huang et al., 2004b; Tourand et al., 2003), Figure 1.5). Although telomere recognition is sequence specific to box 3, cleavage is position-specific and based on the axis of symmetry. This allows for the variation in box 1 regions, and telomere sequence in general (Tourand et al., 2003). However, Type 3 telomeres are generally processed less effectively than Types 1 and 2 that contain a box 1 sequence. Studies have shown that while multiple Type 3 telomeres remain inactive *in vitro*, they can be efficiently processed *in vivo* suggesting a fundamental difference in reaction conditions *in vivo* that facilitates telomere resolution (Tourand et al., 2009). Perhaps, stimulatory proteins are present *in vivo* or the DNA topology differs – ResT's activity was surprisingly shown to be stimulated by positive supercoiling of DNA (Bankhead et al., 2006). Notably, there does not seem to be any correlation between telomere type or reactivity and stable inheritability of the plasmid (Tourand et al., 2009).

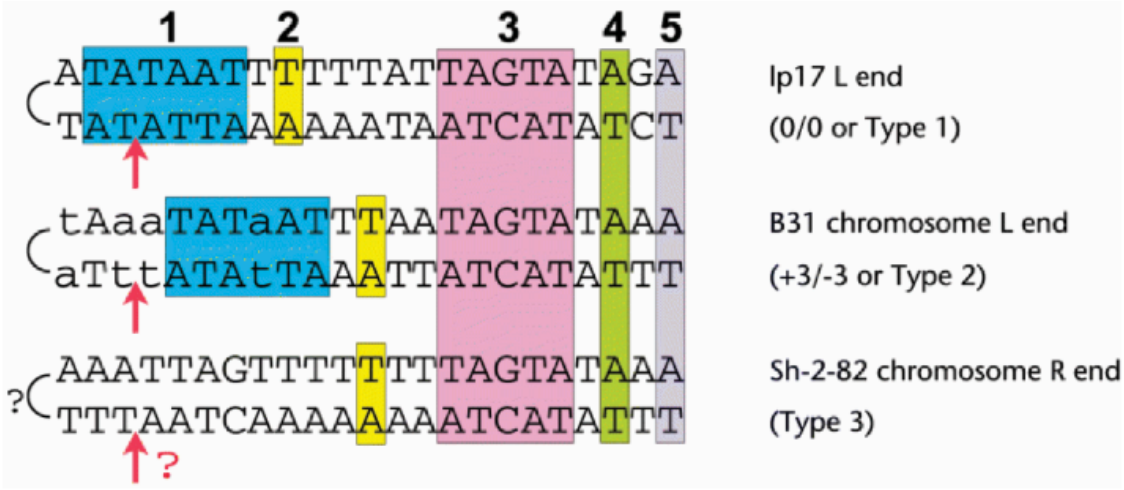

Figure 1.5. Examples of Type 1, 2, and 3 telomeres found in *Borrelia*. A representative of each of the three telomere types found in *B. burgdorferi*. Each conserved sequence "box" is denoted by a unique color and number. Lower case letters indicate known sequence variation in the Type 2 telomere. The red arrows indicate the point of cleavage by ResT and question marks indicate areas of uncertainty in both the identity of the nucleotide around the hairpin and in the exact position of cleavage for the Type 3 telomere. This figure was reprinted with permission from (Chaconas, 2005).

1.4.2.2. Reaction reversal

Another unique feature of *B. burgdorferi* telomeres is the apparent genome plasticity among its linear chromosome and plasmids. The termini of some telomeres appear to possess extended sequences from other plasmids, while multiple subterminal regions contain a patchwork of repeat sequences that suggest some ability for recombination (Casjens et al., 2000). While it is difficult to understand the evolutionary advantage to such events, one study revealed a potential mechanism behind it. ResT was shown to not only be capable of binding already formed hairpin telomeres, but could also perform the reverse reaction of telomere resolution, termed telomere fusion (Kobryn and Chaconas, 2005). Telomere fusion was shown to be possible among differing telomere sequences, although telomeres of different types could not be successfully fused (Kobryn and Chaconas, 2005; Tourand et al., 2003). As telomere fusion is energetically unfavourable, in the majority of situations the fused telomeres are simply resolved back into hairpins. However, at a low frequency a mutation could prevent resolution of the fused telomere resulting in a chimeric plasmid or an extension on the linear chromosome. A

subsequent, relatively large deletion would have to occur to remove one of the sites of telomere resolution and create a stable fusion (Figure 1.6). These fusion products would then be available to participate in future fusion events, potentially contributing to the mosaic nature of borrelial telomeric ends. It has been hypothesized that this event could be apt during infection of the tick, the vector for Lyme disease, as lower temperatures favour the telomere fusion reaction (Kobryn and Chaconas, 2005).

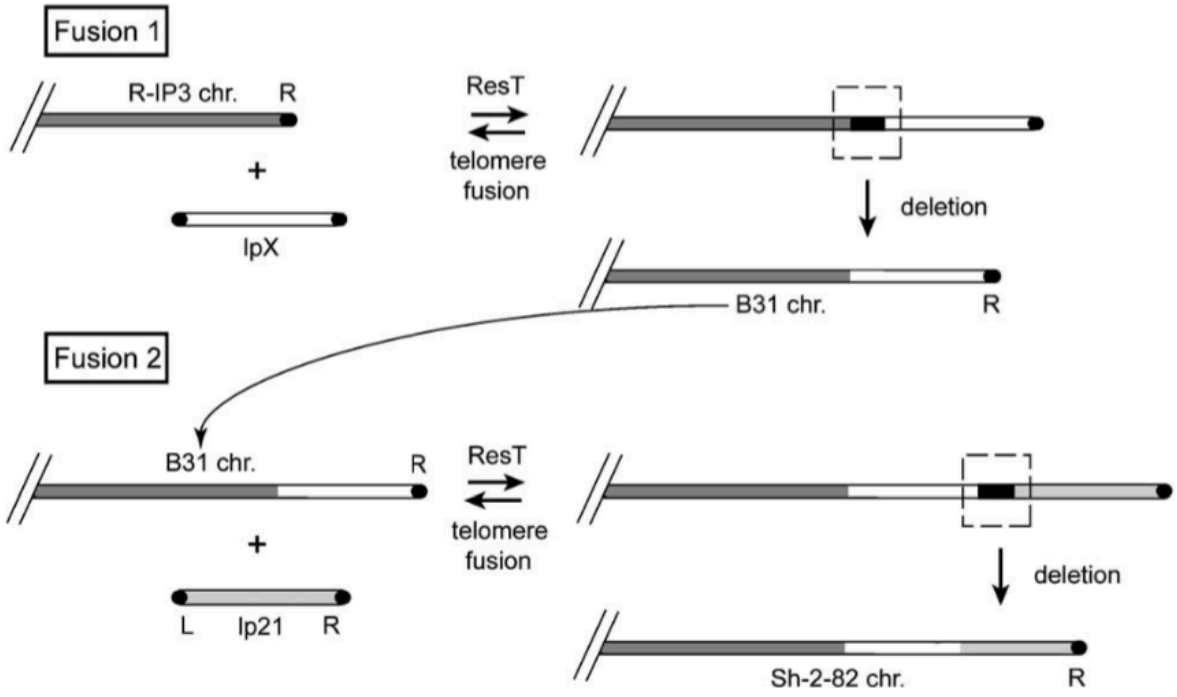

Figure 1.6. A potential mechanism for telomere exchange mediated by ResT. The R-IP3 chromosome is fused to the lpX plasmid (the black tips represent homologous hairpin ends). The identity of the plasmid is variant as the end of the B31 chromosome shares homology with multiple plasmids in *B. burgdorferi* (Casjens et al., 1997, 2000) A subsequently large deletion occurs to remove one site of telomere resolution. In the second fusion the process is repeated with the chimeric end fusing to the lp21 plasmid and another subsequent deletion creating a chimeric end observed with the Sh-2-82 chromosome in *B. burgdorferi* (Casjens et al., 1997; Huang et al., 2004b). Multiple rounds of fusion and deletion could also explain the chimeric ends observed on many *B. burgdorferi* linear plasmids. This figure was reprinted from (Kobryn and Chaconas, 2005)

1.4.2.3. The importance of ResT's hairpin-binding module in DNA cleavage

As previously discussed, telomere resolvases, in general, possess varying N- and C-terminal additions to their highly conserved catalytic domains. ResT can be broadly divided into two regions, ResT (1-163) constituting its N-terminal end and possessing a non-specific DNA binding activity (the source of its annealing activity, which will be discussed later), and its C-terminal end that contains important catalytic residues and displays sequence specific binding to telomere homology boxes 3, 4, and 5 (Tourand et al., 2007). However, within its N-terminal domain, ResT also contains an important region of sequence ranging from residues 139 to 159 that encompasses a hairpin binding module similar to those found in cut-and-paste transposons, Tn5 and Tn10 (Bankhead and Chaconas, 2004; Rice and Baker, 2001). Hairpin binding modules do not exist in either TelK (*K. oxytoca*) or TelA (*A. tumefaciens*) (Aihara et al., 2007; Kobryn and Chaconas, 2014). The hairpin binding module of ResT consists of a hydrophobic binding pocket and a conserved YKEK motif, a derivation of the YREK motif typically observed in the hairpin binding modules of transposons, and has been shown to facilitate DNA cleavage through pre-hairpin formation. Mutation of residues in the hydrophobic binding pocket of ResT produced a telomere resolution defective phenotype that could be rescued by use of a heteroduplex DNA substrate, a substrate in which the two central base pairs have been disrupted and assist this "pre-hairpin formation" (Bankhead and Chaconas, 2004). Furthermore, as these rescued mutants carry out telomere resolution to completion and not just to the step of DNA cleavage, the distortion of the DNA created by the hairpin binding module seems to be important for hairpin formation as well as DNA cleavage. Additional studies suggest the C-terminal domain of ResT that binds boxes 3, 4, and 5, and is responsible for telomere recognition, guides the region of the hairpin binding module to bind box 1 and 2 (Tourand et al., 2007).

1.4.2.4. Strand foldback/hairpin formation

The basic model for hairpin formation by telomere resolvases was based on the TelK-*rTe*l complex in which torsion from the out-of-plane bend in the DNA provided the energy to drive dissolution of the enzyme dimer and subsequent spontaneous strand foldback (Figure 1.7, (Aihara et al., 2007)). However, the unique presence of the hairpin binding module in ResT seemed to provide an alternative mechanism of enzyme-mediated hairpin formation/strand foldback that deviated from this model. Here, it is hypothesized that ResT creates an

underwound conformation in the *rTel* between the scissile phosphates and this allows the catalytic residues of the telomere resolution active site to initiate DNA cleavage. As previously discussed, cleavage incompetent mutants residing within the hairpin-binding module could be rescued and the telomere resolution reaction carried out completion by disruption of the two central base-pairs of the substrate DNA (Bankhead and Chaconas, 2004). Furthermore, the two hairpin products are not released until both are formed (Briffotaux and Kobryn, 2010). More recent work indicates that hairpin formation requires a concerted effort from both the hairpin-binding module and sidechains from the catalytic domain of ResT to create an underwound DNA substrate intermediate that is primed to eject the cleaved strands and drive the telomere resolution reaction forward to completion (Lucyshyn et al., 2015). In contrast to the cleavage incompetent phenotype of the hairpin-binding module mutants, some of the characterized mutants residing in the catalytic domain that contribute to substrate unwinding appeared to undergo abortive cycles of cleavage and rejoining that could be partially rescued through disruption of the base-pairing near the scissile phosphate by using missing base substrates, mismatches or nicks. Loss of these residue's acidic sidechains appeared to attenuate the energy required to expel the cleaved strands away from the phosphor-tyrosine linkage. This proposed "spring loaded pre-cleavage" model for ResT, while contrasting the model for TelK in both cleavage intermediate formation and directionality determinants, holds a similarity in that their reaction intermediates both control reaction directionality (Figure 1.7, (Lucyshyn et al., 2015)). Additionally, structural data for the agrobacterial telomere resolvase, TelA, supports a model of enzyme-mediated hairpin formation during telomere resolution (Figure 1.7, (Shi et al., 2013) that may capture telomere resolvase action in refolding the cleaved DNA strands into a hairpin conformation. It seems plausible that biochemical studies of ResT and TelA structural studies have elucidated different stages of a shared reaction mechanism used to produce hairpin telomeres from a replicated intermediate.

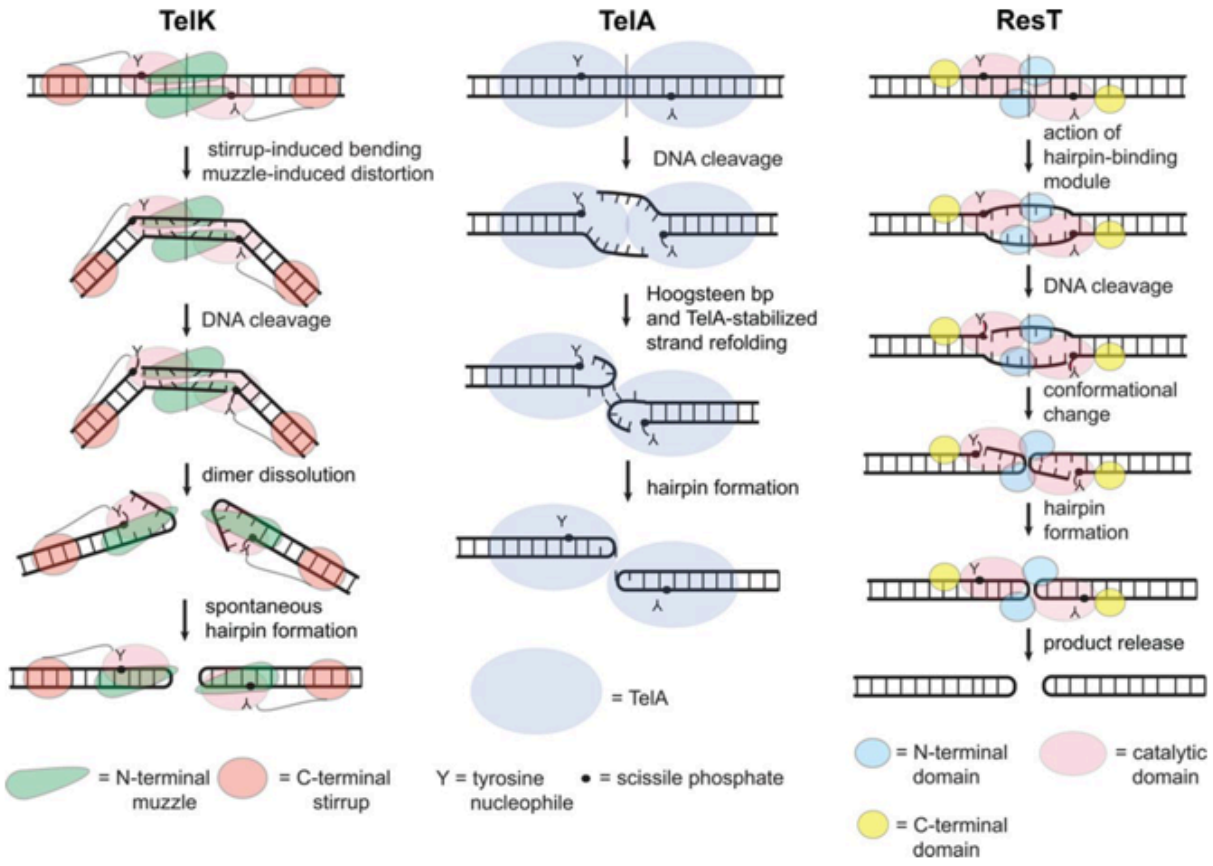

Figure 1.7. Variant models of telomere resolution from different systems. A schematic for the key steps of TelK, TelA, and ResT promoted telomere resolution are shown. The scissile phosphates are represented by black dots in all schematics and the tyrosine nucleophile by Y. **TelK:** binding of TelK to the substrate DNA induces a large 73° bend in the DNA and severely buckles base pairs near the scissile phosphate. This distortion creates a "pre-cleavage intermediate" that stores the energy required to drive the reaction forward with subsequent DNA cleavage, dimer dissolution and spontaneous hairpin formation. This model is supported through a deletion of the stirrup of TelK (pink circle), responsible for DNA bending. This mutant displays cleavage competence, but cannot form hairpins (Aihara et al., 2007). **TelA:** strand refolding is stabilized post cleavage through TelA-DNA interactions and Hoogsteen basepairing across the dimer axis. The entire reaction takes place in the context of the TelA dimer and stabilization of a TelA-hairpin complex post reaction is hypothesized to drive the reaction forward (Shi et al., 2013). **ResT:** binding and dimerization of ResT on the DNA prompts the action of the hairpin binding module of the N-terminal domain. The hairpin binding module distorts the DNA, creating an underwound substrate primed for cleavage by the catalytic domain (Lucyshyn et al., 2015). The reaction occurs entirely in the context of the dimer and is only released when both hairpin products are formed (Briffotaux and Kobryn, 2010). This figure was reprinted from (Lucyshyn et al., 2015).

1.4.2.5. Conditional expression of *res*T *in vivo*

While the original evidence that telomere resolution could be performed *in vivo* came from a demonstration of ResT's activity in borrelial cells (Chaconas et al., 2001), most of the previously discussed biochemical properties have been characterized *in vitro*. *In vitro* conditions are always sub-optimal and do not necessarily reflect what occurs *in vivo*. Recall that although multiple type 3 telomeres from *B. burgdorferi* prototype strain B31 appeared to be inactive *in vitro*, they were readily resolved inside the *Borrelia* cell (Tourand et al., 2009) suggesting additional factors exist *in vivo* to aid telomere resolution. Furthermore, little is known about possible interactions of ResT and telomere resolvases, in general, with other cellular proteins (Kobryn and Chaconas, 2014). Recently, an in-depth study sought to answer some of these questions through conditional expression of the *res*T gene product *in vivo* (Bandy et al., 2014). As *res*T is an essential borrelial gene (Byram et al., 2004), conditional expression was necessary to produce an observable phenotype. Following cellular depletion of ResT, the bacterial cells were expected to filament as is typical when disrupting proteins involved in resolving chromosome dimers (Aroyo et al., 2000; Draper et al., 1998; Wang and Lutkenhaus, 1998). Presumably the DNA would continue to replicate, but would be unable to segregate into daughter cells resulting in an accumulation of DNA dimers and continued elongation of the cell; however, this is not what was observed. Cellular depletion of ResT induced growth arrest and the bacterial cells subsequently ceased DNA replication suggesting the telomere resolvase interacted directly or indirectly with *Borrelia's* replication machinery. The expected accumulation of unresolved dimeric replication intermediates was observed between 24 and 48 hours following ResT depletion, after which they morphed into complex, high molecular weight forms (Bandy et al., 2014). Further studies are needed to explain this unexpectedly complex phenotype.

1.4.2.6. Potential multifunctionality: annealing and unwinding activities

Recently, further *in vitro* biochemical studies on ResT have suggested a functional role for the enzyme beyond telomere resolution. The borrelial telomere resolvase was shown to possess the ability to anneal complementary single-stranded DNA (ssDNA), as well as ssDNA bound with its cognate single-stranded binding protein (SSB) (Huang and Kobryn, 2016; Mir et al., 2013). This activity was shown to stem from the N-terminal domain of the protein, ResT (1-163), as this region alone was sufficient for annealing naked ssDNA. However, the full-length

telomere resolvase still stimulated the reaction above the N-terminal domain alone (Mir et al., 2013). This is consistent with the non-specific DNA binding activity previously identified in the N-terminal domain of ResT (Tourand et al., 2007). Surprisingly, the N-terminal domain alone was not sufficient to promote annealing of ssDNA bound with SSB. Similar results with just the C-terminal end of ResT, ResT (163-449), suggested the region of ResT responsible for interactions with the C-terminal tail of SSB exists between these two domains. ResT's annealing activity could also be extended to plasmid length DNA and therefore, seemed unlikely to only be involved with the 6-base pair region being manipulated during telomere resolution (Huang and Kobryn, 2016). These activities are reminiscent of the *E. coli* protein, RecO, that acts as a recombinational mediator for RecA, as part of the RecF pathway (Kantake et al., 2002a). This pathway mediates RecA-dependent events directed towards recovery from DNA damage and replication stress, (Chow and Courcelle, 2004; Courcelle and Hanawalt, 2003) and is notably absent in *Borrelia* (Fraser et al., 1997) suggesting ResT could fill the role of RecO in this bacterial species.

In addition to ResT's RecO-like properties, the enzyme also displayed a ssDNA-dependent ATPase activity and an ATP-dependent 3'-5' unwinding activity *in vitro,* despite the absence of common helicase motifs or homology to ATP-binding domains in the protein (Huang et al., 2017). ResT's unwinding activity extended to a variety of substrates including replication fork mimics and D-loop mimics. The study also revealed that ResT could only bind ATP in the context of the entire protein – individual domains did not display this property, suggesting that the ATP binding determinants of this protein were not segregated to a particular domain region. Furthermore, ATP binding surprisingly stimulated ResT's annealing activity, dimerization of ResT, and modulated ResT's affinity for replication fork mimics. ResT was also shown to be capable of transferring the gamma phosphate from ATP to itself (unpublished data). ResT's *in vitro* ATPase/unwinding activity was supported through both its hyper- and hypo-activation by mutation of multiple residues. Additionally, mutation of key catalytic residues important for telomere resolution displayed unwinding phenotypes comparable to that of wildtype ResT, supporting a distinct function for these activities from telomere resolution. Finally, ResT also displayed the ability to perform fork regression on a partially mobile synthetic replication fork, *in vitro* (Huang et al., 2017). This activity requires concerted annealing and unwinding and is also found in both the T4 phage UvsW helicase and among many members of

the RecQ helicase family (discussed further in section 1.5.3) (Croteau et al., 2014; Nelson and Benkovic, 2007; Wu and Hickson, 2006).

1.5. Typical annealing and unwinding proteins

1.5.1. Annealing proteins

The annealing of ssDNA is integral to many biological processes, particularly homologous recombination (HR) – a process involved in genetic exchange, double stranded break (DSB) repair, the repair of single-stranded gaps, and restart of stalled or collapsed replication forks (Maher et al., 2011; Mehta and Haber, 2014; Morrical, 2016). While HR is present in all kingdoms of life, mechanisms of prokaryotic HR have been most extensively studied in *E. coli*, where RecA was first identified as the central recombinase and subsequently determined to be highly conserved (Brendel et al., 1997; Clark and Margulies, 1965). However, some HR pathways that function independently of RecA have also been described. The bacteriophage lambda encodes the beta protein, a single-stranded annealing protein, which in combination with an exonuclease is required for HR in a *rec*A$^-$ host strain of *E. coli.* In this model, the exonuclease digests DNA in the 5' to 3' direction, halting at a nick or DSB and leaving an exposed single-stranded 3'-tail. The beta protein then binds to the single-stranded 3'-tails and promotes annealing of homologous single-stranded regions. This complementary single-stranded annealing is likely driven by beta protein binding more strongly to its nascent annealed products then to ssDNA (Karakousis et al., 1998; Muyrers et al., 2000).

In the case of RecA-dependent HR pathways, the annealing of complementary ssDNA presents itself as a common and important activity among recombination mediator proteins (RMP), such as *E. coli's* RecO (Luisi-Deluca and Kolodner, 1994). RMPs primarily function to promote presynaptic RecA filament assembly on SSB-ssDNA (New et al., 1998; Umezu et al., 1993); specifically in *E. coli*, this occurs by RecO stimulating RecA displacement of SSB and subsequent RecA loading to the ssDNA (Umezu et al., 1993). RecO acts as part of a complex with RecF and RecR to perform this function (Gupta et al., 2015; Lenhart et al., 2014; Radzimanowski et al., 2013; Umezu et al., 1993). However, the ability of RecO to promote the annealing of complementary ssDNA, specifically ssDNA bound by its cognate SSB, appears to be distinct from its mediator function. This is supported by the observation that interaction with RecR promotes RecO's mediator activity, while inhibiting its single-stranded annealing activity.

Strand invasion by the presynaptic complex (RecA-ssDNA) displaces one strand of the homologous DNA. It is hypothesized that RecO will bind to this displaced strand and promote annealing with the second processed end of a DSB (a 3' single-stranded overhang), allowing for HR without the need for a second strand invasion event (Kantake et al., 2002b). RMP functional counterparts to RecO including *Saccharomyces cerevisiae's* Rad52 protein and the UsvY protein of T4 bacteriophage also display the ability to promote the annealing of complementary ssDNA bound specifically with their cognate SSBs or functional equivalents (Kantake et al., 2002b; Shinohara et al., 1998; Sugiyama et al., 1998). Furthermore, Rad52's ability to promote second-end DNA capture during HR has been demonstrated (Nimonkar et al., 2009), suggesting the conservation of this dual role for RMP's in HR across divergent systems.

1.5.2. Unwinding proteins

The ability to separate the two strands of duplex DNA is central to almost all DNA metabolic processes, accounting for both the ubiquitous presence of unwinding proteins as well as their variant functions. Helicases possess a distinct directionality, translocating in the 3'-5' direction or the 5'-3' direction across a single-strand of DNA, and can exist in a variety of oligomeric forms (Singleton et al., 2007; Wu and Hickson, 2006). For example, the replicative helicase of *E. coli*, DnaB, forms a hexameric ring and the ssDNA is threaded through its center for loading (Bailey et al., 2007). The unwinding activity of helicases is heavily present at various stages of HR and replication fork repair, the processes where their activity most prominently works in concert with annealing activity. DNA unwinding is required for creating ssDNA tails for RecA loading, the migration and processing of Holliday junctions, and can act in an antagonistic capacity by removing RecA from filaments or through D-loop destruction (Dillingham and Kowalczykowski, 2008; Manosas et al., 2013; Veaute et al., 2005; Wu and Hickson, 2006). The latter function likely acts in a regulatory capacity to prevent inappropriate recombination events. In *E. coli*, the holoenzyme RecBCD is responsible for generating ssDNA tails for RecA loading. The holoenzyme binds to blunt double-stranded ends with RecB and RecD allowing for translocation in both the 3'-5' and 5'-3' direction, respectively, as they possess opposing helicase motors. This bipolar unwinding activity is coupled to degradation of the DNA through RecB's nuclease activity (Dillingham et al., 2003). RecC can recognize a regulatory Chi sequence that prompts a switch to one-stranded degradation, leaving a long 3' ss-

tail ideal for the initiation of HR (Arnold et al., 2000; Dillingham and Kowalczykowski, 2008). Conversely, the UvrD helicase in *E. coli* has been shown to dismantle RecA filaments, antagonizing HR (Veaute et al., 2005); *uvr*D mutants also display hyperactive rates of HR supporting their potential role in regulation (Arthur and Lloyd, 1980).

1.5.3. Proteins with combined annealing and unwinding activity

Despite the opposing nature of annealing and unwinding activities, both play an essential role at various stages of HR. As such, some proteins displaying combined annealing and unwinding properties are particularly apt to perform certain steps in these HR and replication repair pathways (Croteau et al., 2014; Manosas et al., 2013; Nelson and Benkovic, 2007; Wu and Hickson, 2006). When the replication machinery encounters a lesion on the leading strand it often stalls, causing the replisome to disassemble and leaving a fork structure that can be unwound. Both *E. coli's* RecG and the T4 phage helicase, UvsW, can remodel a stalled replication fork through a process called fork regression that requires concerted annealing and unwinding. RecG and UvsW can catalyze unwinding of the DNA strands followed by template switching in which the two nascent strands are annealed to one another and allow the nascent lagging strand to be used as a template for leading strand synthesis. This allows for the unrepaired lesion to be bypassed. It is possible that RecG and UvsW are also involved in subsequently resetting the replication fork through branch migration of the Holliday junction (Manosas et al., 2013; Nelson and Benkovic, 2007). Studies have shown that expression of UvsW in *rec*G mutant *E. coli* cells can rescue their growth suggesting the two proteins are functional analogs of one another (Carles-Kinch et al., 1997). Many members of the highly conserved RecQ helicase family can also perform fork regression and have been proposed to act by similar mechanisms to *E. coli's* RecG in multiple organisms (Bachrati and Hickson, 2008; Ralf et al., 2006; Wu and Hickson, 2006). In *E. coli*, RecQ also acts with the RecJ nuclease as part of the RecFOR pathway to process the nascent lagging strand at stalled replication forks. RecQ's unwinding activity produces a substrate vulnerable to degradation by RecJ, leaving a replication fork that is accessible to the nucleotide excision repair machinery (Courcelle et al., 2006).

Akin to the previously described helicases, ResT also demonstrates the ability to perform fork regression, shown with a partially mobile synthetic replication fork, *in vitro* (Huang et al.,

2017). In concert with the unexpectedly complex phenotype observed in ResT depleted cells (Bandy et al., 2014), these combined annealing and unwinding activities (Huang and Kobryn, 2016; Huang et al., 2017; Mir et al., 2013) suggest a potential role for ResT in DNA replication. While standard models propose that replication proceeds bidirectionally through the hairpin telomeres (see section 1.2.2.), the fate of the replisome as it approaches the hairpins is unknown. It is conceivable that conflict between the replicative helicase and the leading strand polymerase would result in failure to complete replication around the hairpin and leave a leading strand gap conceptually similar to a stalled replication fork. ResT could then remodel the fork to promote leading strand synthesis and subsequent fork reversal, leaving a complete replication intermediate suitable for telomere resolution (Huang et al., 2017). However, the *in vivo* function of ResT's apparent annealing and unwinding activities and whether additional telomere resolvases possess similar properties currently remains unknown. In addition to their conserved telomere resolvase domains, TelN shares weak homology with P-loop NTPases, while TelK displays partial homology to UvrD helicase domains (Figure 1.4b, (Kelley et al., 2015)), but the significance of this has yet to be explored. Additional studies are required to identify the homogeneity of these additional activities across the telomere resolvase enzyme family as well as the functional role these activities play, *in vivo.*

2. Rationale, Hypotheses, and Objectives

2.1. Rationale and Hypotheses

Despite domain diversity among the telomere resolvase enzyme family, their main enzymatic function of telomere resolution – a unique DNA breakage and rejoining reaction, as well as the catalytic domain the activity derives from, are highly conserved. However, recent studies have provided evidence that these enzymes could be multifunctional. Previous work by Bandy *et al.* revealed conditional expression of the borrelial telomere resolvase, ResT, produced a complex phenotype wherein cells depleted of ResT did not filament (as would be expected in cells accumulating DNA dimers) and instead ceased DNA replication (Bandy et al., 2014). These data suggest ResT may be interacting directly or indirectly with the replication machinery. Additionally, the N15 phage telomere resolvase, TelN, was shown to be needed for both linear plasmid lysogenic maintenance, as well as establishing the substrate for lytic replication (Mardanov and Ravin, 2009; Ravin et al., 2003). The possibility of multifunctionality amongst this enzyme family is further supported by a recent *in vitro* biochemical characterization of ResT in which it was demonstrated that aside from its telomere resolution capabilities, this enzyme also unexpectedly displayed the ability to promote the annealing of complementary ssDNA, and an ATP-dependent, 3'-5' unwinding activity (Huang et al., 2017; Mir et al., 2013). Unexpectedly, the ssDNA annealing activity observed in ResT was also stimulated in the presence of ATP. Notably, ResT does not possess an ATP-binding domain or helicase motifs typical of enzymes with these types of activities (Huang et al., 2017), making these results all the more puzzling. Furthermore, these activities currently have no known function *in vivo* and the question of whether all members of this enzyme family possess multifunctionality remains elusive.

This project aims to examine the agrobacterial telomere resolvase, TelA, for these unexpected properties observed in ResT, and if found to identify separation-of-function mutants ideal for eventually assessing the function of these activities, *in vivo*. We hypothesize that ATP-dependent DNA unwinding and ssDNA annealing constitute a property of the telomere resolvase enzyme family and will also be present in the second telomere resolvase, TelA from *Agrobacterium tumefaciens*. We hypothesize TelA will display the ability to anneal complementary ssDNA, bind ATP and by extension possess an ATP-dependent unwinding

activity, in addition to its known function of telomere resolution. We hypothesize it will be possible to separate these distinct activities of TelA from one another by mutation.

2.2. Objectives

1. To determine if these unexpected activities of annealing and unwinding constitute a property of the telomere resolvase enzyme family through purification and *in vitro* biochemical characterization of a second telomere resolvase, TelA from *Agrobacterium tumefaciens.*
2. To understand the mechanistic details of TelA promoted telomere resolution and to determine how those details compare to that of other characterized telomere resolvases.
3. To determine if telomere resolution and any additional activities identified in TelA can be separated from one another through mutation and if so, to generate separation-of-function mutants for future *in vivo* agrobacterial functional studies.

3. Materials and Methods

3.1 DNA cloning and assembly

3.1.1. Synthetic TelA gene codon optimized for expression in *E. coli* and TelA mutant assembly

A codon-optimized synthetic gene encoding TelA (Figure 3.1) that had been blunt-end cloned into a pUC vector was purchased from Integrated DNA Technologies (IDT). For overexpression of a 6X His-tagged TelA in *E. coli*, the gene was excised by NdeI/BamHI and cloned into NdeI/BamHI digested pET15b to create the plasmid construct, pEKK394. The plasmid construct for the N-terminal truncation mutant, TelA (107-442) was created by PCR amplification from the TelA synthetic gene plasmid construct using primers as detailed in Table 1. All other TelA mutants were created through site-directed mutagenesis using primers as detailed in Table 1, followed by DpnI digestion of the parental strand. All plasmids were verified through DNA sequencing and moved into a Novagen Rosetta™(DE3)pLysS expression strain. All plasmid and expression strains were named as detailed in Table 2.

```
   1 catatgctggcggccaagcgtaagacaaaaacgccagtgttagtggaacgtatcgaccaattcgtcggtcaaattaaagaa  81
   1    M  L  A  A  K  R  K  T  K  T  P  V  L  V  E  R  I  D  Q  F  V  G  Q  I  K  E   27

  82 gccatgaaatcggacgatgctagtcgcaatcgcaaaatccgtgatctgtgggatgcggaggtgcgctatcatttcgacaac 162
  28 A  M  K  S  D  D  A  S  R  N  R  K  I  R  D  L  W  D  A  E  V  R  Y  H  F  D  N   54

 163 ggtcgtactgaaaagaccttggagttatacattatgaaatatcgtaatgcattaaaagccgaatttggacccaagtcaaca 243
  55 G  R  T  E  K  T  L  E  L  Y  I  M  K  Y  R  N  A  L  K  A  E  F  G  P  K  S  T   81

 244 ccgctggctatctgtaatatgaagaagttgcgcgagcgcctgaacacatatattgcacgtggcgattatcccaaaaccgga 324
  82 P  L  A  I  C  N  M  K  K  L  R  E  R  L  N  T  Y  I  A  R  G  D  Y  P  K  T  G   108

 325 gtggcgacctctatcgttgaaaagatcgagcgtgccgagttcaataccgcgggccgtaaacctacagttttattgcgtatc 405
 109 V  A  T  S  I  V  E  K  I  E  R  A  E  F  N  T  A  G  R  K  P  T  V  L  L  R  I   135

 406 gcagacttcattgctgcaatgaacggtatggatgctaaacaagacatgcaggccctttgggacgccgaaattgctattatg 486
 136 A  D  F  I  A  A  M  N  G  M  D  A  K  Q  D  M  Q  A  L  W  D  A  E  I  A  I  M   162

 487 aacggccgtgctcagacaactatcatctcctacattacaaaataccgcaatgcgattcgcgaagcttttggggacgaccac 567
 163 N  G  R  A  Q  T  T  I  I  S  Y  I  T  K  Y  R  N  A  I  R  E  A  F  G  D  D  H   189

 568 ccaatgttgaaaattgccactggcgacgctgctatgtacgacgaagctcgtcgtgttaagatggaaaaaatcgcgaataaa 648
 190 P  M  L  K  I  A  T  G  D  A  A  M  Y  D  E  A  R  R  V  K  M  E  K  I  A  N  K   216

 649 cacggtgcacttatcacgtttgaaaattatcgccaggtcctgaaaatctgcgaggattgcttgaaaagctccgacccactt 729
 217 H  G  A  L  I  T  F  E  N  Y  R  Q  V  L  K  I  C  E  D  C  L  K  S  S  D  P  L   243

 730 atgatcgggattggccttattgggatgacggggcgtcgcccctacgaagtctttactcaagctgagtttagtccagctccg 810
 244 M  I  G  I  G  L  I  G  M  T  G  R  R  P  Y  E  V  F  T  Q  A  E  F  S  P  A  P   270

 811 tacggaaaaggggtatcgaagtggtcgatccttttttaacggacaggccaagactaagcaaggtgagggaacgaagtttggg 891
 271 Y  G  K  G  V  S  K  W  S  I  L  F  N  G  Q  A  K  T  K  Q  G  E  G  T  K  F  G   297

 892 atcacgtacgaaatccctgtcttgacccgctcagaaactgtccttgccgcctacaagcgcctgcgtgaaagtggccaaggc 972
 298 I  T  Y  E  I  P  V  L  T  R  S  E  T  V  L  A  A  Y  K  R  L  R  E  S  G  Q  G   324

 973 aagttgtggcatggcatgtcgatcgacgacttctcgtccgagacacgtctgctgttacgcgatacggtctttaacttgttt 1053
 325 K  L  W  H  G  M  S  I  D  D  F  S  S  E  T  R  L  L  L  R  D  T  V  F  N  L  F   351

1054 gaggatgtttggccgaaggaagagcttccgaaaccgtacggtcttcgccacttgtacgctgaagtggcataccataatttt 1134
 352 E  D  V  W  P  K  E  E  L  P  K  P  Y  G  L  R  H  L  Y  A  E  V  A  Y  H  N  F   378

1135 gcacctccgcacgtcactaaaaacagttatttcgcagccatcctgggccacaacaataatgacttagaaacaagtctttct 1215
 379 A  P  P  H  V  T  K  N  S  Y  F  A  A  I  L  G  H  N  N  N  D  L  E  T  S  L  S   405

1216 tacatgacttatacgctgcctgaggaccgtgataacgcactggcgcgcctgaagcgcaccaacgaacgcacattgcaacag 1296
 406 Y  M  T  Y  T  L  P  E  D  R  D  N  A  L  A  R  L  K  R  T  N  E  R  T  L  Q  Q   432

1297 atggccaccattgcgcccgtaagtcgtaaggggtaaggatcc 1338
 433 M  A  T  I  A  P  V  S  R  K  G  *
```

Figure 3.1. Synthetic TelA gene sequence. The gene sequence and corresponding amino acid sequence for the synthetic TelA gene are shown and numbered, respectively. The NdeI and BamHI restriction sites are **bolded** and the stop codon introduced into the synthetic gene is highlighted in red. The synthetic gene was blunt-end cloned into pUCIDT by IDT and verified by DNA sequencing. This figure was generated from https://www.bioinformatics.nl/cgi-bin/emboss/prettyseq

Table 1. Oligonucleotide primers used for mutant construction in this study.

Mutation	Primers for Mutant Plasmid Constructs	
(107-442)	OGCB794	5′-**ATACCGGATCC**TTACCCCTTACGACTTACGGGCGC-3′
	OGCB795	5′-**CACCATGGCATATG**GGAGTGGCGACCTCTATCGTTGAAAAG-3′
D202A	OGCB772	5′-GCTGCTATGTACGCGGAAGCTCGTCGT-3′
	OGCB773	5′-ACGACGAGCTTCCGCGTACATAGCAGC-3′
Y405F	OGCB778	5′-TTAGAAACAAGTCTTTCTTTCATGACTTATACGCTGCCT-3′
	OGCB779	5′-AGGCAGCGTATAAGTCATGAAAGAAAGACTTGTTTCTAA-3′
R205A	OGCB780	5′-TACGACGAAGCTGCGCGTGTTAAGATG-3′
	OGCB781	5′-CATCTTAACACGCGCAGCTTCGTCGTA-3′
S238A	OGCB802	5′-GATTGCTTGAAAGCGTCCGACCCACTTATG-3′
	OGCB803	5'-CATAAGTGGGTCGGACGCTTTCAAGCAATC-3'
R318A	OGCB804	5′-AAGCGCCTGGCGGAAAGTGGC-3′
	OGCB805	5'-GCCACTTTCCGCCAGGCGCTT-3'

Codons highlighted in red indicate the amino acid that was altered from the parental strand. In the case of TelA (107-442), the red codon TTA introduces a stop codon at that position and the bolded sequences contain the BamHI and NdeI sites and flanking DNA introduced into the primer for cloning.

Table 2. Assigned plasmid and expression strain numbers for TelA and mutants

Mutation	Plasmid Strain	Expression Strain
wildtype TelA	pEKK394	pEKK395
(107-442)	pEKK406	pEKK408
D202A	pEKK396	pEKK401
Y405F	pEKK399	pEKK402
R205A	pEKK397	pEKK403
S238A	pEKK416	pEKK425
R318A	pEKK417	pEKK426
S238A/R318A	pEKK428	pEKK431

3.2. TelA expression and purification

3.2.1. Wildtype TelA

Expression of TelA was performed in 500 mL of LB broth containing 100 μg/mL ampicillin and 30 μg/mL chloramphenicol. A seed culture of the expression strain containing 100 μg/mL ampicillin, 30 μg/mL chloramphenicol, and 1% glucose was grown overnight at 37°C. The 500 mL culture was seeded 1 in 100 from the overnight culture of the expression

strain and grown at 37°C to an A_{600nm} of 0.4. The temperature was reduced to 24°C for 20 min followed by induction with 500 μM Isopropyl β-D-1-thiogalactopyranoside (IPTG). The culture was induced overnight at 24°C. Lysate was prepared from the pelleted cells by the freeze-thaw method previously described by (Bankhead and Chaconas, 2004). The salt concentration of the lysate was adjusted to 0.5 M with Ni-load buffer (50 mM NaH_2PO4, 10 mM imidazole, 10% glycerol) not containing NaCl and the lysate was loaded to a 10 mL Ni-NTA affinity column. The column was washed with 10 column volumes of 0.5 M NaCl Ni-wash buffer (50 mM NaH_2PO4, 20 mM imidazole, 10% glycerol) and TelA was eluted with 15 mL of 0.5 M NaCl Ni-elution buffer (50 mM NaH_2PO4, 400 mM imidazole, 10% glycerol) into 1 mL aliquots. Peak fractions were identified by sodium dodecyl sulfate (SDS) polyacrylamide gel electrophoresis (PAGE) and pooled. The combined Ni-elutions were diluted in HG buffer (25 mM HEPES [pH 7.6], 0.2 mM EDTA, 10% glycerol) containing no salt to reduce the salt concentration to 0.25 M NaCl and loaded to a 6 mL Heparin-Sepharose CL6B column (HS). The HS column was washed with 10 column volumes of 0.25 M NaCl HG and 2 column volumes of 0.35 M NaCl HG. TelA was eluted from the HS column with 9 mL of 0.5 M NaCl HG followed by 9 mL of 1.5 M NaCl HG in 1.5 mL fractions. Peak fractions from 1.5 M NaCl HG fractions were pooled and the protein concentration determined by using BioRad's protein dye reagent (Bradford, 1976).

3.2.2. TelA mutants

TelA (D202A), (Y405F) and (R205A) were overexpressed and purified as previously described for wildtype TelA. TelA (107-442) was induced at 27°C overnight with 250 μM IPTG. Lysate preparation, Ni-NTA affinity purification were performed as with wildtype TelA. The HS purification was performed similarly to the previously described protocol, however the column was eluted on a 14 mL linear gradient (0.25 M NaCl HG – 1.5 M NaCl HG). Peak fractions were identified by SDS-PAGE and tested for nuclease activity with the 3'-partial duplex substrate assembled from labelled OGCB666 and unlabeled OGCB692 (see Table 3.). Fractions containing the least amount of nuclease activity were pooled and the salt adjusted to 0.5 M NaCl. Pooled elutions were loaded to a 3 mL hydroxyapatite (HAP) column equilibrated with 0.5 M NaCl HG. The column was washed with 10 column volumes of 0.5 M NaCl HG + 10 mM sodium phosphate (NaPi) buffer. TelA (107-442) was eluted with a 9 mL linear gradient (HG 0.5M NaCl + 10 mM NaPi – HG 0.5M NaCl + 0.3M NaPi).

TelA (S238A), (R318A) and the double mutant (S238A/R318A) were induced overnight at 24°C with 250, 500, and 250 μM of IPTG, respectively. TelA (S238A) and (R318A) were originally purified in a manner similar to what was previously described for TelA (107-442). The double mutant was purified in a manner similar to wildtype TelA. Notably, attempts to repurify TelA (S238A) required constant modification of the lysate making protocol, as the lysate produced was very gluey and the soluble portion could not be successfully separated for loading onto the Ni-NTA affinity column.

3.3. Substrate assembly

3.3.1. Plasmid substrate for telomere resolution

A 36 bp synthetic *rTel* was assembled from oligonucleotides OGCB763/764 with 5' GATC overhangs purchased from IDT. The assembled *rTel* was cloned into BamHI digested pUC19, verified by DNA sequencing and subsequently named pEKK392. pEKK392 was linearized by SspI for use in plasmid length telomere resolution assays.

3.3.2. Oligonucleotide substrate assembly

Substrates were constructed by 5'-^{32}P endlabelling the oligonucleotides with 4 units of T4 polynucleotide kinase (PNK) and 66 nM [γ-^{32}P] ATP at 37°C for 1 hour. The oligonucleotides were subsequently annealed in buffer containing 25 mM 4-(2-hydroxyethyl)-1-piperazineethanesulfonic acid (HEPES) pH 7.6, 0.1 mM Ethylenediaminetetraacetic acid (EDTA) and 50 mM NaCl by bringing reactions to a boil in a water bath and allowing slow cooling to room temperature overnight. Substrate assemblies used for replication fork and D-loop mimics were recovered by excision from 8% PAGE 1X Tris Acetate EDTA (TAE) gels followed by a crush and soak elution overnight at 4°C, separation of gel remnants by application to 0.45 μm Costar® cellulose acetate columns, and ethanol precipitation to concentrate the substrates. A detailed list of oligonucleotides used for the various substrates can be found in Table 3.

3.3.3. Telomere binding substrates

A synthetic *rTel* was assembled from oligonucleotides OGCB763/764. These oligos were annealed together as previously described to create an *rTel* half site with 5'-GATC overhangs

and -ATAT overhangs. OGCB764 was treated with T4 PNK to produce a half site that could be ligated to form a fully assembled *rTel*. Unligated half sites were gel purified away from the fully assembled *rTel* with an 8% PAGE 1X TAE gel followed by crush and soak of the gel slice, application to a 0.45 μm Costar® cellulose acetate column, and ethanol precipitation to concentrate the DNA. The assembled *rTel* was then 5'-radiolabelled for use in binding assays. Mock *rTel*s were constructed in a similar manner using OGCB 832 and 833.

Table 3. Oligonucleotides used for substrate construction in this study.

Oligo name	Oligo sequence	Use
OGCB455	5′-GATCATATCCTTTCTTTAAACTTCTATCATTGATTCTTACTAG TCTTTACCTTACTATACTTCTATCAGTTTATCGATTCTTCTTTA-3′	87 nt ssDNA; used in annealing assays.
OGCB456	5′-GATCTAAAGAAGAATCGATAAACTGATAGAAGTATAGTAAG GTAAAGACTAGTAAGAATCAATGATAGAAGTTTAAAGAAAGGATAT-3′	Complement of 455 to make a duplex DNA in annealing assays.
OGCB409	5′-TCTGCGCCTCGTTCCGGCTAAGTAACATGGAGCAGGTCGCGGATT TCGACACAATTTATCAGGCGATGATACAAATCTCCGT TGTACTTTGTTTCGCGCTTGGTATAATCGCTGGGGGTCAAAGAT-3′	126 nt bottom strand of polarity test substrate.
OGCB666	5′-GTTACTTAGCCGGAACGAGGCGCAGA-3′	26 nt strand to make polarity test substrate
OGCB667	5′-ATCTTTGACCCCCAGCGATTATACCA-3′	26 nt strand to make polarity test substrate.
OGCB669	5′-GTCGGATCCTCTAGACAGCTCCATGATCACTGGCACTGGT AGAATTCGGC-3′	50 nt leading template strand for fork mimic.
OGCB670	5′-CAACGTCATAGACGATTACATTGCTACATGGAGCTGTCTAG AGGATCCGA-3′	50 nt lagging template strand for fork mimic.
OGCB671	5′-TGCCGAATTCTACCAGTGCCAGTGAT-3′	26 nt nascent leading strand for fork mimic.
OGCB672	5′-TAGCAATGTAATCGTCTATGACGTT-3′	26 nt nascent lagging strand for fork mimic.
OGCB681	5′-TGTGGAATGCTACAGGCGTTCTAGTTTGTACTGGTGACGAA ACTCAGTGTTACGGTACATGGGTTCCTATTGGGCTTGCTATCCCTGAAAA TGAGGGTGG-3′	100 nt top strand for D-loop substrates.
OGCB686	5′-CCACCCTCATTTTCAGGGATAGCAAGCCCAATAGGGGTAC CGAGCTCGAATTCACTGGCCGTCGTTCCAGTACAAACTACAACGCCTGTA GCATTCCACA-3′	100 nt bottom strand for D-loop substrates.

OGCB687	5′-AACGCCGGCCAGTGAATTCGAGCTCGGTACC-3′	31 nt strand with complementarity to the centre of 686; used to make D-loop.
OGCB688	5′-AGTCTTAAGCCTTGACTAGTCAGCTTGACTAAGCGATTGAC TAACGACGGCCAGTGAATTCGAGCTCGGTACCC-3′	74 nt strand to make 5'-D-loop
OGCB689	5′-AACGACGGCCAGTGAATTCGAGCTCGGTACCCAGTCTTAA GCCTTGACTAGTCAGCTTGACTAAGCGATTGACT-3′	74 nt strand to make 3'-D-loop.
OGCB692	5′-TCTGCGCCTCGTTCCGGCTAAGTAACATGGAGCAGGTC GCGGATTTCGACACAATTTATCAGGCGATGATACAAAT-3′	76 nt strand to make 3'-partial duplex with 50 nt 3'-tail, use with 666.
OGCB763	5′-gatcCATAATAACAATAT-3′	Oligo to make telomere half-site; annealed with 764; used to make pEKK392, used for EMSA.
OGCB764	5′-CATGATATTGTTATTATG-3′	Oligo to make telomere half-site; annealed with 763; used to make pEKK392, used for EMSA.
OGCB827	5′-gatcCCTCTAACCATTGCGCGATCGATCATAATAACAATATCATGAT ATTGTTATTGTAATCGATCGCGGATCCCGGGCGTAGCCACGTAGGTA-3′	used to make oligo telomere resolution substrate; annealed with 828
OGCB828	5′-gatcTACCTACGTGGCTACGCCCGGGATCCGCGATCGATTACAATA ATATCATGATATTGTTATTATGATCGATCGCGCAATGGTTAGAGG-3′	Used to make oligo telomere resolution substrate; annealed with 827
OGCB832	5′-gatcGTATTATTGTTATA-3′	oligo to make mock telomere half-site; annealed with 833; used for EMSA
OGCB833	5′-GTACTATAACAATAATAC-3′	oligo to make mock telomere half-site; annealed with 832; used for EMSA

3.4. Telomere resolution assays

3.4.1. Plasmid substrate telomere resolution assays

All plasmid substrate telomere resolution assays were performed in buffer containing 25 mM HEPES (pH 7.6), 1 mM 1,4-dithiothreitol (DTT), 100 μg/mL bovine serum albumin (BSA), and 50 mM potassium glutamate, with or without a divalent metal ion present. The reactions were incubated at 30°C. The conversion of 1.75 μg/mL of SspI linearized pEKK 392 into two hairpins was monitored with both timecourse and endpoint reactions. Timecourses were set up as 120 μL reactions with 18 μL aliquots removed at indicated timepoints and combined with SDS loading dye to a 1X final concentration (1X SDS load dye contains 20 mM EDTA, 3.2% glycerol, 0.1% SDS and 0.0024% bromophenol blue)

3.4.2. Telomere resolution assays using an oligonucleotide substrate

All oligonucleotide telomere resolution assays were performed in buffer containing 25 mM HEPES (pH 7.6), 1 mM DTT, 4 mM $CaCl_2$, 100 μg/mL BSA, and 50 mM potassium glutamate, with or without 2 mM ATP present. 76 nM of TelA was incubated with 5 nM of the 5' radiolabelled substrate (OGCB827*/828*) at 30°C and the conversion of OGCB827*/828* into two radiolabelled hairpins was monitored through timecourse reactions. Timecourses were set up as 120 μL reactions with 18 μL aliquots removed at indicated timepoints and combined with SDS loading dye to a 1X final concentration.

3.5. Electrophoretic mobility shift assays

Binding reactions were performed by incubating TelA with 1 nM of its assembled *rTel* or a mock *rTel* at 0°C for 20 min. Reaction buffer contained 25 mM HEPES (pH 7.6), 1 mM DTT, 4 mM $CaCl_2$, 100 μg/mL BSA, 50 mM potassium glutamate, and 76 ng/mL heparin sulphate, with or without the addition of 2 mM ATP. Load dye (- SDS) was added to a 1X final concentration and samples were loaded to 6% PAGE/ 0.5X Tris Borate EDTA (TBE) gels that were electrophoresed 15V/cm at 4°C. The gels were dried and exposed to a phosphor-imaging screen for visualization.

3.6. Annealing assays

3.6.1. Oligonucleotide substrate annealing assays

This is a gel-based method for tracking mobility differences between ssDNA and that of the annealed product for analysis of TelA's annealing activity. Annealing assays were performed by mixing 15 nM of the labelled reporter oligonucleotide (OGCB455*) with buffer containing 25 mM HEPES (pH 7.6), 1 mM DTT, 2 mM $CaCl_2$, 100 μg/mL BSA, 50 mM potassium glutamate. Reactions were placed on ice for 2 min prior to addition of 15 nM of the complementary unlabeled oligonucleotide (OGCB456) and TelA to reduce the spontaneous rate of annealing. Following the addition of TelA, the reactions were incubated at 30°C and 18 μL aliquots were removed at 0.16, 0.5 1, 2 and 5 min and mixed with pre-aliquoted SDS loading dye containing an excess of the unlabeled reporter oligonucleotide to prevent further annealing. In annealing assays using 7.5 nM of the 3'-partial duplex substrate to compare annealing *vs.* unwinding activity, the reactions were incubated at 37°C for 60 min, with or without the addition of 2 mM ATP to the buffer, and $CaCl_2$ was replaced with $MgCl_2$. All annealing reactions were loaded to 8% PAGE/ 1X TAE/ 0.1% SDS gels and electrophoresed at 13V/cm. Timecourse assays were performed for 120 min and endpoint assays were performed for 105 min. The gels were dried and exposed to phosphor-imaging screens.

3.6.2. Plasmid annealing assay

5'-^{32}P endlabelled pUC19 ssDNA was prepared by digesting pUC19 DNA with BamHI followed by dephosphorylation with antarctic phosphatase, and by endlabelling with T4 polynucleotide kinase. Enzymes, ATP and buffer were removed/changed with G-25 Sephadex microspin columns. ssDNA was generated for the annealing experiments by heat treatment conducted in a PCR machine (99.9^{o}C, 5 min) followed by snap cooling of the denatured DNA in ice water to prevent reannealing. Annealing reactions were performed in 25 mM HEPES (pH 7.6), 2 mM $MgCl_2$, 1 mM DTT, 100 μg/mL BSA and 50 mM potassium glutamate. The annealing reactions contained 1.78 mM nucleotides of substrate DNA and 76 nM TelA and were incubated at 37^{o}C for the times indicated. The samples were deproteinated by addition of SDS load dye to a 1X concentration and applied to an agarose gel. Gel electrophoresis was performed with a 0.7% agarose 1X TAE gel at 1V/cm for 15 h. The gels were dried onto P81 chromatography paper and exposed to a phosphor-imaging screen.

3.7. ATP binding experiments

3.7.1. Surface Plasmon Resonance

Surface Plasmon Resonance measures protein-ligand interactions through immobilizing the protein of interest and exposing the bound protein to a range of ligand concentrations. Interactions are measured as a change in mass of the bound protein, indicative of binding events. Analysis of ATP binding to the telomere resolvase, TelA, as well as the TelA (D202A) mutant and LexA from *E. coli* were carried out with the Reichert SR7500DC dual channel instrument in running buffer containing 25 mM HEPES (pH 7.6), 0.2 mM EDTA (pH 8.0), and 50 mM potassium glutamate at 25°C. Buffer exchange of the system was performed prior to conducting experiments. Purified TelA, TelA (D202A) or LexA was immobilized on a carboxymethyl dextran 500k chip, suitable for small proteins, through a standard amine coupling protocol. Briefly, a 4:1 mixture of *N*-(3-dimethylaminopropyl)-*N*'-ethylcarbodiimide hydrochloride (EDC) and *N*-hydroxysuccinimide (NHS) was injected over the chip to modify the surface carboxylate groups into esters. A sample of the protein to be bound in 10 mM sodium acetate (pH 5.2) was injected across the left channel of the chip forming covalent amide bonds between primary amine groups on the protein and the chip surface. In the final step, an injection of 1 M ethanolamine HCl (pH 8.5) flows over the chip, blocking any exposed surface by deactivating remaining esters and removing any loosely bound protein. The right channel (containing no bound protein) served as a reference channel. Binding analyses were then performed by flowing a titration of ATP injections in running buffer across both channels. 25 μM, 50 μM, 100 μM, 125 μM, 200 μM, 250 μM 500 μM, 1 mM and 2 mM injections were performed in triplicate with an injection of 1.5 M NaCl in running buffer following each ATP injection. This regeneration step removed any ATP accumulating on the chip. Analysis of SPR data was conducted with TraceDrawer software. The SPR response (uRUI) was compared to the reference channel and the data was fit to a 1:1 binding model.

3.7.2. Assaying ATP binding through photoaffinity crosslinking

TelA's ability to bind ATP was assayed by incubating 550 nM of protein (wt TelA, TelA (107-442), TelA (D202A), TelA (R205A) or LexA at 0°C for 5 min in buffer containing 25 mM HEPES (pH 7.6), 0.2 mM EDTA (pH 8.0), 1 mM DTT, 50 mM potassium glutamate, 25 μM ATP and 33 nM [γ^{32}-P] ATP. This allowed any potential interactions between the protein and

ATP to occur. Following incubation, the 1.5 ml Eppendorf tubes containing the reaction were placed on a transilluminator and exposed to UV radiation (312 nm) for 2- or 10-min intervals (as indicated in Figure 4.10) to induce crosslinking. Protein-ATP interactions can now be identified as they are covalently linked to one another. The samples were then prepared for gel loading with the addition of SDS-load dye to a 1X final concentration and incubated at 95°C for 6 min. Following gel electrophoresis, the gel was washed with multiple changes of ddH_2O for 30 min and then fixed using the Pierce™ silver staining kit as per the manufacturer's instructions. The gel was then wrapped and exposed to a phosphor-imaging screen to detect [γ^{32}-P] ATP that had become crosslinked with protein. The silver staining protocol was finished following exposure to the phosphor-imaging screen to detect the migration of the proteins within the gel.

3.8. Thin Layer Chromatography ATPase assay

ATPase assays were performed by incubating TelA in buffer containing 25 mM HEPES (pH 7.6), 1 mM DTT, 2 mM $MgCl_2$, 100 μg/mL BSA, 50 mM potassium glutamate, 100 μM ATP and 66 nM [γ^{32}-P] ATP at 30°C for 120 min. When present, DNA effectors ϕX174 virion DNA (ssDNA) or ϕX174 RFI (dsDNA) were added to 10 μg/mL. Reactions were terminated by the addition of 3 mM EDTA and an aliquot was spotted onto a polyethyleneimine thin-layer chromatography sheet. The sheets were developed in 1M formic acid and 0.5 M lithium chloride and allowed to air dry. Sheets were exposed to a phosphor-imaging screen to visualize the conversion of [γ^{32}-P] ATP to free [γ^{32}-P] phosphate and ADP.

3.9. Unwinding assays

3.9.1. Polarity test substrate assays

Polarity Assays were performed at 37°C in buffer containing 25 mM HEPES (pH 7.6), 1 mM DTT, 2 mM $MgCl_2$, 100 μg/mL BSA, 50 mM potassium glutamate and 2 mM ATP. The polarity substrate (OGCB666 + OGCB667/OGCB409) was alternatively radiolabelled with either the OGCB666* or OGCB667* oligonucleotide to differentiate which strand is preferentially unwound, and is then annealed to unlabelled versions of the other two oligonucleotides to construct the full substrate. 15 nM of the assembled polarity substrate was incubated with TelA and aliquots of the reaction were removed at 15, 30, and 60 min and mixed with 5X SDS load dye supplemented with 600 nM of unlabelled OGCB666 or OGCB667 to a

1X final concentration to halt the reaction. The samples were loaded to an 8% PAGE/ 1X TAE/ 0.1% SDS gel and electrophoresed at 13V/cm for 105 min. The gels were dried and the unwound products visualized by phosphor imaging.

3.9.2. 3'-partial duplex unwinding assays

Unwinding assays were performed at 37°C in buffer containing 25 mM HEPES (pH 7.6), 1 mM DTT, 2 mM $MgCl_2$, 100 μg/mL BSA, 50 mM potassium glutamate, and 2 mM ATP. A constructed partial duplex substrate with a 50 nucleotide 3'-tail (OGCB666, radiolabelled and annealed to OGCB692) was incubated with TelA for 60 min and terminated with the addition of 5X SDS loading dye containing 600 nM of the unlabelled 666 oligonucleotide to a 1X final concentration. The samples were loaded to an 8% PAGE/ 1X TAE/ 0.1% SDS gel and electrophoresed at 13V/cm for 105 min. The gels were dried and the unwound products visualized by exposure to phosphor imaging screens.

**All phosphor-imaging screens were visualized with a Typhoon phosphor-imaging machine and quantitated with Quantity one software. All graphing and statistical analyses were performed with Prism's GraphPad 6.0.

3.10. Protein band isolation by SDS-PAGE

This method allows for the separation of our protein of interest (TelA) away from any contaminants present in the protein preparation. 20 μg of TelA (supplemented with 20 μg of lysozyme, as a carrier protein) was loaded to a 15% SDS-PAGE gel with a 5% stacking gel. An identical sample was loaded to an adjacent lane. Protein bands were identified by staining one set of samples with Imperial™ Protein stain (Thermofisher) and aligning with unstained sample. Gel slices were extracted from the unstained sample and placed in 1.5 mL Eppendorf tubes. Protein elution and acetone precipitation were performed as described by Hager and Burgess (Hager and Burgess, 1980) with some modifications. Proteins were eluted in 0.3 mL of 50 mM HEPES (pH 7.6), 0.15 M NaCl, 0.1 mM EDTA, 1 mM DTT, 100 μg/mL BSA and 0.1% SDS and proteins were precipitated with cold acetone (-20°C) overnight at -20°C. Protein samples were denatured in 50 μL of 6M GuHCl, 50 mM HEPES (pH 7.6), 0.15 M NaCl, 0.1 mM EDTA, 1 mM DTT, 100 μg/mL BSA and 20% glycerol for 20 min at room temperature and renatured by dialyzing against 500 mL of 50 mM HEPES (pH 7.6), 0.15 M NaCl, 0.1 mM EDTA and 20% glycerol (1

change of buffer) for 4 hours. The renaturation step was modified by Vales *et. al*. to remove the GuHCl by dialysis (Vales et. al. 1982), instead of by dilution as originally described by Hager and Burgess. The renatured proteins from each gel slice were assayed for ssDNA-dependent ATPase, unwinding activity, annealing activity, and telomere resolution as previously described to determine which bands possessed these activities.

4. Results

4.1 Biochemical characterization of TelA promoted telomere resolution

4.1.1. Telomere resolution is stimulated by the presence of a divalent metal ion

In the biochemical characterization of TelA, we first assessed the enzyme's ability to perform telomere resolution on a plasmid substrate, *in vitro*. The buffer conditions for these assays were optimized to include 25 mM HEPES (pH 7.6), 1 mM DTT, 100 µg/ml BSA and 50 mM potassium glutamate. The addition of TelA stimulated the conversion of the linearized, 36 bp *rTel* containing plasmid into two distinct hairpin products (Figure 4.1a), and this telomere resolution was stimulated in the presence of a divalent metal ion (Figure 4.1b). We observed a preference for calcium over magnesium, although the enzyme was active over a larger titration of magnesium; calcium levels above 4 mM became inhibitory, whereas magnesium was stimulatory at levels up to 8 mM (Figure 4.2). TelA promoted telomere resolution could also be stimulated by manganese (data not shown). The requirement for a divalent metal ion could explain why previous studies reported needing µM concentrations of TelA to stimulate telomere resolution (Huang et al., 2012; Shi et al., 2013). With a divalent metal ion, we only required low nM concentrations of the enzyme to stimulate the reaction. The telomere resolution activity of TelN was also reported to be stimulated in the presence of a divalent metal ion (Deneke et al., 2000). Conversely, with the borrelial telomere resolvase, ResT, the presence of a divalent metal ion does not affect the enzyme's ability to perform telomere resolution, *in vitro* (Kobryn and Chaconas, 2002).

4.1.2. An N-terminal truncation mutant produces a divalent metal independent phenotype

The initial characterization of TelA reported that its N-terminal domain was dispensable for telomere resolution (Huang et al., 2012). Furthermore, a later reported set of DNA-TelA crystal structures show that TelA only starts to resolve at residue 102, suggesting the N-terminal domain may have other functions (Kobryn and Chaconas, 2014; Shi et al., 2013). Construction, purification, and subsequent analysis of an N-terminal truncation mutant of TelA revealed a divalent metal independent phenotype (Figure 4.1c). However, the addition of calcium or magnesium eventually became inhibitory to the reaction, with concentrations above 2 mM or 8 mM, respectively (Figure 4.2). Similar to the wildtype enzyme, calcium becomes inhibitory at lower levels than magnesium. Relief from the divalent metal requirement observed in the

wildtype enzyme by truncation of the N-terminal domain suggests TelA may be subject to autoinhibition by its N-terminal end. This autoinhibition could be relieved by removal of the N-terminal domain or by addition of a divalent metal ion. The borrelial telomere resolvase, ResT, has also been shown to be subject to autoinhibition by its N-terminal domain (Tourand et al., 2007).

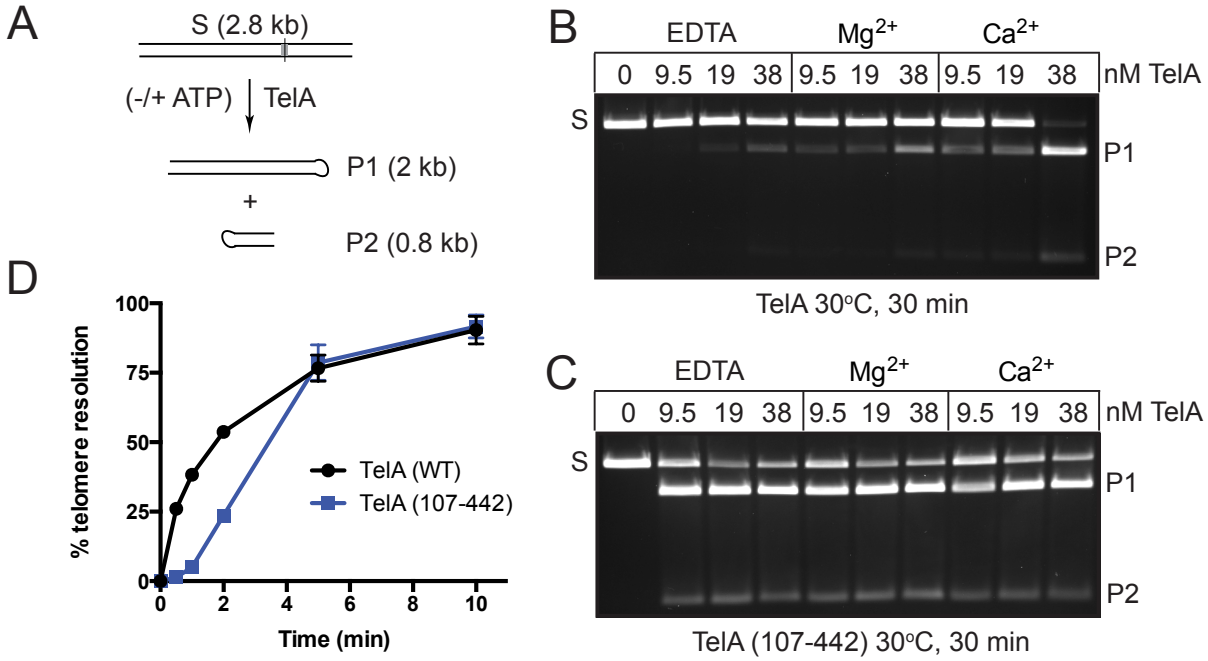

Figure 4.1. Telomere resolution of wt TelA is stimulated in the presence of a divalent metal ion (A) Schematic of the linearized plasmid substrate used to perform telomere resolution assays. The 36-basepair *rTel* (represented by the grey shaded area) is cloned into pUC19 and linearized with SspI. Addition of TelA promotes the conversion of the substrate (S) into two hairpin products (P1, P2) at the point where the shaded region is bisected by a line. **(B, C)** Ethidium bromide stained 0.8% agarose 1X TAE gel panels incubated at 30°C for 30 min with the indicated concentration of wt TelA (B) or TelA (107-442) (C). The reaction buffer contained 1 mM of EDTA, magnesium or calcium as indicated. **(D)** Timecourse plots of wt TelA *vs.* TelA (107-442). Reactions were performed with 1 mM $CaCl_2$ and 19 nM of protein.

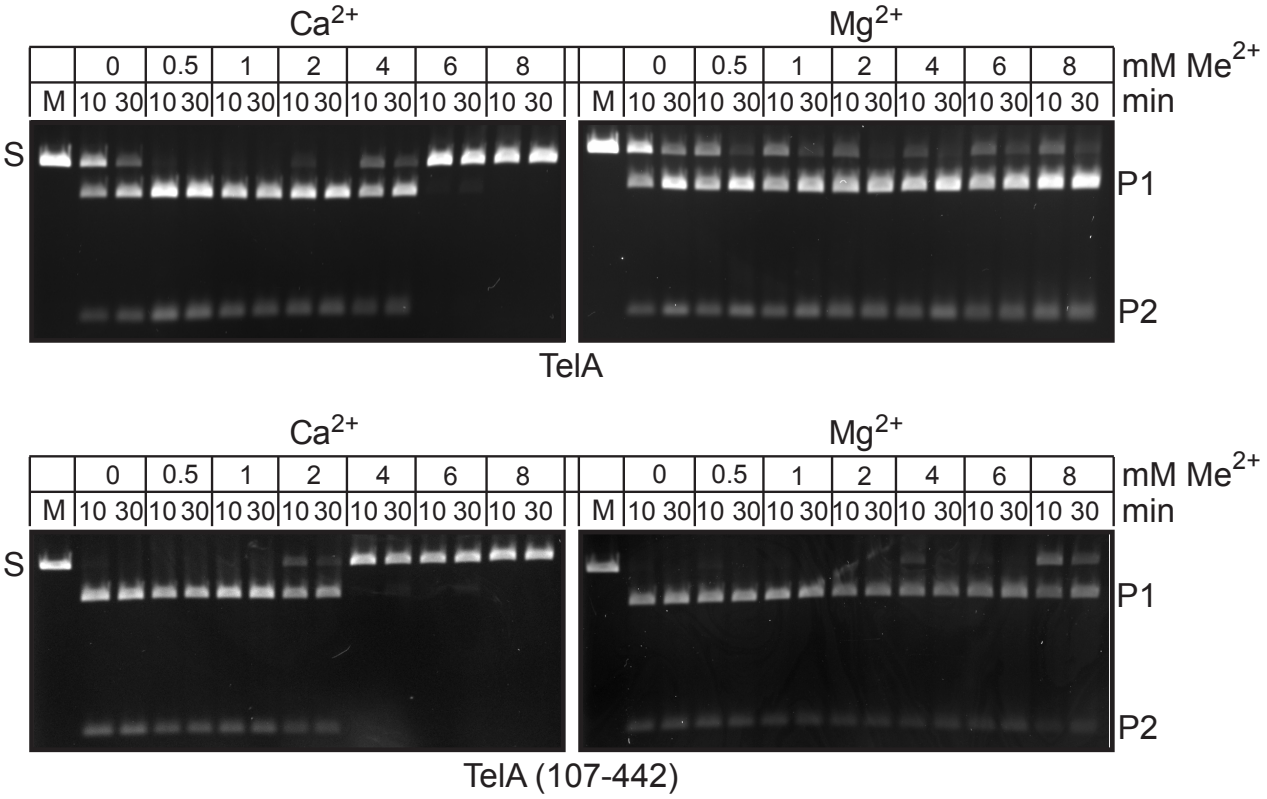

Figure 4.2. TelA's response to a divalent metal ion concentration. 0.8% agarose 1X TAE gel panels of telomere resolution reactions performed with metal titrations of either calcium or magnesium. The top panel displays reactions with wt TelA while the bottom panel shows TelA (107-442) reactions. Both proteins were present at 38 nM.

4.1.3. Differential effects of mutating key residues involved in telomere resolution - Y405F, R205A, D202A

To further understand the mechanism by which TelA performs telomere resolution in *A. tumefaciens*, we again examined the series of crystal structures reported by Shi *et al*. One structure uses a substrate on which hairpin formation has been prevented and the resulting interactions captured are hypothesized to represent a refolding intermediate of telomere resolution (Figure 4.3). Notably, the last 3 nucleotides of each cleaved strand are too mobile to be resolved in these structures (Figure 4.3b). In this, multiple residues are implicated in stabilizing this step including TelA D202 and R205. While this study did not include a biochemical analysis of TelA (D202A), the researchers did conclude that mutation of the R205 residue produced a mutant that was cleavage competent, but could no longer form hairpin

telomeres (Shi et al., 2013). We included the mutants D202A and R205A in our analysis as well as a mutant of the telomere resolution active site nucleophile (Y405F), known to be inactive for telomere resolution activity, as a negative control. Based on the previously discussed crystal structure, we expected TelA (D202A) and (R205A) to possess similar phenotypes. Preliminary characterization of these mutants revealed TelA (Y405F) to be inactive as expected, while R205A and D202A were hypoactive and hyperactive for telomere resolution activity, respectively (Figure 4.4). These contrasting phenotypes suggest these residues have differential roles in telomere resolution.

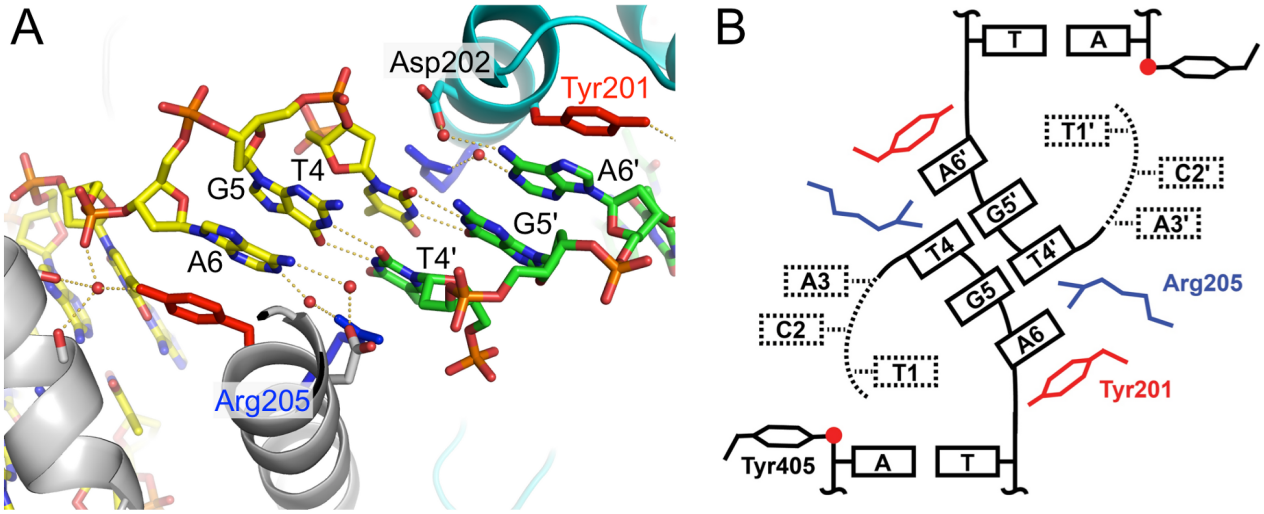

Figure 4.3. The strand refolding intermediate of telomere resolution. (A, B) Schematic diagrams of the refolding intermediate of telomere resolution. This structure was obtained by introducing a nick one base 3' to the scissile phosphates so that subsequent cleavage by TelA would result in shortened 5' overhangs only 5 nucleotides long and leaving no appropriately positioned 5'-OH group available for strand ligation. The phosphor-tyrosine complex can be visualized, as well as the flipped-out adenine base at the sixth position (A6, A6') being stabilized through stacking interactions and hydrogen bonding. (taken from (Shi et al., 2013) PDB ID: 4e0y) doi: https://doi.org/10.1371/journal.pbio.1001472.g007

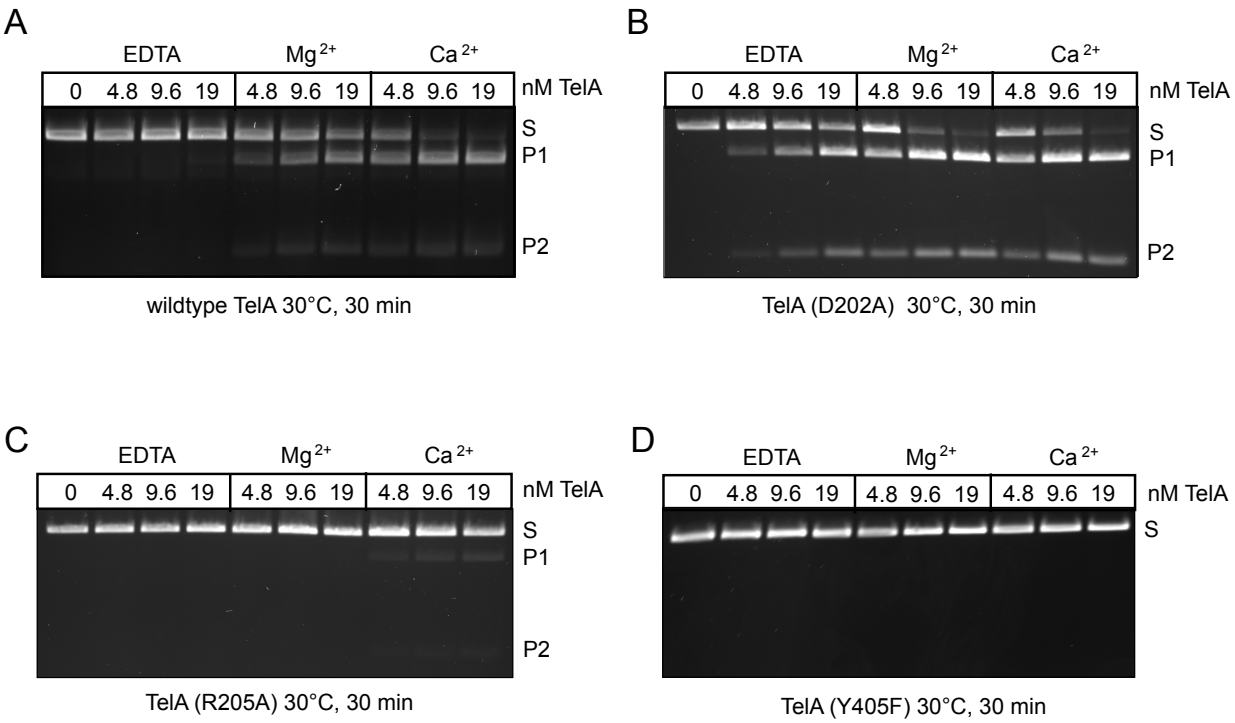

Figure 4.4. Mutation of TelA residues involved with telomere resolution produces differential phenotypes. (A, B, C, D) 0.8% agarose 1X TAE gel panels of telomere resolution reactions incubated at 30°C with the indicated concentration of TelA present. All reactions with wt TelA **(A)**, TelA (D202A) **(B)**, TelA (R205A) **(C)**, or TelA (Y405F) **(D)** included 2 mM EDTA, magnesium or calcium.

Although it was previously reported that TelA (R205A) was cleavage competent, but inactive for telomere resolution, our recent finding of divalent metal ion stimulation of telomere resolution by wildtype TelA prompted us to examine this mutant more thoroughly. Further characterization of TelA (R205A) revealed this mutant could still stimulate telomere resolution in the presence of calcium, although not comparably to wildtype levels (Figure 4.5). The presence of calcium in the buffer stimulated telomere resolution by TelA (R205A) over the entire range tested (0.5 mM – 8 mM), with increasing calcium levels corresponding to increased product formation (Figure 4.5b). Addition of magnesium to the buffer failed to significantly stimulate telomere resolution by the R205A mutant (Figure 4.5a). Even in the presence of calcium, TelA (R205A) requires higher enzyme levels and a longer incubation time than the wildtype enzyme or the D202A mutant to significantly stimulate telomere resolution (Figure 4.5c).

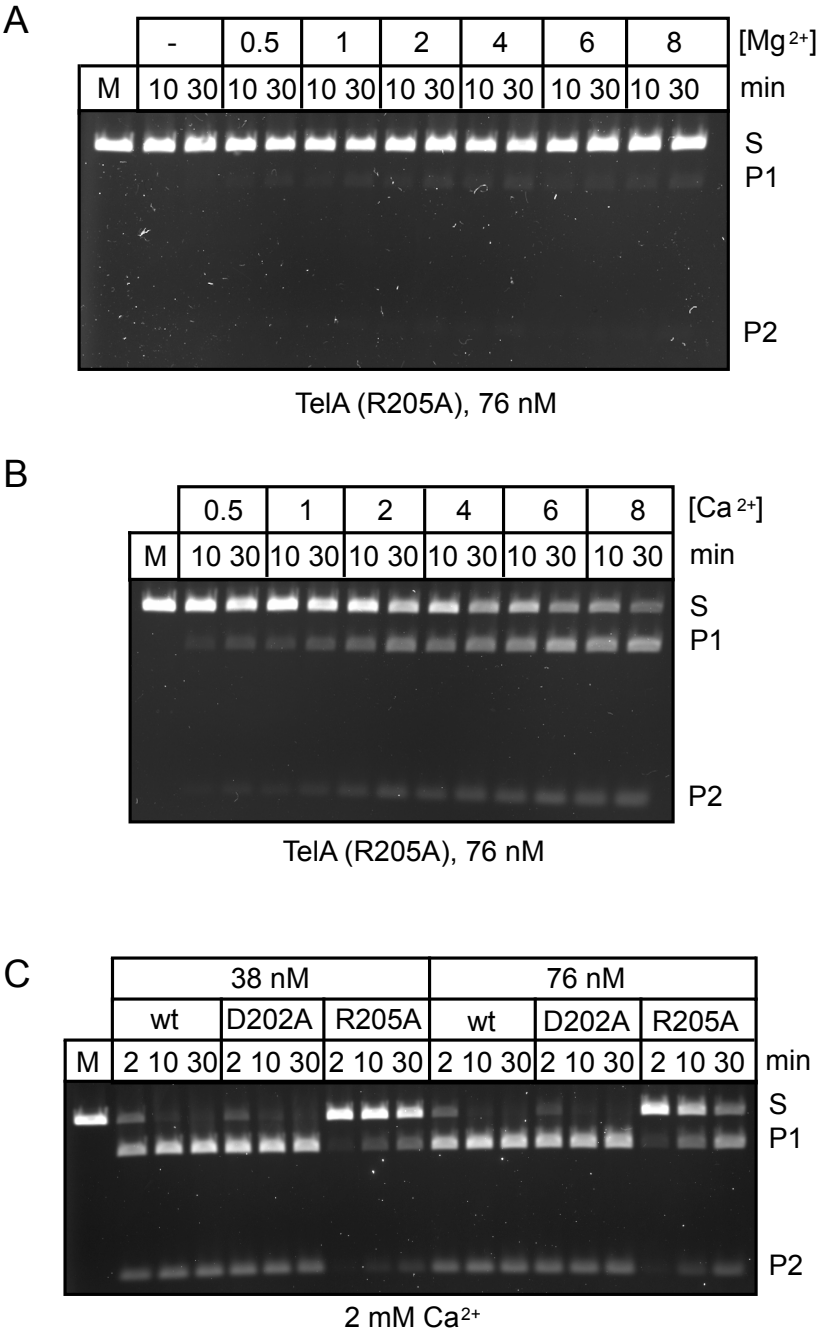

Figure 4.5. TelA (R205A) displays hypoactive telomere resolution activity that can be partially reconstituted in the presence of calcium. (A, B) 0.8% agarose 1X TAE gel panels of telomere resolution reactions with TelA (R205A) incubated at 30°C for the indicated lengths of time. A titration of magnesium **(A)** or calcium **(B)** was present in the buffer. **(C)** Telomere resolution timecourses comparing the activity of wt TelA, and the D202A and R205A mutants in the presence of calcium.

Along with its hyperactive phenotype, TelA (D202A) promoted telomere resolution appears to be partially metal independent as well, although not as starkly as the N-terminal truncation mutant. While the D202A mutant was able to promote telomere resolution in the absence of a divalent metal ion, the presence of both low levels of magnesium or calcium still stimulated the reaction (Figure 4.6ab). This partial metal independence suggests the D202 residue may also be involved with autoinhibition of TelA. The mutant's hyperactivity, in comparison to the wildtype enzyme, is most pronounced in the presence of magnesium (Figure 4.6b).

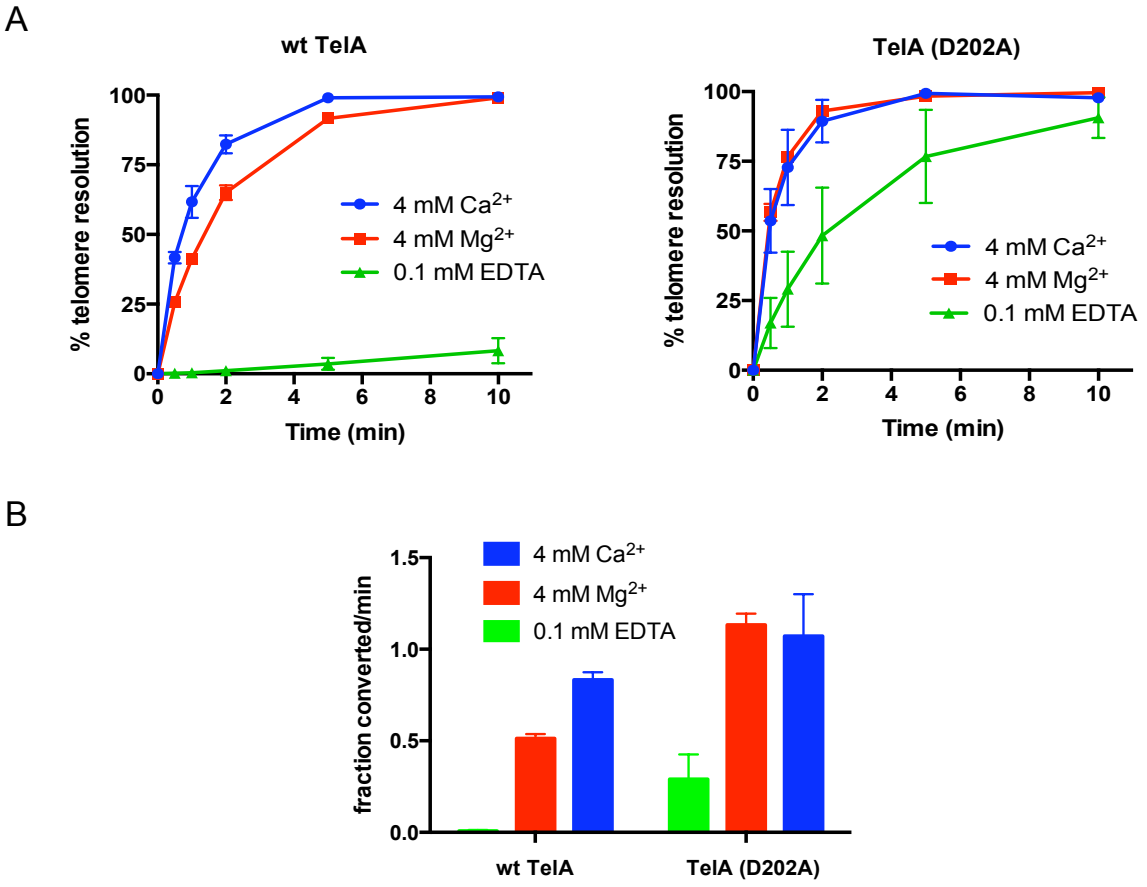

Figure 4.6. TelA (D202A) can perform telomere resolution independently of a divalent metal ion. (A) Telomere resolution timecourse plots and **(B)** Initial rates for 38 nM of TelA and TelA (D202A) with or without a divalent metal ion present. Data shows the mean and standard deviation of three independent experiments.

4.1.4. ATP appears to interfere with TelA's ability to perform telomere resolution

When testing for the optimal buffer conditions under which TelA performs telomere resolution *in vitro* we also included high-energy cofactors, such as ATP in our analysis. We found that not only could TelA perform telomere resolution independently of such high energy cofactors, the presence of ATP unexpectedly inhibited the enzyme's ability to perform telomere resolution when calcium was present in the buffer. Under similar conditions, both the D202A and R205A mutant's ability to perform telomere resolution were unaffected by the addition of ATP to the buffer (Figure 4.7b).

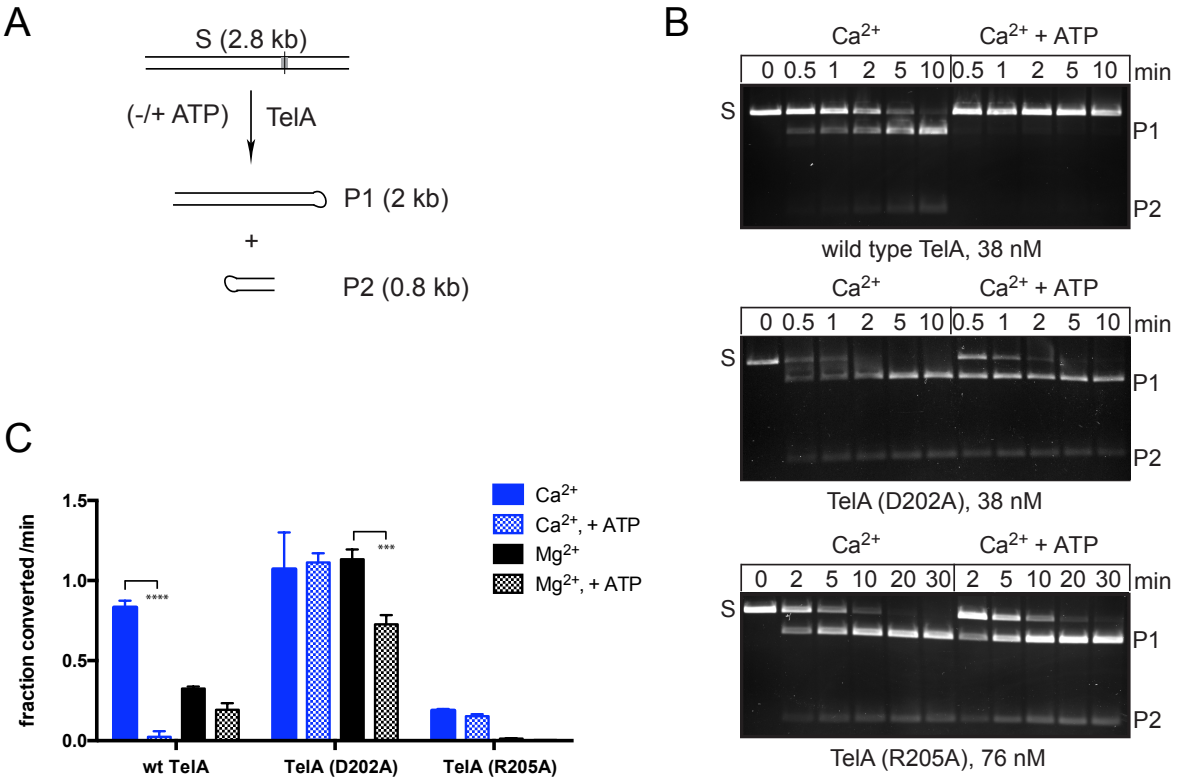

Figure 4.7. Apparent inhibition of telomere resolution in wt TelA by ATP can be relieved through mutation. (A) Schematic of the linearized plasmid substrate used to perform telomere resolution assays. The 36-basepair *rTel* (represented by the grey shaded area) is cloned into pUC19 and linearized with SspI. Addition of TelA promotes the conversion of the substrate (S) into two hairpin products (P1, P2) at the point where the shaded region is bisected by a line. **(B)** Ethidium bromide stained 0.8% agarose 1X TAE gel analysis of telomere resolution timecourses for wt TelA, TelA (D202A) and (R205A) in the presence of calcium, with or without ATP present in the buffer. **(C)** Plots of telomere resolution initial rates for wt TelA, TelA (D202A) and TelA (R205A) in the presence of calcium or magnesium, with or without ATP being present in the buffer. Mg^{2+} was present at 4 mM concentrations. In the case of wildtype TelA and the D202A mutant Ca^{2+} was present at 4 mM and ATP was present at 2 mM. With TelA (R205A) Ca^{2+} was present at 2 mM concentrations and ATP at 1 mM. The mean and standard deviation of three independent experiments are shown.

To further explore the relationship between telomere resolution and this apparent ATP interference, we performed a set of titration experiments in which the optimum calcium levels (4 mM Ca^{2+}) were tested with a range of ATP concentrations from 0 - 2 mM. As the concentration of ATP increased, the enzymes ability to perform telomere resolution decreased (Figure 4.8a). Conversely, the D202A mutant's ability to perform telomere resolution remained unaffected over the same titration of ATP and identical divalent metal conditions (Figure 4.8a). With the knowledge that ATP binds divalent metals at roughly a 1:1 ratio and that TelA (D202A) displays a metal-independent phenotype, we performed a secondary set of experiments to determine if the apparent ATP inhibition of telomere resolution observed in the wildtype enzyme was merely an artifact of decreasing free calcium levels in the reaction. These experiments did not contain ATP, but contained fluctuating calcium levels comparable to that of the unbound, free calcium that would have been present in the reactions containing ATP. We found that the decreasing levels of free calcium alone could not account for the inhibition observed in the wildtype experiments containing ATP (Figure 4.8b). Furthermore, the D202A mutant displayed the expected indifference to fluctuating calcium levels consistent with its divalent metal independent phenotype (Figure 4.8b). Finally, we analysed the effect of alternative nucleotides (GTP, ADP) and ATP homologs (AMP-PNP, ATPγS) on wildtype TelA stimulated telomere resolution to determine if they could produce similar inhibition to that of ATP. Under 4 mM Ca^{2+} conditions, we observed that although the presence of GTP in the buffer resulted in approximately 50% inhibition, both ADP and the ATP homologs, AMP-PNP and ATPγS did not significantly inhibit TelA's ability to perform telomere resolution (Figure 4.8c and data not shown).

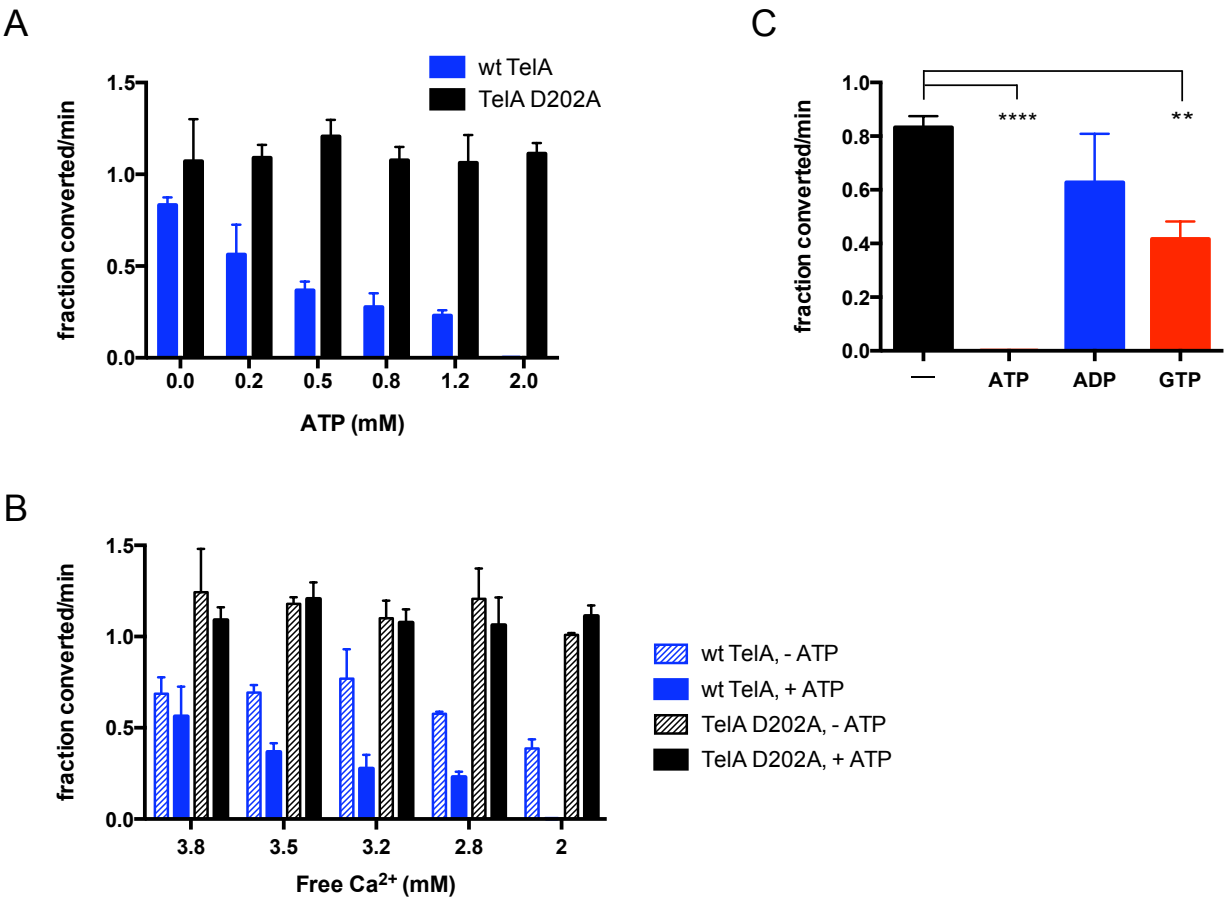

Figure 4.8. "ATP interference" of wt TelA promoted telomere resolution is ATP concentration dependent. For all experiments the mean and standard deviation of three separate experiments are shown. **(A)** Plots of telomere resolution initial rates *vs.* ATP concentration for wt TelA and the D202A mutant. These reactions were performed in the presence of 4 mM Ca^{2+}. **(B)** Plots of telomere resolution initial rates *vs.* unbound, free calcium in the reaction. These reactions were performed with or without ATP present in the buffer and 38 nM of wt TelA or TelA (D202A). **(C)** Plots comparing telomere resolution initial rates for wt TelA across various triphosphate conditions, including no ATP (–), 2 mM ATP, 2 mM GTP, or 2 mM ADP. These experiments were performed with 4 mM Ca^{2+} and 38 nM of TelA.

4.1.5. TelA can bind ATP

Having identified ATP as a seemingly potent inhibitor of TelA promoted telomere resolution, we sought to analyse whether TelA was capable of binding ATP and if so, whether a difference in binding affinity between the wildtype enzyme and its mutants could be responsible for their contrasting "ATP interference" phenotypes. We chose to use a technique called Surface Plasmon Resonance (SPR) to determine an ATP binding affinity for our enzyme. While primarily used for protein-protein or protein-nucleotide binding studies, a previous study had successfully implemented this technology for use in testing ATP binding affinities (Hirata et al., 2014), highlighting the potential in this technique. I performed multiple sets of experiments as previously described in the methods section to compare the ATP binding affinities of wildtype TelA and mutant TelA (D202A). I also performed a control set of experiments using *E. coli's*, LexA, a DNA-binding protein that does not bind ATP. However, LexA is not a perfect control for SPR, as its isoelectric point differs from TelA. LexA is slightly acidic with a pI of 6.2, while TelA is a basic protein with a pI of 9.4. Furthermore, we were limited by the equipment itself. Ideally, with a 4-channel system the experiment could be set up with a control channel (no protein bound), a channel with our protein of interest bound, and a third channel with LexA bound as a protein control. With this set up, the experiments for multiple proteins could be performed simultaneously. However, we only possessed a 2-channel system and with the constant necessity of a control channel (no protein bound) we were forced to perform each experiment individually. The SPR experiments revealed wildtype TelA and the D202A mutant to have comparable K_d values of 0.383 mM ± 0.003 and 0.299 mM ± 0.0106, respectively (Figure 4.9b). These data suggest that the difference in ATP's apparent interference of telomere resolution between the wildtype and D202A enzyme is not a result of differential ATP binding affinities. However, SPR experiments performed with LexA also generated a usable binding curve that suggested a K_d value of about half the previously determined ATP binding affinities (0.153 mM ± 0.0097) (Figure 4.9b). These data suggest that SPR is not the most reliable method for determining if a protein binds ATP. When an analyte binds to the ligand that is coupled to the chip, the change in mass is directly proportional to the change in resonance angle that is then measured by the machine. For this reason, SPR is not an ideal instrument for measuring the binding affinities of small molecules, as their masses are quite small and do not produce a significant change in resonance angle. This can be observed in Figure 4.9b. where the Signal

(uRIU) range of the y-axis is quite small, whereas with protein-protein or protein-nucleotide binding curves you would expect to see a range within the thousands. Furthermore, the type of binding that is observed is referred to as square wave (Figure 4.9a) and suggests a rapid association and dissociation of the analyte (ATP) that in itself is difficult to measure.

As an alternative method, we used a photoaffinity crosslinking approach to see if we could detect any ATP binding for TelA and its various mutants (TelA (107-442), TelA (D202A), TelA (R205A)). We once again included LexA in our experiments as a negative control. These experiments showed that while wildtype TelA, the D202A mutant, and the R205A mutant were capable of binding ATP, we see very little ATP binding to the N-terminal truncation mutant of TelA and no visible binding could be seen with the negative control (Figure 4.10). TelA appears to be capable of binding ATP, but we cannot conclude the ATP binding affinity of this enzyme with any certainty. However, the crosslinking experiments show similar levels of ATP binding among wildtype TelA and the two mutants (D202A and R205A) supporting the results from the SPR experiments that showed comparable ATP binding affinities for wt TelA and TelA (D202A). It is therefore unlikely that a difference in ATP binding affinity can account for the ATP interference of telomere resolution observed in wildtype TelA. Furthermore, the inconsistencies observed in TelA's ability to perform telomere resolution when replacing ATP with alternative nucleotides and ATP homologs (Figure 4.8c), and the differential effects observed with the presence of calcium verses magnesium (Figure 4.7c) in the buffer further support a more complex explanation than interference of TelA promoted telomere resolution through ATP binding alone.

A

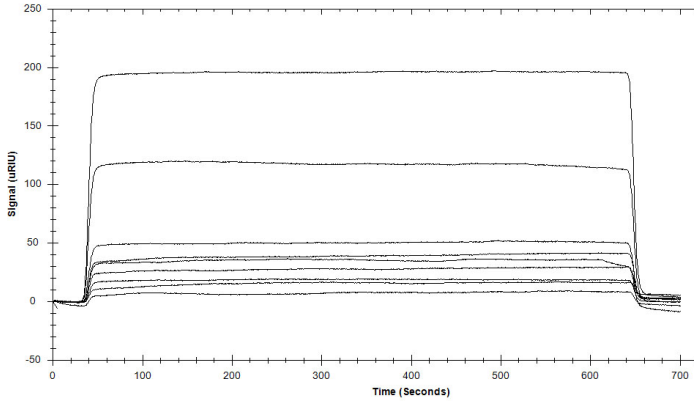

B

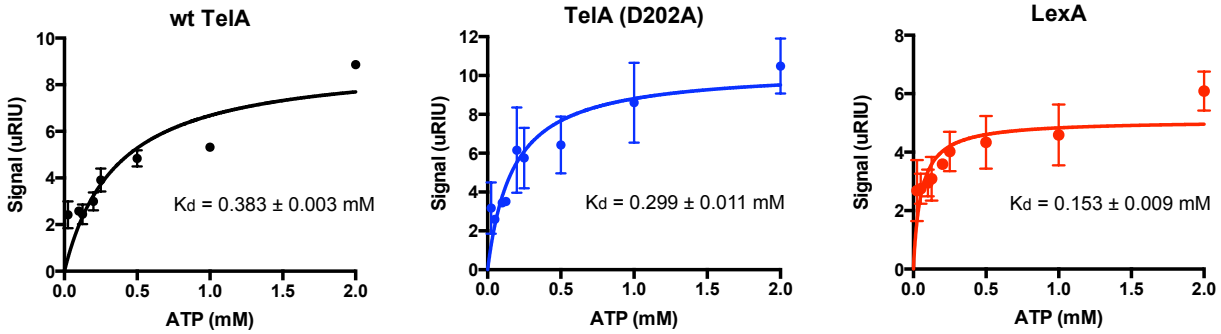

Figure 4.9. Using Surface Plasmon Resonance, wildtype TelA and TelA (D202A) display comparable ATP binding affinities. (A) A set of unprocessed wildtype TelA Surface Plasmon Resonance data. These data show the protein immobilized channel in the presence of running buffer with increasing concentrations of analyte (ATP). Each ATP concentration was tested in triplicate and each line shows a single representation of one concentration as a response (uRIU) against time. uRIU are microrefractive index units. **(B)** Affinity binding curves of wt TelA (black), TelA (D202A) (blue), and LexA (red) binding to ATP. For wt TelA and LexA the data points show the mean and standard deviation of triplicate trials. For TelA (D202A) the data points show the mean and standard deviation of duplicate trials. wt TelA: Bmax = 9.25; χ^2 = 0.836. TelA (D202A): Bmax = 9.53; χ^2 = 1.66. LexA: Bmax = 4.22; χ^2 = 0.454.

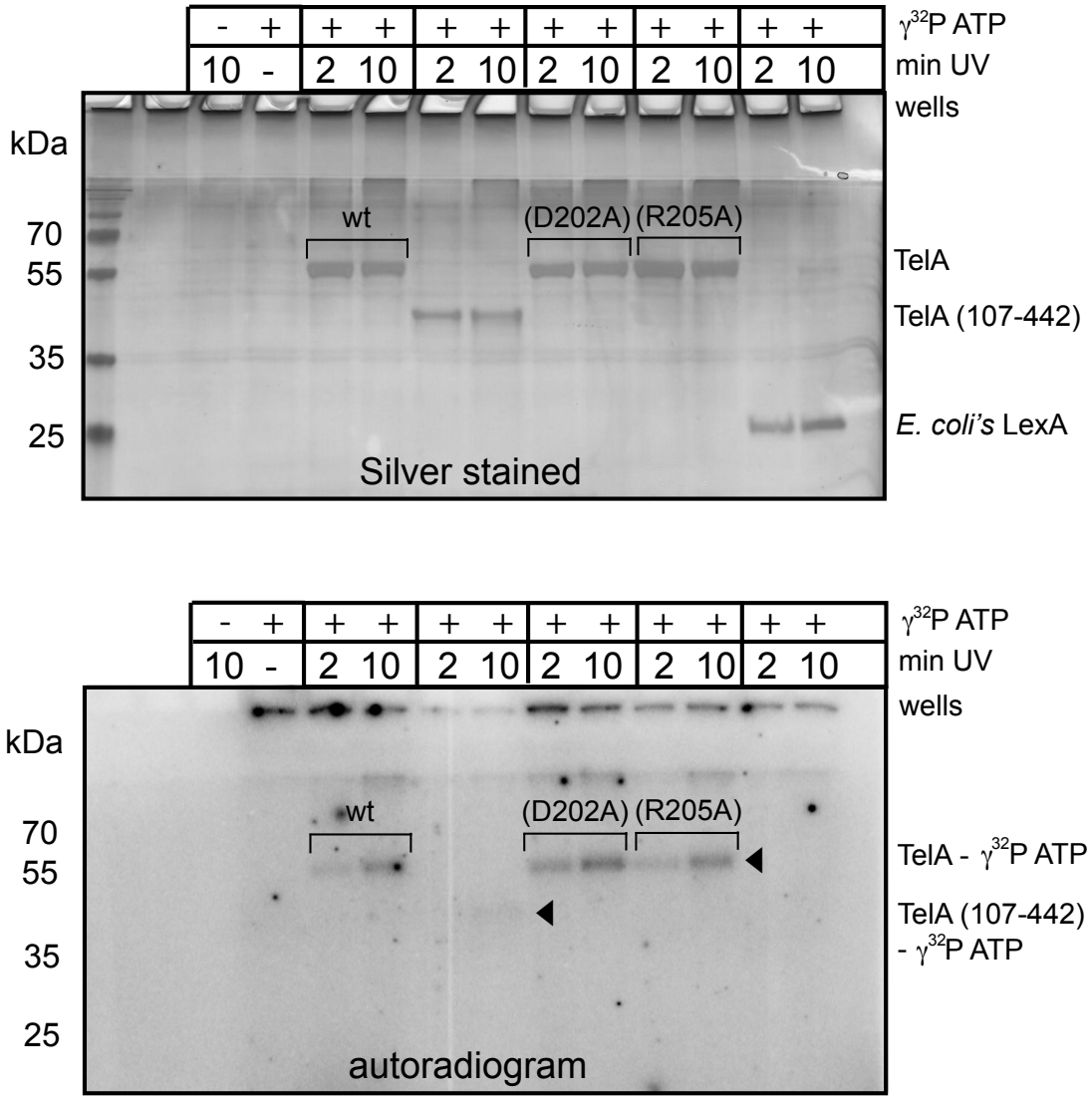

Figure 4.10. TelA can bind ATP. 15% SDS-PAGE gel analysis of ATP photoaffinity crosslinking assays for TelA, TelA (107-442), TelA (D202A), TelA (R205A), and LexA from *E. coli* as a control. The migration positions of wildtype (wt) TelA and its various mutants are shown as labelled on the silver stained gel. Any binding of γ^{32}P ATP to TelA that occurred can be visualized on the autoradiogram of the same gel as indicated with the labelling arrows.

4.1.6. Investigating the difference in "ATP interference" between TelA and ResT

As the binding of ATP to wt TelA did not prove a sufficient explanation for the observed "ATP interference" of TelA promoted telomere resolution, we began to search for alternative explanations. Notably, when previously characterizing the borrelial telomere resolvase, ResT, the Kobryn lab found that high energy cofactors such as ATP, as well as the poorly hydrolysable

ATP analog, ATPγS had no effect on ResT's ability to perform telomere resolution (Huang et al., 2017). The contrasting results between these two telomere resolvases lead us to examine the differences among the components of their *in vitro* reactions. Telomere resolution assays with ResT were performed using a constructed 50 bp *rTel* oligonucleotide substrate (Huang et al., 2017); whereas, a 36 bp *rTel* sequence cloned into pUC19 and linearized with SspI was used in telomere resolution assays for characterizing TelA (Figure 4.11a). The plasmid substrate used to characterize TelA contains an excess of non-target DNA from the plasmid backbone that is not present in the assays that use an oligonucleotide substrate. We hypothesized that the lack of "ATP interference" observed in ResT was due to the use of the oligonucleotide substrate, as opposed to the plasmid substrate used in TelA assays.

To test this hypothesis, we first looked at TelA's ability to perform telomere resolution on an oligonucleotide substrate more comparable to that used in telomere resolution assays with ResT (Figure 4.11b). Using similar buffer conditions to those optimized for plasmid telomere resolution assays we found, that similar to ResT, there was no discernable difference between conditions with and without ATP present using the oligonucleotide substrate (Figure 4.12ab). Furthermore, with the addition of equal nanomolar concentrations of pUC19 to the reaction to mimic the presence of a plasmid backbone and thus, of the abundance of non-target DNA present in the plasmid substrate, we could reproduce the inhibition observed when using the plasmid substrate; more inhibition was observed in the presence of ATP (Figure 4.12ab). We also examined TelA (D202A), previously shown to be hyperactive for telomere resolution with the plasmid substrate, and found it was still able to efficiently perform telomere resolution on the oligo substrate, even in the presence of non-target DNA (Figure 4.12cd). This is consistent with the apparent abolition of "ATP interference" afforded by mutation of the D202 residue under conditions using the plasmid substrate in the presence of calcium (Figure 4.7bc). Additionally, we can recapitulate this apparent ATP interference in ResT when alternatively using a plasmid substrate. Similar to TelA, ResT's ability to perform telomere resolution on a plasmid substrate, in the presence of Ca^{2+}, was inhibited by the addition of ATP to the reaction buffer (Figure 4.13).

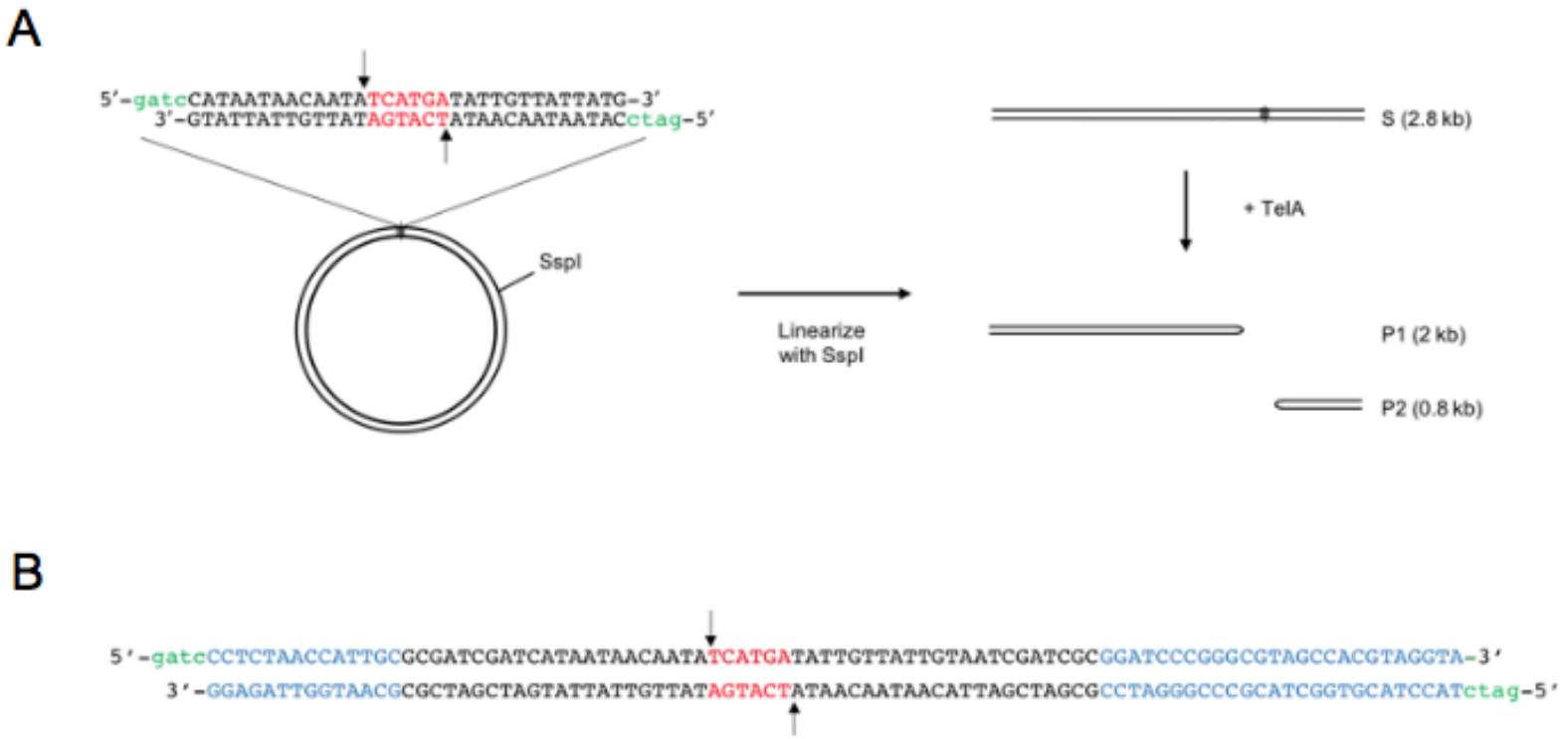

Figure 4.11. Plasmid *vs.* oligonucleotide substrate used for telomere resolution assays. (A) Full schematic of the inverted repeat 36 bp *rTel* sequence containing 5′ -gatc overhangs (green) cloned into pUC19. The nucleotides that form the two hairpins are in red with arrows indicating the position of the scissile phosphate being cleaved. The plasmid is linearized with SspI where indicated and with the addition of TelA produces two hairpin products (P1, P2). Conversion of the substrate to the two hairpin products can be visualized through ethidium bromide staining **(B)** Schematic of the oligonucleotide substrate used for telomere resolution. It contains the *rTel* sequence, represented in black with extensions of pUC19 sequence on either side (blue) to increase GC content, create asymmetrical cleavage, and for ease of annealing when assembling the substrate. The six nucleotides involved in hairpin formation are indicated in red with the scissile phosphates indicated by the arrows. The substrate is 5' radiolabelled on both strands to visualize product formation.

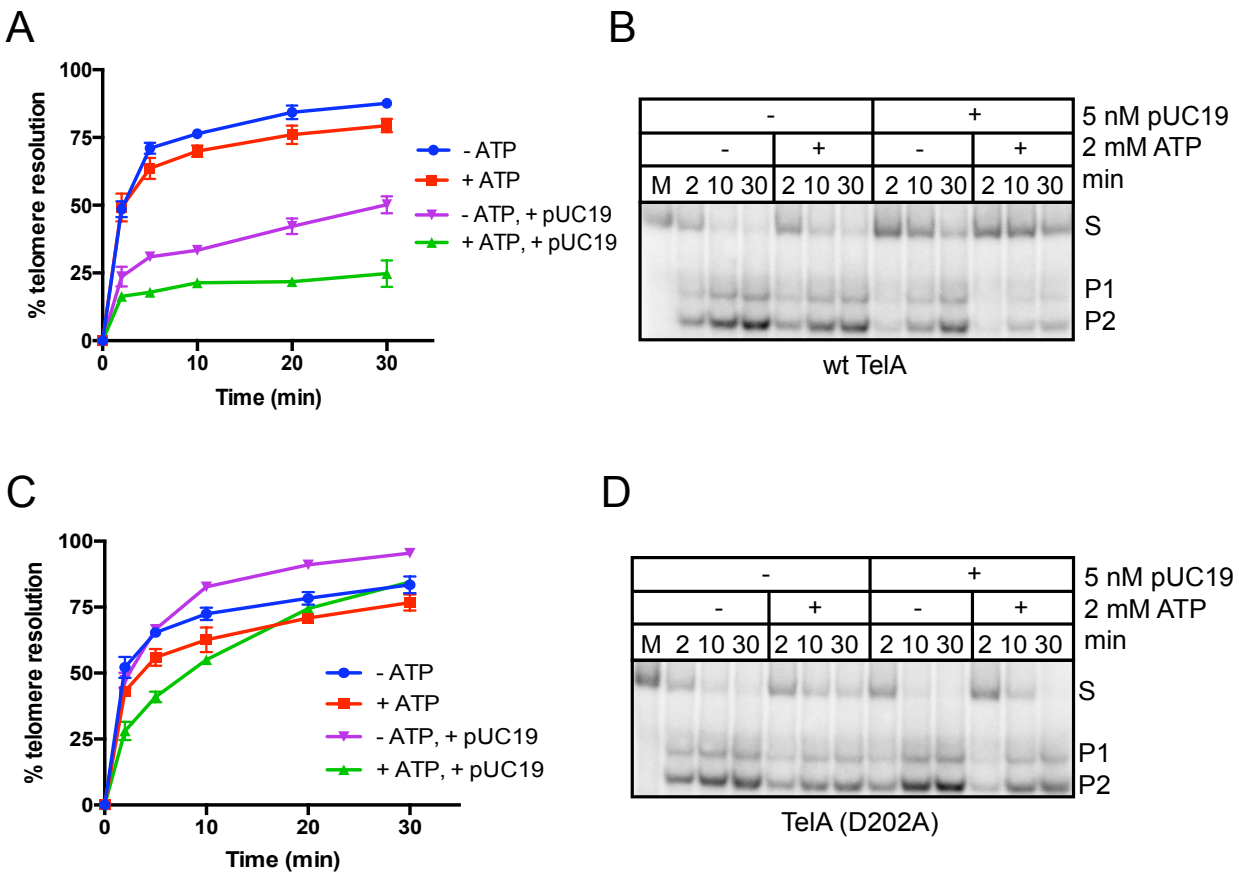

Figure 4.12. The ability of TelA to perform telomere resolution on an oligo substrate is inhibited in the presence of non-target DNA. (A, C) Plots of telomere resolution timecourses for 76 nM of (A) TelA and (C) TelA (D202A) performed in the presence of calcium, with or without 2 mM ATP and with or without the addition of 5 nM pUC19. All data is represented by the mean and standard deviation of three independent experiments. **(B, D)** 8% PAGE/ 1X TAE/ 0.1% SDS gel analysis of telomere resolution with 76 nM of (B) TelA and (D) TelA (D202A) performed at 30ºC in the presence of 4 mM calcium. The substrate is present at 5 nM and incubated with or without ATP and with or without 5 nM of pUC19.

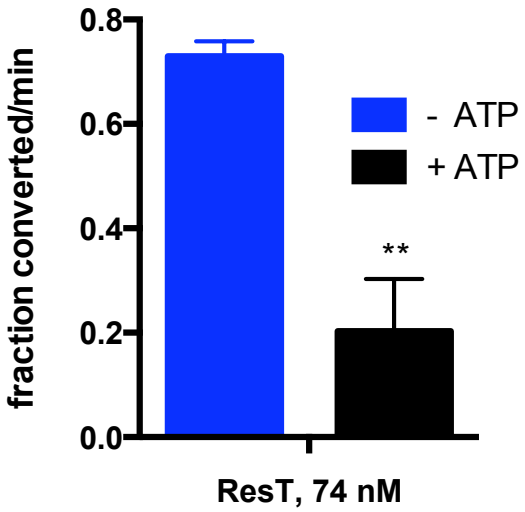

Figure 4.13. The ability of ResT to perform telomere resolution on a plasmid substrate is hindered in the presence of ATP. Summary plot of telomere resolution initial rates with 74 nM ResT at 37 ºC. Reactions were performed in the presence of 2 mM Ca^{2+} with or without the addition of 1 mM ATP. All rates were calculated as the mean and standard deviation of three independent experiments.

We hypothesized that ATP lowered TelA's affinity for its *rTel* sequence, and in the presence of an excess of non-target DNA (coming from the plasmid backbone) TelA is provided with many alternative binding sites and thus, ATP appears to inhibit telomere resolution in the plasmid substrate telomere resolution reactions. To test this, we examined TelA's affinity for its *rTel* under varying conditions, through a series of electrophoretic mobility shift assays (EMSA). A titration of TelA was incubated at 0°C with 1 nM of either a radiolabelled constructed *rTel* or a mock *rTel* (a construct in which the telomere sequence has been scrambled, but the inverted repeat sequence composition is maintained) in buffer similar to telomere resolution assays with the addition of 76 ng/mL of heparin sulphate to reduce non-specific binding. We compared wt TelA's affinity for its *rTel* to the mock *rTel* and found very little difference in binding affinity, but a difference in binding mode between the two substrates (Figure 4.14a). Furthermore, with both the *rTel* and the mock *rTel* we see a slight decrease in TelA's binding affinity for the substrate in the presence of ATP. This effect is most pronounced under conditions including the *rTel* substrate and 115 nM of TelA. Although slight, this reduction in TelA's affinity for its *rTel* in the presence of ATP could hinder the enzyme's ability to locate its substrate and perform telomere resolution, *in vitro*. In the presence of 115 nM TelA, the addition of a titration of

pUC19 to the reactions abolished TelA-*rTel* binding, as well as any binding observed with the mock *rTel* (Figure 4.14b). The stark effect produced by the addition of non-target DNA and the minimal difference between *rTel* and mock *rTel* binding affinities suggests that TelA does not possess a significant differential between its affinity for its *rTel* verses bulk DNA. A set of similar EMSAs were performed with TelA (D202A) and we found the mutant possesses a slightly higher affinity for its *rTel* as compared to wt TelA (Figure 4.15a). However, the D202A mutant displayed a similar inability to locate its *rTel* in the presence of an excess of non-target DNA, especially in the upper range of the pUC19 titration (Figure 4.15b).

Collectively, these data suggest that TelA has difficulty binding it's *rTel* in the presence of ATP where the difference in affinity between the *rTel* and non-target DNA is even lower than without ATP present. Although TelA (D202A) can still perform telomere resolution in the presence of non-target DNA, a slightly elevated affinity for its *rTel* cannot alone account for this phenotype and its *rTel* affinity is still significantly affected in the presence of non-target DNA. When characterizing this mutant, its telomere resolution activity was found to be hyperactive as well as less dependent on the present of a divalent metal ion (Figure 4.4, 4.6). This divalent metal ion independent telomere resolution activity was also observed, although more strongly, in our N-terminal truncation mutant and hypothesized to result from relieving autoinhibition in TelA through the removal of the N-terminal domain. As previously mentioned, the D202 residue of TelA is likely also involved in autoinhibition and mutation of this residue provides some relief from this regulatory mechanism. Perhaps TelA (D202A)'s slightly elevated affinity for its *rTel* combined with its partial independence from a divalent metal ion requirement are enough to overcome the presence of ATP while performing telomere resolution. However, in demonstrating such low affinity for its *rTel*, it is still unclear how wildtype TelA locates its substrate, *in vivo*. It is possible that the presence of a metal ion or some other factor guides the enzyme to its target. Alternatively, telomere resolution could be tethered to the metabolic status of the cell with the enzymatic function being repressed in an ATP-rich environment. These data may also help explain the observation that ResT is highly abundant at about 15, 000 monomers per cell, notably high for a protein with defined sites of action (Bandy et al., 2014). Perhaps the enzyme's low affinity for its substrate is compensated for by an overabundance of the enzyme being present in the bacterial cells. However, the relative abundance of TelA *in vivo* is currently unknown.

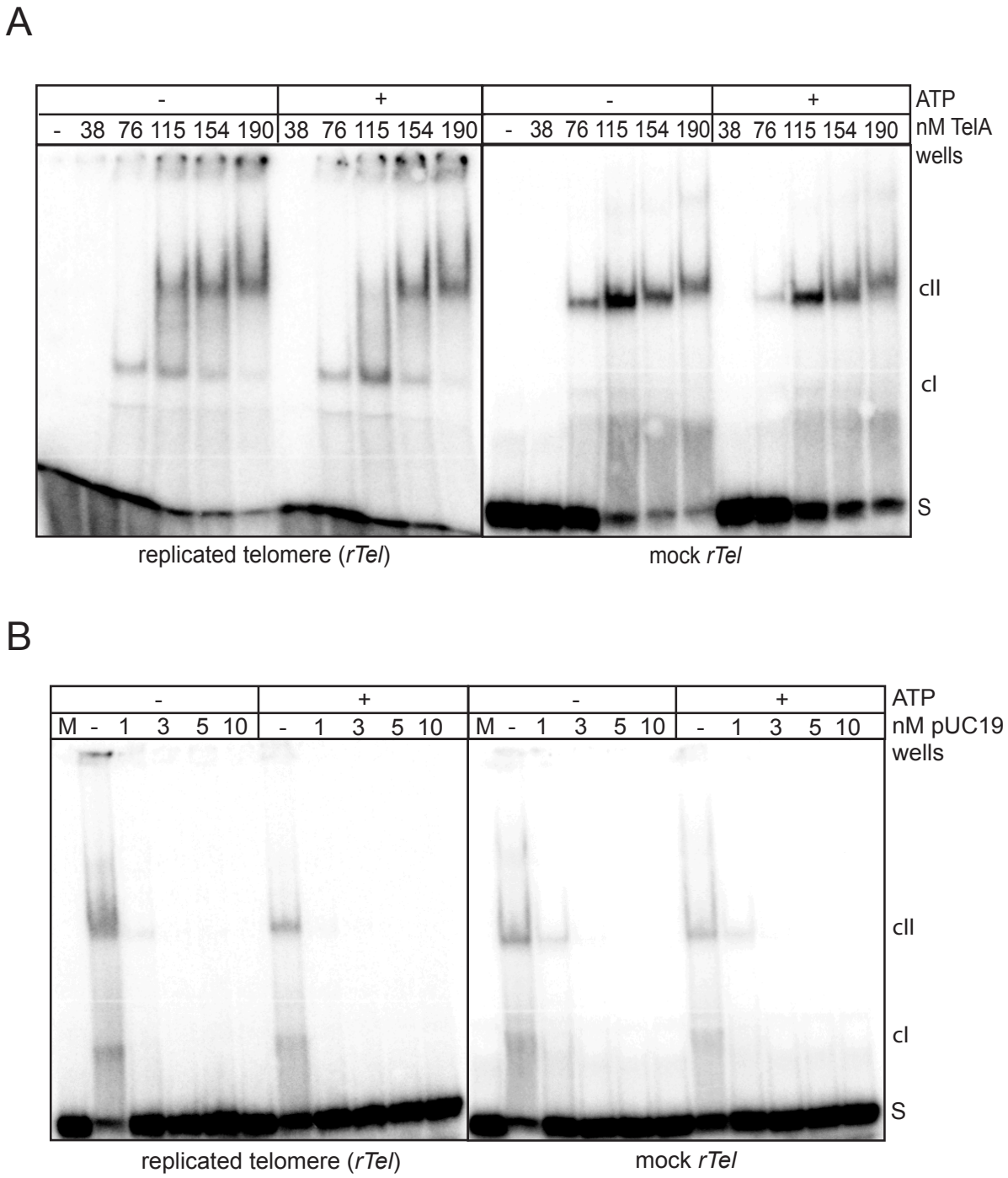

Figure 4.14. TelA displays a low differential between its affinity for its *rTel* sequence and non *rTel* sequences. 6% PAGE 0.5X TBE gel analyses of TelA incubated at 0ºC for 20 min with 1 nM of its assembled ^{32}P 5'-endlabelled *rTel* or a mock *rTel* (scrambled *rTel*). Heparin sulfate was present at 76 ng/mL to reduce non-specific binding **(A)** Binding reactions were performed with a titration of TelA with or without the addition of 2 mM ATP to the binding buffer. **(B)** Binding reactions were performed with 115 nM of TelA and a titration of pUC19, with or without the addition of ATP to the binding buffer.

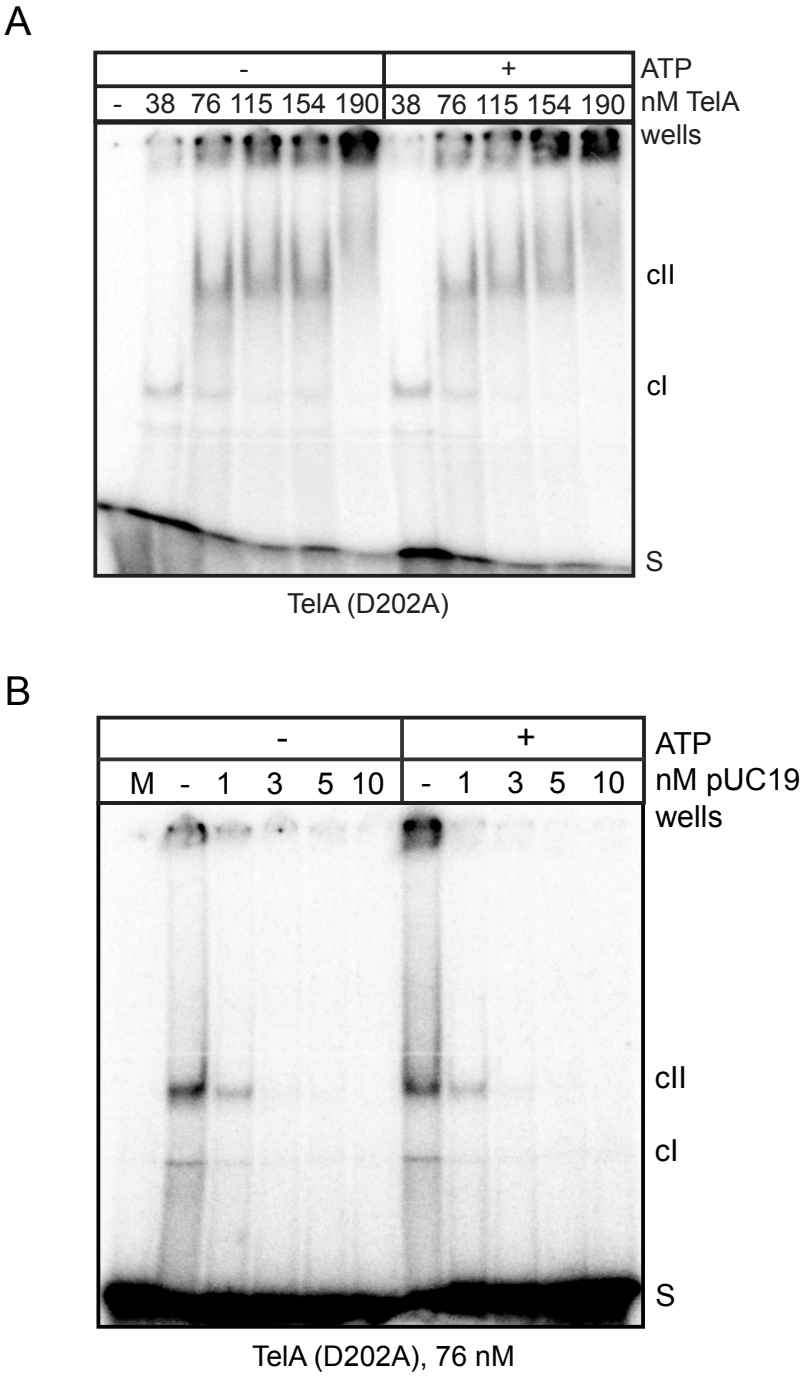

Figure 4.15. TelA (D202A) demonstrates a higher affinity for its replicated telomere than the wildtype enzyme. 6% PAGE 0.5X TBE gel analysis of TelA (D202A) incubated at 0ºC for 20 min with 1 nM of its assembled ^{32}P 5'-endlabelled *rTel*. Heparin sulfate was present at 76 ng/mL to reduce non-specific binding. **(A)** Binding reactions contained a titration of TelA (D202A) with or without the addition of ATP to the binding buffer. **(B)** Binding reactions were performed with 76 nM of TelA (D202A), with or without ATP and a titration of pUC19.

Summary Results for Section 4.1: Biochemical characterization of TelA promoted telomere resolution

- TelA promoted telomere resolution is stimulated in the presence of a divalent metal ion, with a preference for calcium (Figure 4.1).
- Truncation of the N-terminal domain of TelA relieves the enzyme of this divalent metal dependence (Figure 4.1). Mutation of the D202 residue partially relieves this dependence as well (Figure 4.6).
- TelA (D202A) and (R205A) display differential telomere resolution phenotypes, being hyperactive and hypoactive, respectively (Figure 4.4).
- TelA can bind ATP (Figure 4.10).
- TelA possesses a low differential between its affinity for its *rTel vs.* bulk DNA (Figure 4.14). ATP further reduces TelA's affinity for its *rTel*, giving ATP the appearance of being a potent inhibitor of telomere resolution, *in vitro* (Figure 4.7).
- TelA (D202A) appears to overcome this ATP interference of telomere resolution through possession of an elevated affinity for its *rTel* (Figure 4.15) and its semi-metal independence (Figure 4.6).

4.2. Does TelA promote DNA annealing and ATP-dependent DNA unwinding?

4.2.1. Annealing activity

4.2.1.1. TelA can promote the annealing of complementary ssDNA

We chose to continue our biochemical characterization of TelA by next examining it's potential multifunctionality. Having established that the borrelial enzyme, ResT, was capable of annealing complementary ssDNA (Mir et al., 2013) , we sought to determine if TelA possessed a similar activity. To test for annealing properties, we used two complementary 87 nucleotide strands with 26% GC content and 5'-GATC overhangs (see Table 3. or (Mir et al., 2013)). One strand was radiolabelled and the conversion of ssDNA into the annealed product was visualized by a shift in the migration of the bands on a polyacrylamide gel (Figure 4.16b). Buffer conditions similar to those optimized for telomere resolution were used including the presence of Ca^{2+} ions in the buffer. We found that TelA was capable of annealing complementary ssDNA above the spontaneous rate (Figure 4.16bc). An analysis of TelA's concentration dependence on annealing rate revealed a non-linear response in which a TelA concentration between 75 and 100 nM produced a half maximal annealing rate. Additionally, TelA was able to anneal plasmid DNA into a unit-length duplex (Figure 4.17). Although we can visualize some plasmid length annealing, much of the product remains in the wells and likely represents a network of partially annealed substrate. This remained true over a variety of conditions and TelA concentrations (data not shown).

We also examined TelA (Y405F), proven to be deficient in telomere resolution, for potential annealing activity and found it was capable of annealing ssDNA with a response curve comparable to that of the wildtype enzyme (Figure 4.16c). These data suggest TelA (Y405F) displays separation-of-function potential by being deficient for telomere resolution while still maintaining annealing activity comparable to that of the wildtype enzyme.

4.2.1.2 The deletion of the N-terminal domain of TelA produces an annealing deficient mutant

We also included an N-terminal truncation mutant of TelA in our analysis of annealing activity. The N-terminal domain of TelA was shown to be expendable for telomere resolution suggesting the N-terminal domain may have other functions (Figure 4.1c and (Huang et al., 2012)). We found that deletion of the N-terminal domain abolished TelA's ability to anneal

complementary ssDNA over the spontaneous rate (Figure 4.16bc). This was true over a wide TelA (107-442) concentration range, suggesting the N-terminal domain to be essential for annealing activity. A similar truncation was constructed in ResT, ResT (163-449), however this mutant while inactive for annealing also did not retain its telomere resolution activity (Huang et al., 2017; Mir et al., 2013; Tourand et al., 2007). Therefore, it does not represent the same separation of function demonstrated by TelA (107-442).

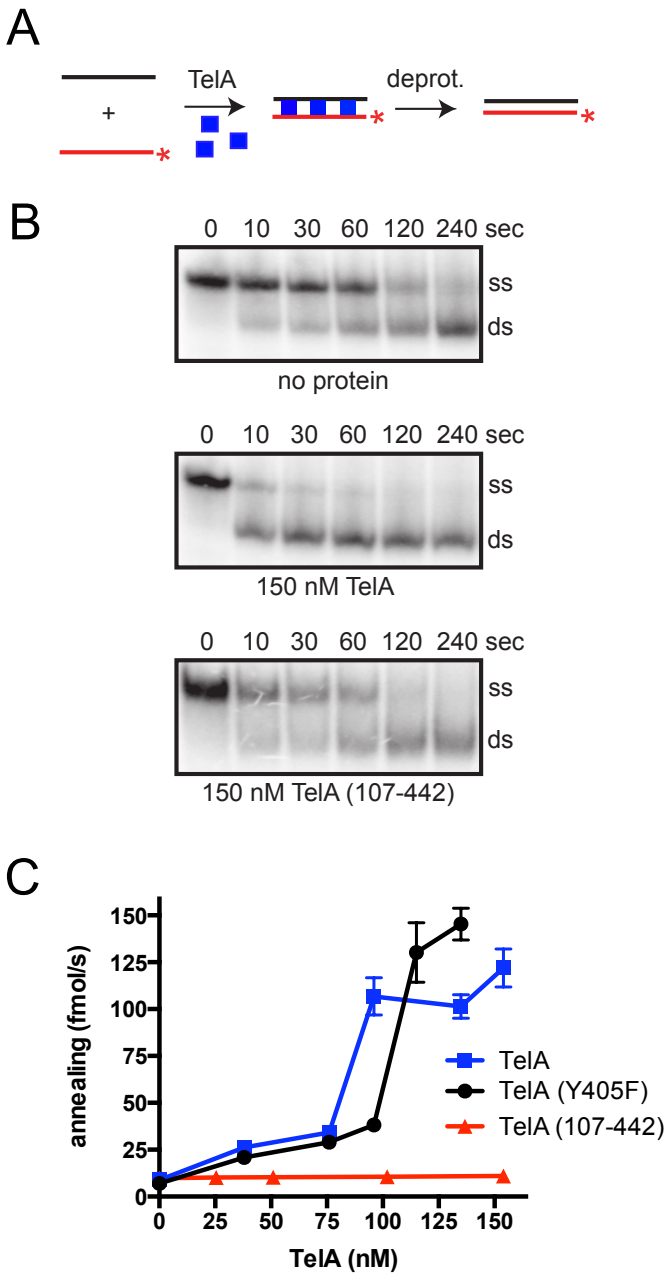

Figure 4.16. TelA promotes the annealing of complementary ssDNA. (A) Schematic of the annealing assay. The tested complementary DNA strands (OGCB455 and 456) anneal into an 83 bp duplex product with 5' GATC overhangs (Table 3). The 5'-^{32}P labelled reporter strand is shown in red while the complementary, unlabeled, strand is shaded black, TelA is represented by blue squares. The red asterisk represents the 5'-^{32}P endlabel. **(B)** 8% PAGE/ 1X TAE/ 0.1% SDS gel panels of timecourse annealing reactions, including spontaneous annealing (no protein), wt TelA, and TelA (107-442). The migration positions on the gel are labelled as the reporter oligonucleotide (ss) and the duplex product (ds). **(C)** A plot of annealing rates *vs.* TelA concentration comparing wt TelA, TelA (Y405F), and TelA (107-442). The mean and standard deviation are shown and are derived from three independent experiments.

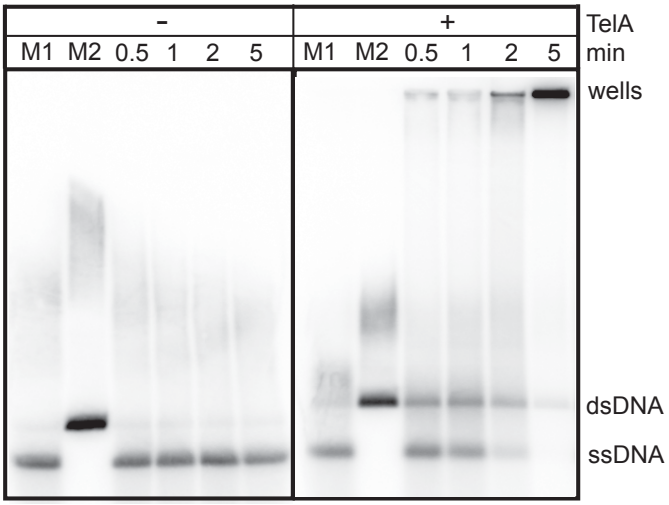

Figure 4.17. TelA can anneal plasmid length DNA. 0.7% agarose 1X TAE gel panels showing plasmid annealing reactions. The migration patterns of heat denatured pUC19 (ssDNA) and the unit-length plasmid duplex (dsDNA) are labelled as shown. Reaction timepoints and the presence or absence of reaction components are indicated in the key above the gel. 76 nM of TelA was incubated with 1.78 mM nucleotides of the plasmid substrate in buffer containing 25 mM HEPES (pH 7.6), 2 mM $MgCl_2$, 1 mM DTT, 100 μg/mL BSA and 50 mM potassium glutamate. The pUC19 was linearized and ^{32}P endlabelled as described in the methods section.

4.2.2. ATPase and unwinding activities

4.2.2.1. TelA appears to be active as a ssDNA-dependent ATPase

Our examination of the telomere resolution properties of TelA uncovered an unexpected inhibitory effect of ATP, and we subsequently demonstrated through photoaffinity crosslinking that TelA appeared to bind ATP as well. The characterization of the borrelial telomere resolvase, ResT, revealed similar ATP binding properties that were indicative of the enzyme's ATPase and unwinding activities. We sought to identify whether TelA was capable of hydrolyzing ATP as well. To test for ATPase activity in TelA, the conversion of γ-^{32}P ATP to ADP and free γ-^{32}P phosphate was monitored at 30°C in the presence of 10 μg/mL ϕx174 DNA effectors and visualized with polyethyleneimine thin-layer chromatography (Figure 4.18b). We found that TelA appeared to possess a ssDNA-dependent ATPase activity (Figure 4.18c) with a specific activity of 7.45 pmol/min/pmol of enzyme (Figure 4.18d), comparable to that of a weak DNA helicase or an RNA helicase (Huang et al., 2017; Salman-Dilgimen et al., 2013). In comparison, the N-terminal truncation mutant of TelA appeared to have slightly hypoactive ATPase activity, with a specific activity of about half of wildtype TelA (3.68 pmol/min/pmol of enzyme) (Figure 4.18d). TelA's ATPase activity was shown to be dependent upon the presence of Mg^{2+} ions in the buffer, as expected. Notably, the enzyme can bind ATP without a divalent metal ion present (Figure 4.10). ATP hydrolysis could be supported to a lesser extent by the presence of manganese in the buffer; calcium could not support ATP hydrolysis (data not shown).

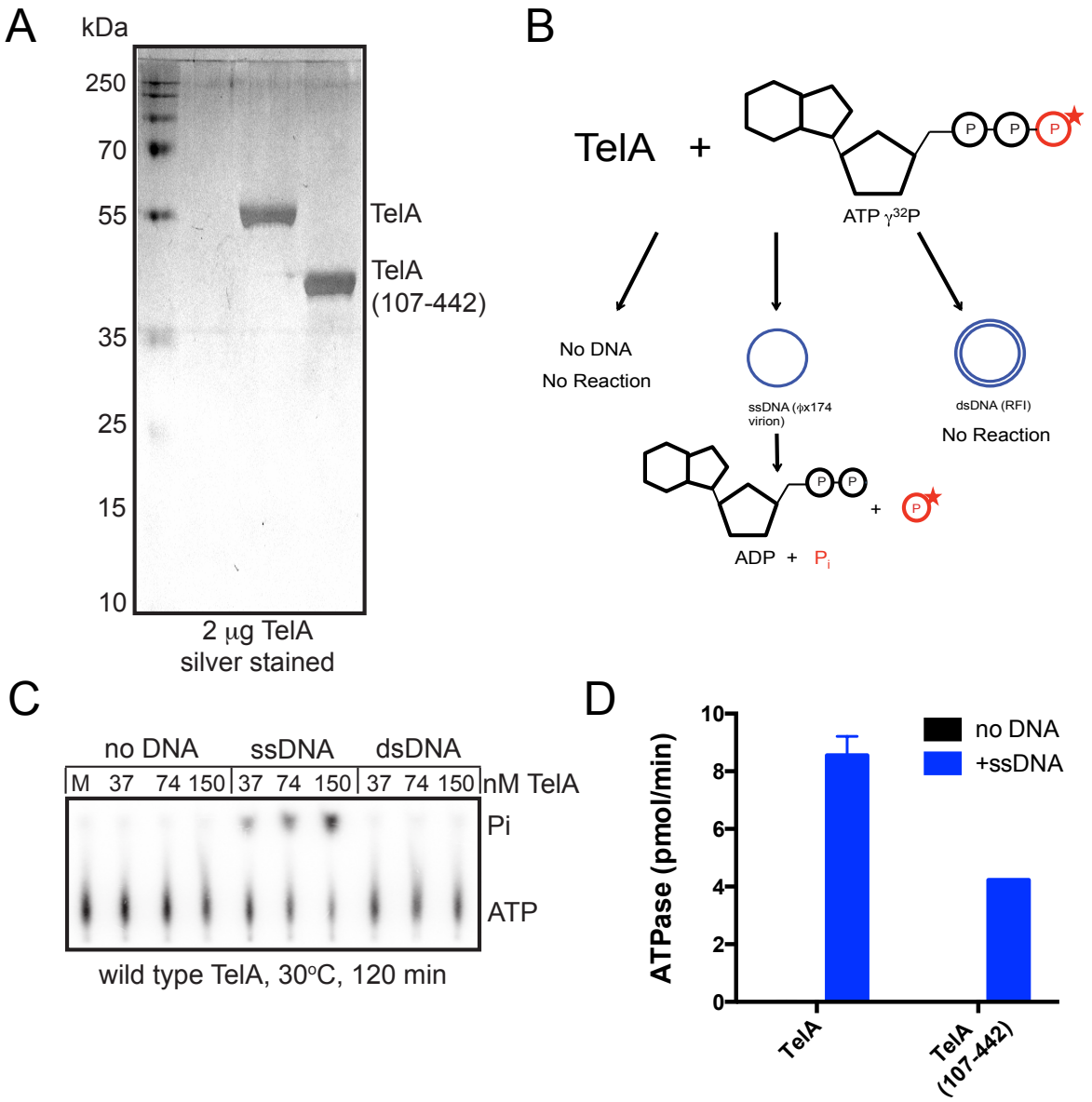

Figure 4.18. TelA possesses a ssDNA-dependent ATPase activity. (A) 15% SDS-PAGE analysis of 2 µg of TelA and TelA (107-442), visualized by silver staining. A molecular weight marker was loaded with one lane separation from the samples and labelled to the left of the gel. **(B)** A schematic of the ATPase assay. In the presence of a ssDNA effector (ϕX174 virion) γ-^{32}P ATP can be hydrolysed, converting it into ADP and γ-^{32}P phosphate. **(C)** Polyethyleneimine thin-layer chromatography result for ATPase assays with wildtype TelA. DNA effectors were present at 10 µg/mL using either no DNA, ϕX174 virion (ssDNA), or ϕX174 RFI DNA (dsDNA). **(D)** Summary of ATPase results -/+ ϕX174 virion DNA (ssDNA) for 74 nM wildtype TelA and TelA (107-442). The average and standard deviation are a representation of three independent experiments.

4.2.2.2. TelA appears to be active on a variety of unwinding substrates

The presence of ssDNA-dependent ATPase activity in enzymes is often correlated with the possession of helicase-like properties. As ResT was unexpectedly found to have unwinding activity despite its lack of signature helicase motifs in its primary sequence (Huang et al., 2017), we sought to identify whether TelA also possesses a similar type of activity. We first tested TelA for a DNA unwinding activity using a polarity substrate. This substrate contained two 26 bp duplexed regions separated by a 74 nt single-stranded gap; either end of the partial duplex was alternatively radiolabelled to identify a potential polarity bias of any DNA unwinding that may occur (Figure 4.19). As we were aware of TelA's annealing activity, an excess of the unlabelled reporter strand was added to one set of these experiments to identify whether a strong annealing capacity could be masking any potential unwinding activity. We found that TelA was capable of unwinding the polarity substrate with a 3'-5' polarity bias, in respect to the single-stranded portion of the substrate (Figure 4.19). This unwinding activity was dependent on both the presence of Mg^{2+} and ATP in the buffer, as well as the hydrolysis of ATP (unwinding was not observed in the presence of the poorly hydrolysable ATP analog, ATP γS, data not shown). TelA was also shown to be able to unwind other types of substrates including synthetic replication forks and strand invasion intermediates like D-loop mimics (data not shown). One activity that TelA was not able to perform that was observed in ResT was fork regression, an activity that requires concerted annealing and unwinding (Huang et al., 2017).

4.2.2.3. TelA's annealing and unwinding activities appear to have different concentration optima

Given that TelA appeared to possess the ability to both unwind and anneal DNA, but could not perform fork regression, we thought perhaps these two activities could be in competition with one another. To test this, we annealed a substrate that could also be unwound by TelA, a partially duplexed substrate with a 50 nt-3'-tail (OGCB666*/692, see Table 3). We conducted both annealing and unwinding reactions over a large concentration range of TelA, with or without ATP present in the buffer (Figure 4.20a). In conditions lacking ATP, TelA was unable to unwind the 3'-partial duplex, but readily annealed the two strands. The annealing *vs.* TelA concentration profile demonstrated a linear relationship with complete annealing by 76 nM of TelA (Figure 4.20b). However, with ATP present in the buffer TelA readily unwound the

substrate at lower protein concentrations, with optimum activity between 37 and 115 nM of TelA. At TelA concentrations greater than 150 nM, the annealing reaction appeared to be completely dominant (Figure 4.20b). These data suggest that in the presence of ATP these two activities have different concentration optima. Notably, when examining the unwinding *vs.* TelA (107-442) concentration profile it showed that without the ability to anneal complementary ssDNA the unwinding reaction was able to move to completion at higher TelA (107-442) concentrations. The N-terminal truncation mutant also appears to be slightly hypoactive for the unwinding activity, consistent with the ATPase results for this mutant (Figure 4.20c).

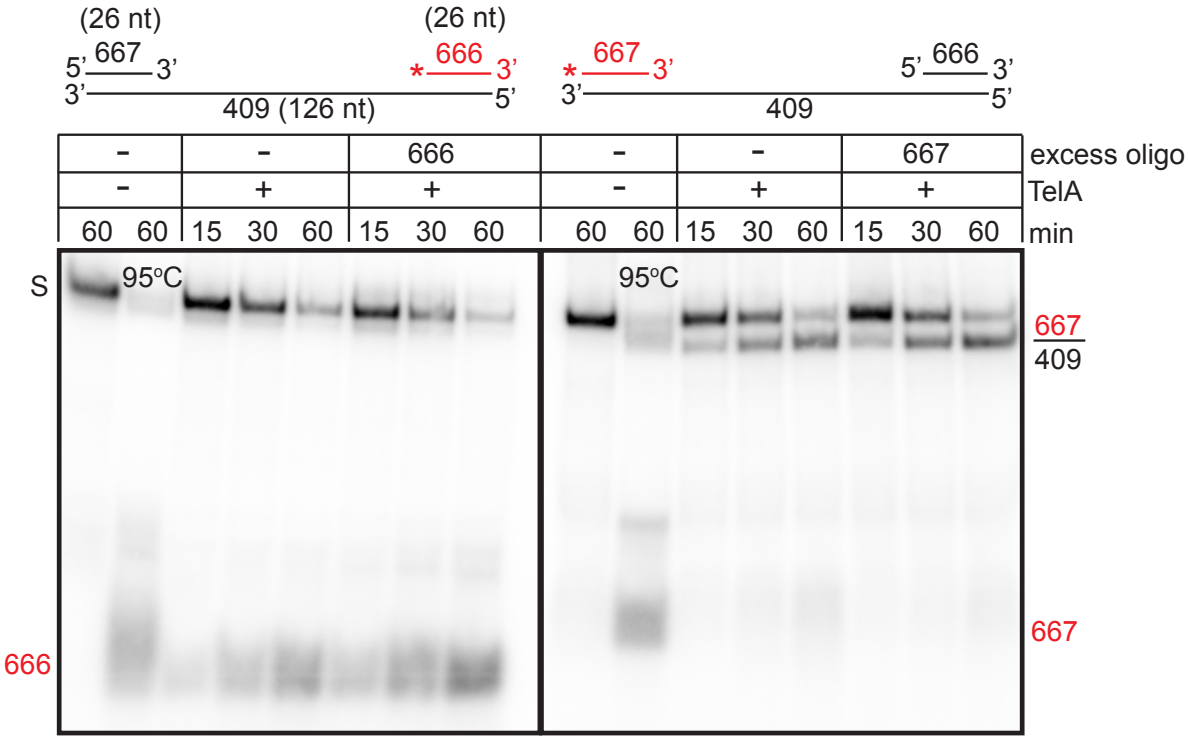

Figure 4.19. TelA appears to unwind DNA with 3'-5' polarity bias. 8% PAGE/ 1X TAE/ 0.1% SDS gel analysis of DNA unwinding polarity. In the substrate schematics above the DNA strands that are 5'-radiolabelled are indicated in red and with an asterisk, unlabeled strands are shown in black. Also indicated is the name and length of the oligonucleotides used to assemble the substrates. The gel migration position of displaced 666 strand and the partial duplex product 667/409 are shown to the right of the gel. S, indicates the gel migration position of the full substrate. The 95°C lane shows a substrate that has been heat denatured prior to loading. Unwinding reactions were performed in a buffer containing ATP and were either performed with 38 nM TelA and 15 nM substrate DNA, alone, or supplemented with 45 nM unlabeled 666 or 667 oligonucleotide to prevent reannealing of any displaced labeled strand. This eliminates differential reannealing ability from the interpretation of unwinding polarity results.

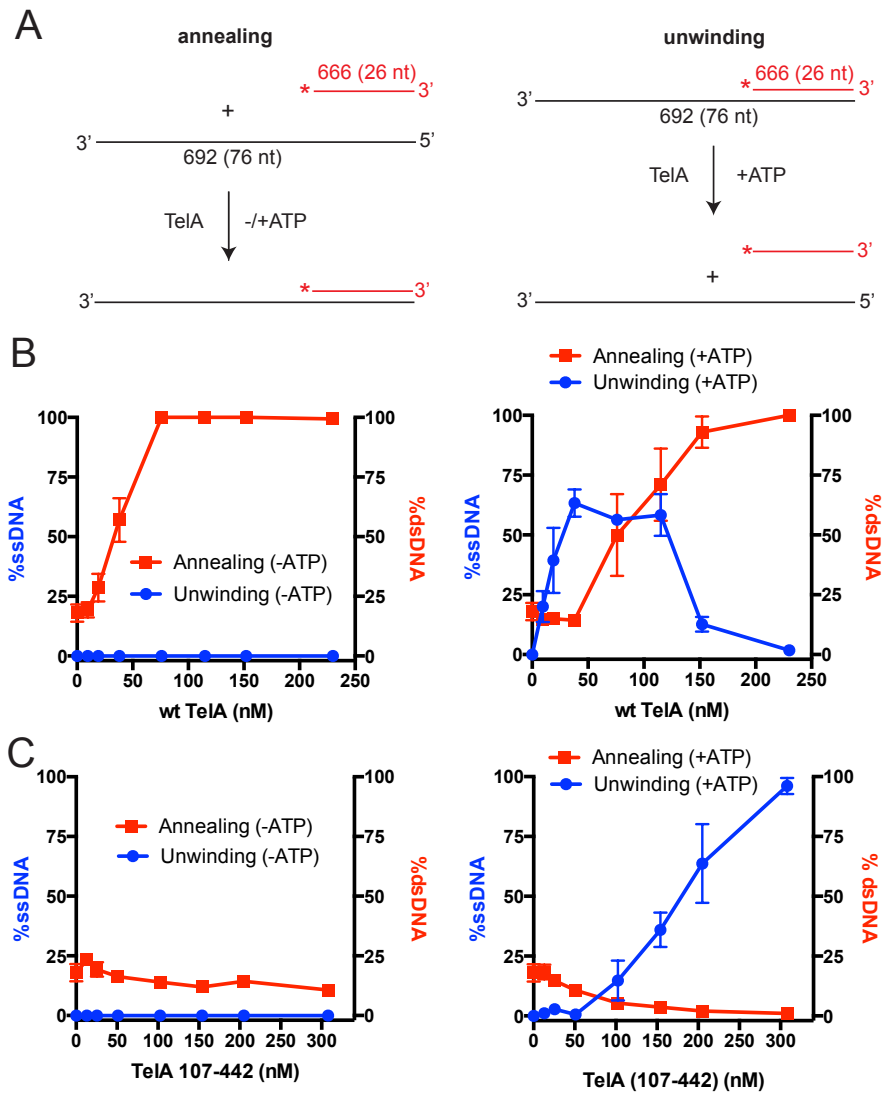

Figure 4.20. TelA's annealing and unwinding activities have different concentration optima. (A) Schematic of the substrates and reactions performed to compare TelA concentration optima of annealing and unwinding reactions using substrates that TelA can both anneal or unwind. For annealing reactions, the 26 nt OGCB666 oligonucleotide is 5'-^{32}P endlabelled and mixed with a 76 nt cold partner oligonucleotide (OGCB692) that can anneal into a partial duplex DNA with a 50 nt 3'-tail. For the unwinding reactions a 666*/692 substrate previously annealed by heat denaturation/renaturation is used and dissociation of the labeled 666* strand from the partial duplex is followed via gel analysis. **(B, C)** Plots of % ssDNA and % dsDNA (secondary y-axis) *vs.* TelA concentration (nM) in the absence or presence of ATP. Reactions for wildtype TelA (B) and TelA (107-442) (C) are shown. Unwinding reactions are represented by % ssDNA (blue) and annealing reactions are represented by % dsDNA (red). Spontaneous annealing accounts for about 20% of the conversion to dsDNA and is represented by the protein-free reaction of the y-axis intercept. The average and standard deviation are shown and are derived from three independent experiments.

4.2.2.4. Attempting to identify unwinding separation-of-function mutants: Characterization of TelA (S238A) and (R318A)

TelA's apparent telomere resolution, complementary ssDNA annealing, and ATP-dependent unwinding activities suggested a multifunctionality similar to the borrelial telomere resolvase, ResT. However, these annealing and unwinding properties still had no known *in vivo* function. Having established a promising annealing separation-of-function mutant in the N-terminal truncation mutant of TelA for future *in vivo* studies and separating TelA's telomere resolution activity from its annealing with TelA (Y405F), we moved forward trying to identify a separation-of-function mutant for TelA's apparent unwinding activity. We identified TelA residues S238 and R318 as both highly conserved, but not part of the telomere resolution active site from an alignment of the most diverse telomere resolvase domain containing proteins, as identified by the conserved domain database (CDD) (Figure 4.21). Mutation, overexpression and subsequent purification of these two mutants (see Methods section and Table 1 for details) revealed promising preliminary results. Both TelA (S238A) and (R318A) appeared to be significantly compromised for ATPase and unwinding activities, while maintaining their ability to perform telomere resolution and anneal ssDNA *in vitro* (Figure 4.22). However, an attempt to characterize mutants of equivalent residues in ResT showed inconsistent results. While ResT (S182A) still appeared deficient for unwinding activity, ResT (R253A) displayed significantly hyperactive unwinding activity in comparison to wt ResT (Figure 4.23). Furthermore, characterization of a TelA double mutant, S238A/R318A showed further inconsistencies. TelA (S238A/R318A) displayed increased unwinding activity as compared to the two single mutants, a puzzling result for combining two significantly compromised unwinding mutants (Figure 4.22b). This double mutant displayed similar telomere resolution capabilities as the two single mutants, as well as a decreased annealing capacity in comparison (Figure 4.22ac).

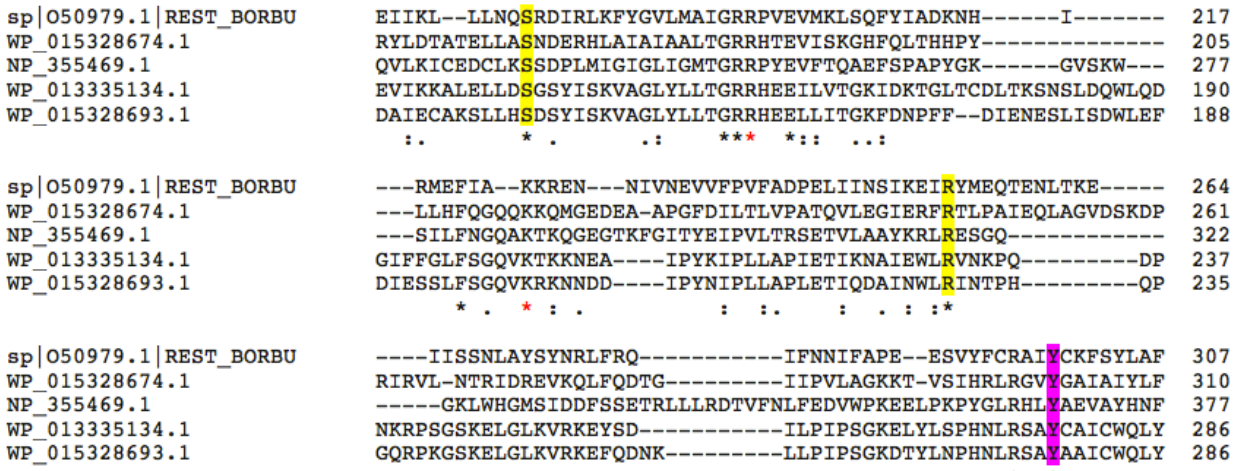

Figure 4.21. Conserved Domain Database (CDD) alignment of telomere resolvase domain containing proteins (pfam 16684). A section of a full multiple sequence alignment of telomere resolvase domain containing proteins as defined by the CDD (pfam 16684) using the greatest diversity setting. This alignment was performed with full protein sequences. Accession numbers: O50979.1, ResT from *Borrelia burgdorferi*; WP_015328674.1, hypothetical protein from cyanobacteria; NP_355469.1, TelA from *Agrobacterium tumefaciens* C58; WP_013335134.1, hypothetical protein from *Cyanothece sp.* PCC 7822; WP_015328693.1, hypothetical protein from *Stanieria cyanosphaera*. Conserved residues highlighted in yellow indicate the position of the two potential ATPase/unwinding separation-of-function mutants. The conserved residue highlighted in pink indicates a mutant we could not construct in TelA (Marchler-Bauer et. al., 2015).

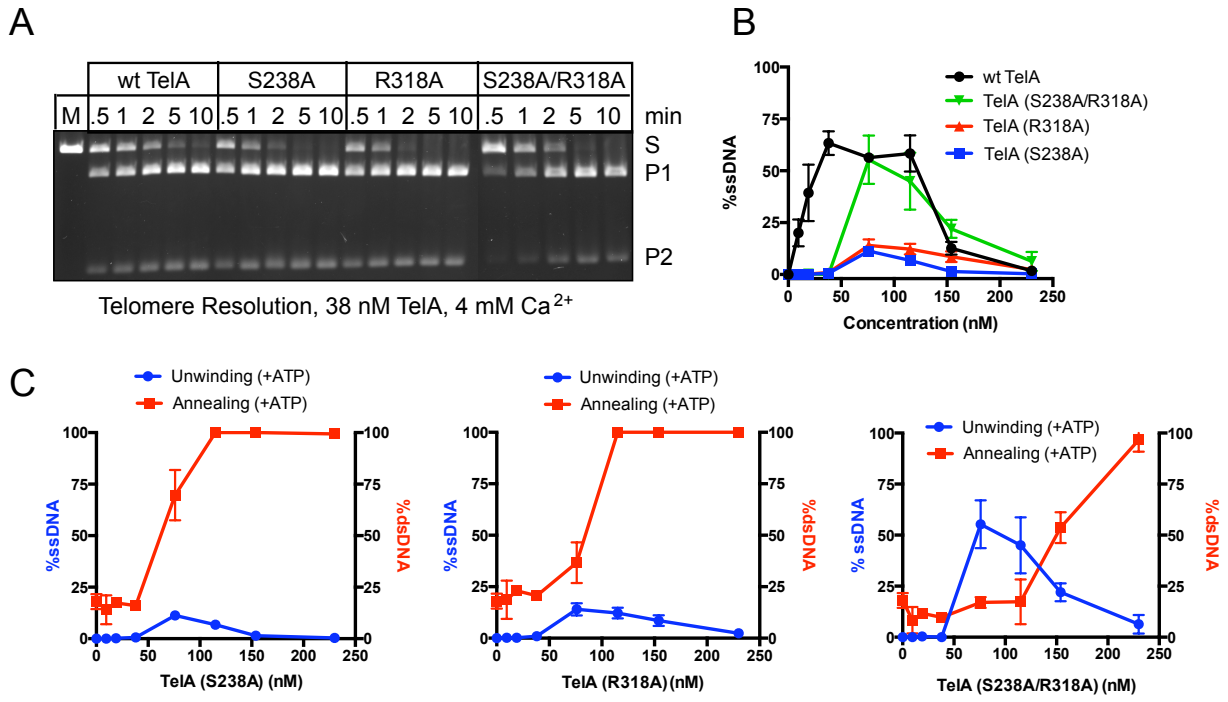

Figure 4.22. TelA single mutants, S238A and R318A display contradicting phenotypes to a double mutant (S238A/R318A) of both residues. (A) 0.8% agarose 1X TAE gel analysis of telomere resolution timecourses for wt TelA, TelA S238A, TelA R318A, and the double mutant TelA S238A/R318A. TelA was present at 38 nM, with 4 mM Ca^{2+} and incubated at 30°C. This figure is a combination of two separate gel panels. **(B)** % ssDNA *vs.* TelA concentration (nM) analysis comparing wt TelA, TelA S238A, TelA R318A and TelA S238A/R318A. **(C)** Plots of % ssDNA and % dsDNA (secondary y-axis) *vs.* TelA concentration (nM) for TelA S238A, TelA R318A and TelA S238A/R318A. Unwinding reactions are represented by % ssDNA (blue) and annealing reactions are represented by % dsDNA (red). Spontaneous annealing accounts for about 20% of the conversion to dsDNA and is represented by the protein-free reaction of the y-axis intercept. The average and standard are shown and are derived from three independent experiments.

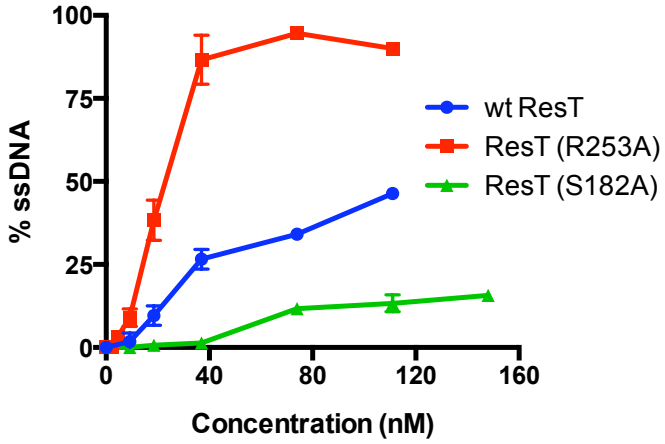

Figure 4.23. Equivalent potential unwinding separation-of-function mutants in ResT display conflicting phenotypes to their TelA counterparts. Plots of % ssDNA *vs.* ResT concentration (nM) comparing wt ResT, ResT (S182A), and ResT (R253A).

As we grew more concerned over the inconsistencies surrounding our potential unwinding separation-of-function mutants, we attempted to repurify TelA (S238A), the more seemingly promising of the two TelA unwinding mutants. Following our original purification protocols, we continuously encountered obstacles in lysate preparation. The lysate produced for this mutant was gluey and it was difficult to separate the soluble portion for loading onto the Ni-NTA affinity column. Despite many modifications to the lysate making procedure to try to recover a larger soluble portion for loading, we encountered little success. Over our variety of purification attempts, experiments using the resulting TelA (S238A) preparations displayed varying levels of apparent unwinding activity ranging from wildtype comparable to hyperactive, with no observable consistency among protein preparations. In addition, TelA appeared to lack many other unwinding-centric properties that were observed in ResT. ResT displayed the ability to perform fork regression (Figure 4.24) while TelA could not (data not shown), suggesting TelA's apparent annealing and unwinding activities could not function in a collaborative manner. Furthermore, these activities appeared to be in competition with one another when presented with a substrate that could be both unwound and annealed (Figure 4.20). TelA also failed to demonstrate ATP-mediated dimerization, nor could it transfer the phosphate group from ATP to itself, despite these activities being present in ResT (unpublished data, (Huang et al., 2017)). In combination, these results heightened our suspicions of not just the validity of our unwinding mutants, but TelA apparent unwinding activity, in general.

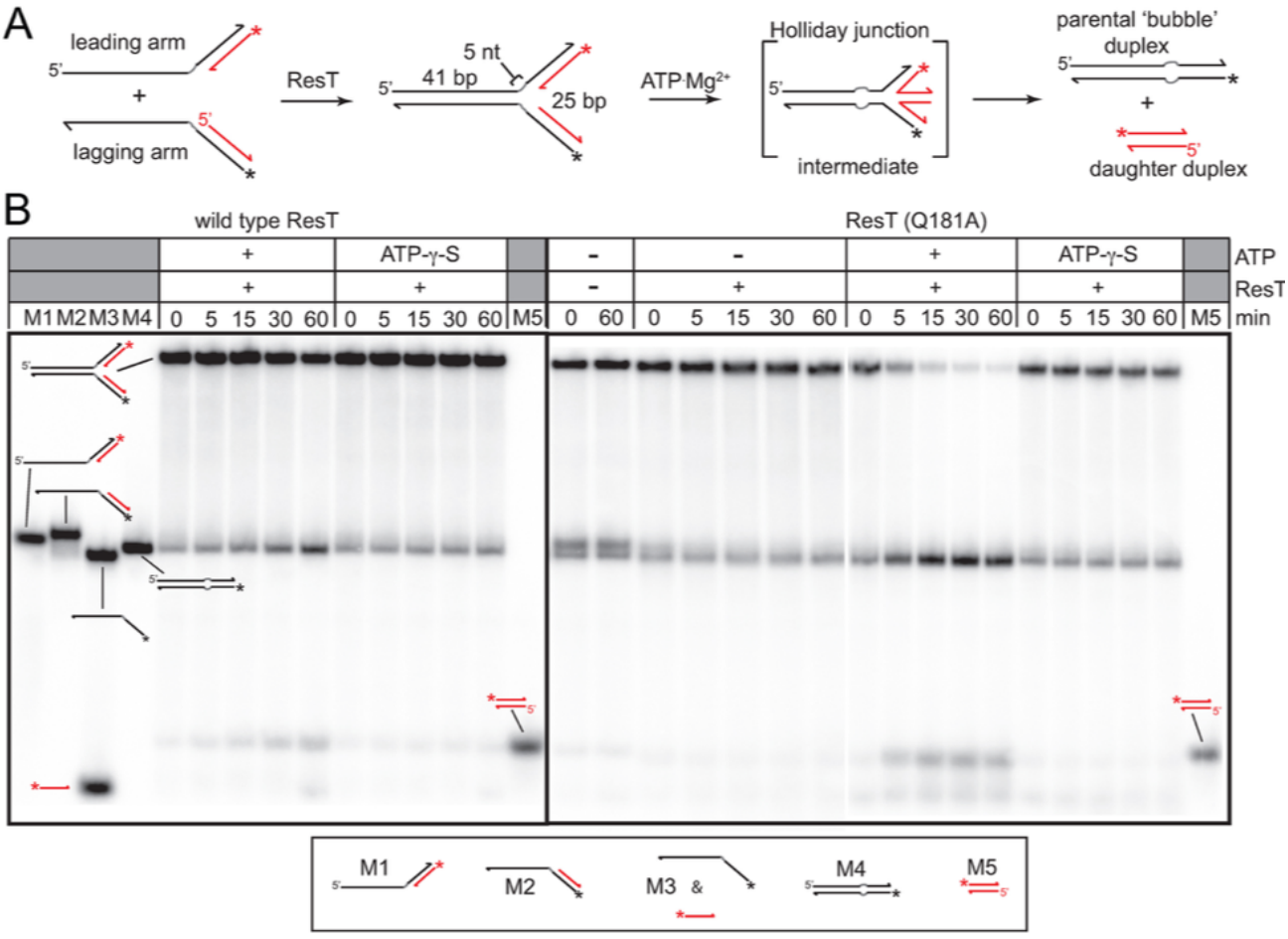

Figure 4.24. ResT can perform fork regression. (A) A schematic of the fork regression assay. Two homologous arms representing the lagging and leading arm of a replication fork are annealed together with the addition of ResT to create a replication fork mimic. Both arms contain a 5-nucleotide heterologous gap at the ssDNA dsDNA junctions to prevent spontaneous branch migration. ATP·Mg is added to induce ResT's unwinding activity. The resulting products (parental bubble duplex and daughter duplex) indicate successful template switching and regression of the replication fork mimic. **(B)** 8% PAGE/ 1X TAE/ 0.1% SDS gel analysis of fork regression promoted by both wt ResT and the hyperactive unwinding mutant, ResT (Q181A). The substrate was present at 15 nM and ResT present at 37 nM. Following addition of ResT, the annealing step proceeds for 10 min. This is followed by addition of ATP·Mg to induce unwinding and the various products can be identified by M1-5 that have been individually loaded. The structures of these products are indicated in the legend below. Reprinted from (Huang et al., 2017).

4.2.2.5 Assessing the purity of TelA purification with Mass Spectrometry

Despite previous assessments that our wt TelA purification was highly homogenous (Figure 4.18a), our inconsistent results in trying to identify an unwinding separation-of-function mutant lead us to question whether the observed ATPase/unwinding was coming from our enzyme or an *E. coli* contaminant in the TelA preparation. We loaded 10 μg of our wt TelA (pEKK 395, see Table 2.) to a 15% SDS-PAGE gel and stained with a sensitive (< 6 ng of protein), mass spectrometry compatible, Imperial™ stain (Thermofisher). Identified contaminant bands (Figure 4.25a) were excised and submerged in 1% acetic acid for Mass Spectrometry. Mass Spectrometry results for all excised bands can be seen in Figure 4.25b. One notable result from the Mass Spectrometry data was the presence of the *E. coli* helicase, HelD, as a small percentage of the entire spectra for contaminant band 2 (highlighted in Figure 4.25b). Despite its low abundance within the wt TelA protein preparation, *hel*D encodes a ssDNA-dependent ATPase with ATP-dependent 3'-5' unwinding activity (Wood and Matson, 1987) and thus, we needed to identify whether our observed unwinding activity originated from TelA or the contaminant.

A

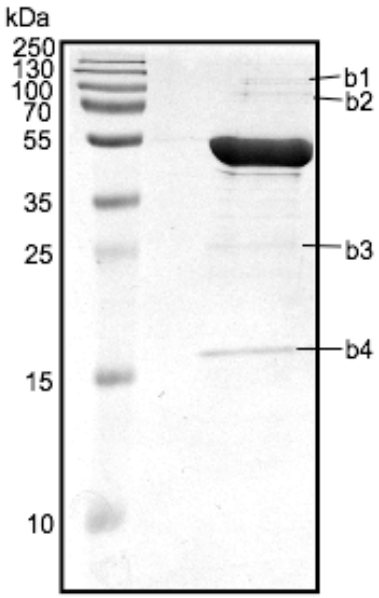

10 µg TelA
Imperial stained

B

Mass Spectrometry Summary Table

band	spectra	unique peptides	% cover-age	% total spect-ra	protein MW (kDa)	species	uniprotKB #	protein name
$b1_{.1}$	115	26	62	2.7	52.5	A. tum	custom database	TelA
$b1_{.2}$	104	45	53	2.5	99.7	E. coli	P0AFG8	AceE
$b1_{.3}$	101	38	44	2.4	105	E. coli	P0AFG3	SucA
$b1_{.4}$	49	33	48	1.2	97.4	E. coli	P06612	TopA
$b2_{.1}$	107	31	49	2.6	66.1	E. coli	P06959	AceF
$b2_{.2}$	79	23	53	1.9	52.5	A. tum	custom database	TelA
$b2_{.3}$	74	32	39	1.8	90.5	E. coli	P0AC86	GlgP
$b2_{.4}$	41	28	37	1.0	77.9	E. coli	P15038	HelD
$b3_{.1}$	165	30	68	5.5	52.5	A. tum	custom database	TelA
$b3_{.2}$	66	14	53	2.2	29.7	E. coli	P16528	IclR
$b3_{.3}$	32	10	39	1.1	27.3	E. coli	P0A8I5	TrmB
$b3_{.4}$	29	8	48	0.96	25.3	E. coli	P0AGJ2	TrmH
$b4_{.1}$	152	16	80	5.9	16	E. coli	P0AA10	RplM
$b4_{.2}$	48	22	49	1.9	52.5	A. tum	custom database	TelA
$b4_{.3}$	24	10	51	0.93	20	E. coli	P02359	RpsG
$b4_{.4}$	21	8	57	0.82	17.6	E. coli	P0A7W1	RpsE

Figure 4.25. Mass Spectrometry of TelA to identify potential ATPase/helicase contaminants. (A) 15% SDS-PAGE analysis of 10 μg TelA stained with a colloidal Coomassie R250 stain (Imperial™ protein stain; Thermofisher) with the ability to visibly stain < 6 ng of protein. Regions of the gel indicated by b or 'band' designations b1-b4 were cut from a lane wherein 20 μg of TelA was loaded. These gel slices were subjected to in-gel tryptic digest and LC-MS/MS to identify contaminating *E. coli* proteins and TelA breakdown fragments. **(B)** Summary table of the 4 most abundant hits for each gel region excised from the preparative gel identified by LC-MS/MS against *E. coli* and custom TelA databases. For region b1 the proteins with the most spectra are TelA (the telomere resolvase), AceE (pyruvate dehydrogenase E1), SucA (2-oxoglutarate dehydrogenase E1) and TopA (DNA topoisomerase I). For region b2 the proteins with the most spectra are AceF (acetyltransferase of pyruvate dehydrogenase), TelA, GlgP (Glycogen phosphorylase) and HelD (an UvrD-like DNA helicase). For region b3 the proteins with the most spectra are TelA, IclR (a transcriptional repressor), TrmB and TrmH (tRNA methyltransferases). For region b4 the proteins with the most spectra are RplM (a 50S ribosomal protein), TelA, RpsG and RpsE (30S ribosomal subunit proteins). The relevant contaminant, HelD is highlighted in yellow.

4.2.2.6. TelA's apparent ATPase and unwinding activities come from a contaminant

To identify whether this small amount of HelD from band 2 was an issue in our TelA characterization, we sought to isolate the TelA protein away from all its contaminants. We implemented a method originally described by Hager and Burgess (Hager and Burgess, 1980) and subsequently modified by Vales *et. al.* (Vales et al., 1982) in which excised protein bands were eluted from a gel followed by denaturation and subsequent renaturation by dialysis (Figure 4.26, see Methods section for details). Isolation of TelA away from its contaminants revealed that although both the telomere resolution and annealing activity originated from the TelA protein (Figure 4.27ac), the unwinding activity observed only came from the isolated bands containing HelD (Figure 4.27b). Similar experiments performed with the TelA (107-442) protein preparation revealed comparable results (Figure 4.28). The slightly hypoactive ATPase and unwinding activity originally observed with the N-terminal truncation mutant was likely a reflection of decreased levels of HelD present in this prep. This is supported by the fact that TelA (107-442) was purified with the additional HAP column (see Methods section) in comparison to the wildtype enzyme, presumably decreasing HelD's abundance. It is important to note that the whole wildtype TelA preparation (pEKK395) was preliminarily denatured and renatured with guanidine hydrochloride prior to conducting these experiments to test for proper refolding. The whole preparation retained all originally observed activities including telomere resolution, annealing, and unwinding (data not shown). Additionally, it would be highly unlikely for TelA to maintain its telomere resolution capabilities if improperly folded, thus supporting the validity of our results, as a whole. From these, we have concluded that TelA does not possess ATPase or unwinding activity, but still constitutes a multifunctional enzyme with its combined telomere resolution and ssDNA annealing properties. Additionally, TelA appears to bind ATP despite its lack of ATPase or unwinding activity (Figure 4.10). It is currently unknown why an enzyme that does not utilize ATP for its activity would still possess ATP binding capabilities.

1. Protein Isolation from SDS-PAGE

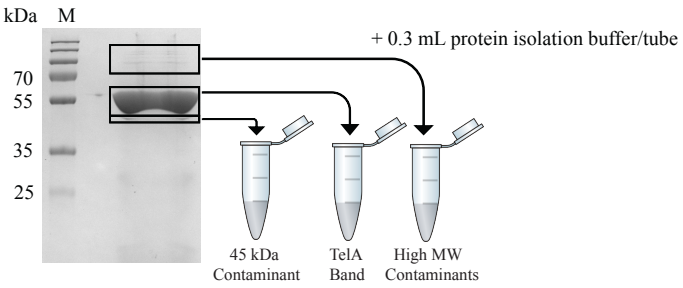

Crush and soak, O/N

2. Acetone Precipitation of Protein/ SDS Removal

Add 4X volume ice cold acetone, -20ºC O/N

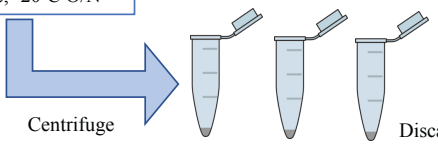

Centrifuge

Discard supernatant, retain protein pellet

3. Protein Denaturation and Renturation

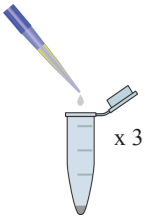

resuspend pellet in 6 M GuHCl

x 3

20 min, RT

Renaturation of Isolated Proteins by Dialysis against buffer w/o GuHCl

Testing for enzyme activity

If TelA refolded properly and possesses unwinding activity

Telomere Resolution: **Active**
Unwinding Activity: **Active**

If TelA **did not** refold properly

Telomere Resolution: **Dead**
Unwinding Activity: **Dead**

If TelA refolded properly, **but** unwinding activity originates from a contaminent

Telomere Resolution: **Active**
Unwinding Activity: **Dead**

Figure 4.26. Workflow of Protein Band Isolation by SDS-PAGE. 1. Desired protein bands are excised from a 20 μg sample loaded on an SDS-PAGE gel. The excised bands are transferred to separate Eppendorf tubes and crushed in 0.3 mL of protein isolation buffer containing 50 mM HEPES (pH 7.6), 0.15 M NaCl, 0.1 mM EDTA, 1 mM DTT, 100 μg/mL BSA and 0.1% SDS (as described in the methods section). The protein is left to elute out of the gel slices overnight at room temperature. **2.** Four volumes of ice-cold acetone were added to each tube to induce protein precipitation. Precipitation is allowed to proceed at -20°C overnight. The precipitated proteins are then pelleted by centrifugation and the supernatant removed. **3.** The protein pellets are resuspended in 50 μL of 6 M guanidine hydrochloride, 50 mM HEPES (pH 7.6), 0.15 M NaCl, 0.1 mM EDTA, 1 mM DTT, 100 μg/mL BSA and 20% glycerol and left to denature at room temperature for 20 min. Renaturation is performed by dialysis against denaturation buffer lacking guanidine hydrochloride, BSA and DTT. The resulting isolated protein preparations are then assayed for TelA's previously determined activities, most importantly unwinding activity. In the case of the isolated TelA band, the three possible outcomes are indicated. Telomere resolution would not occur if TelA misfolded and thus, can be used as an indicator for activity.

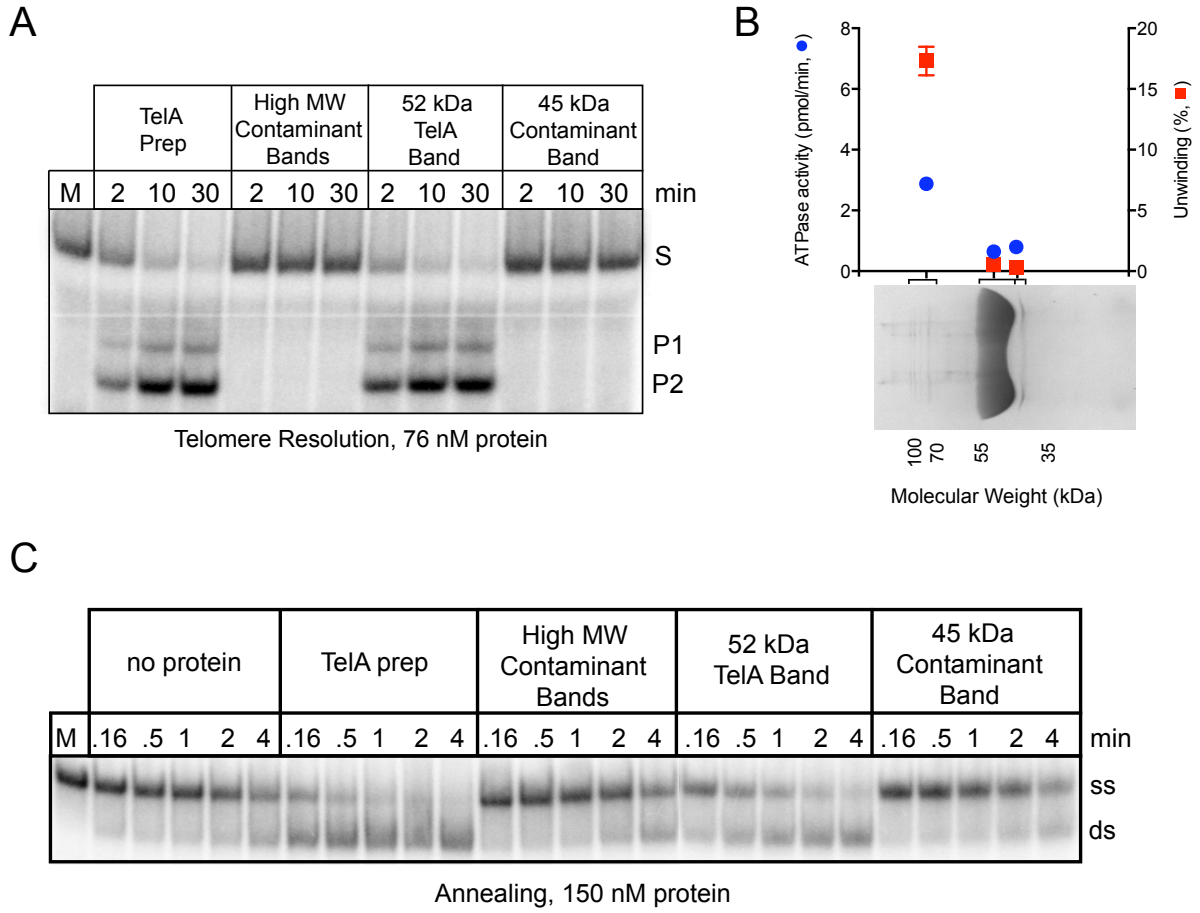

Figure 4.27. Activity assays performed on TelA and isolated contaminant bands. (A) 8% PAGE/ 1X TAE/ 0.1% SDS SDS gel analysis of telomere resolution timecourses with the complete TelA prep (pEKK 395) compared to isolated contaminant bands and isolated TelA. Telomere resolution was visualized by the conversion of the radiolabelled rTel substrate (S) into two hairpin products (P1, P2). These assays were performed at 30°C in the presence of 4 mM calcium. The substrate is present at 5 nM. **(B)** An Imperial™ stained lane of the TelA protein prep is shown (20 µg) and the isolated bands indicated on the gel. The graph depicts the ssDNA-dependent ATPase (●) and ATP dependent unwinding (■) activity profiles for the isolated bands following renaturation by dialysis. ATPase assays were performed with 76 nM of protein and unwinding assays were performed with 115 nM of protein. Concentrations were based off of the TelA band and equal parts of contaminant bands were added to maintain ratios true to the original protein prep. **(C)** 8% PAGE/ 1X TAE/ 0.1% SDS SDS gel analysis of annealing reactions. Gel panels representative of spontaneous annealing (no protein), the TelA protein prep, the isolated contaminant bands and the isolated TelA band are shown. Annealing is measured by the migration of the radiolabelled reporter strand (ss) into an annealed product with its complementary unlabeled strand (ds). The figure is composed of two separate gels shown as one panel.

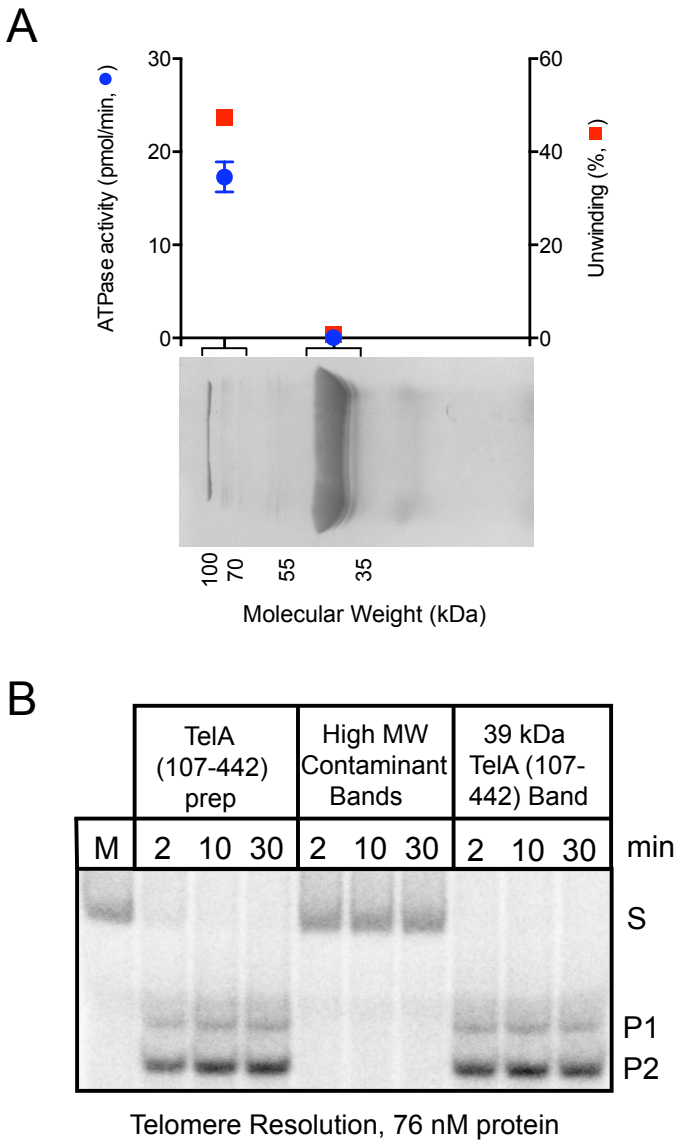

Figure 4.28. Activity assays performed on TelA (107-442) and isolated contaminant bands. **(A)** An Imperial™ stained lane of the TelA (107-442) protein prep is shown (20 µg) and the isolated bands indicated on the gel. The graph depicts the ssDNA-dependent ATPase (•) and ATP-dependent unwinding (■) activity profiles for the isolated bands following renaturation by dialysis. ATPase assays were performed with 76 nM of protein and unwinding assays were performed with 115 nM of protein. Concentrations were based off of the TelA (107-442) band and equal parts of contaminant bands were added to maintain ratios true to the original protein prep. **(B)** 8% PAGE/ 1X TAE/ 0.1% SDS SDS gel analysis of telomere resolution timecourses with the full TelA (107-442) prep compared to isolated contaminant bands and isolated TelA (107-442). Telomere resolution is visualized by the conversion of the radiolabelled rTel substrate (S) into two hairpin products (P1, P2). These assays were performed at 30°C in the presence of 4 mM calcium. The substrate is present at 5 nM.

Summary Results for Section 4.2: Does TelA promote DNA annealing and ATP-dependent DNA unwinding?

- TelA can anneal complementary ssDNA (Figure 4.16).
- The N-terminal truncation mutant of TelA, TelA (107-442) cannot anneal ssDNA above the spontaneous rate (Figure 4.16). This suggests TelA annealing activity stems from its N-terminal domain.
- The telomere resolution inactive mutant, TelA (Y405F), displays annealing activity comparable to that of the wildtype enzyme (Figure 4.16).
- Thus, there is a clean separation of function between TelA's annealing and telomere resolution activities.
- TelA cannot unwind DNA. All unwinding activity was determined to stem from a contaminant in the protein preparation (Figure 4.27).

5. Discussion

While all characterized members of the telomere resolvase enzyme family share the common core function of telomere resolution, stemming from its highly conserved telomere resolvase domain (pfam 16684), the N- and C- terminal extensions of these enzymes are quite variable. Additionally, most research to date is difficult to compare with structural data available for both the klebsiellal telomere resolvase, TelK, and the agrobacterial telomere resolvase, TelA, while most biochemical studies have focused on the study of the borrelial telomere resolvase, ResT. This provides a challenge in compiling mechanistic similarities and differences across this diverse enzyme family, as well as in identifying the full range of activities for each protein. Recently, the borrelial telomere resolvase, ResT, was shown to possess the ability to promote the annealing of complementary ssDNA (Mir et al., 2013) and an ATP-dependent, 3'-5' unwinding activity *in vitro* (Huang et al., 2017), in addition to its main activity of telomere resolution. This was unexpected as ResT lacks domains typical of these functions nor does it contain any recognizable helicase motifs in its primary sequence. Due to the domain diversity across the telomere resolvase enzyme family, it was unclear whether additional members would also possess these activities. Furthermore, while these additional activities are distinct from telomere resolution, their *in vivo* functions remain elusive. Through an *in vitro* biochemical study of the agrobacterial telomere resolvase, TelA, we sought to identify whether these unexpected activities of ssDNA annealing and ATP-dependent unwinding would be present in a second telomere resolvase and, if so, to identify whether these activities could be separated from one another by mutation. TelA was selected for this study due to its available partial structural data and its comparability to ResT in both size and sequence homology. Additionally, we aimed to expand upon the limited data available for TelA promoted telomere resolution. We examined the mutant phenotypes of multiple TelA residues, some of which had been previously implicated to play roles in telomere resolution (Shi et al., 2013), to further assess mechanistic similarities and differences between TelA and other previously characterized telomere resolvases.

5.1 The biochemical characterization of TelA promoted telomere resolution

Our initial characterization of TelA's telomere resolution activity showed that the reaction was stimulated in the presence of a divalent metal ion, with a preference for calcium (Figure 4.1). This was in contrast to ResT, which performed telomere resolution, *in vitro*,

independently of a metal ion's presence. However, there is precedent for this phenotype as the telomere resolution activity of the *E. coli* N15 phage telomere resolvase, TelN, was also stimulated in the presence of a divalent metal ion (Deneke et al., 2000). This would also explain why previous characterization of wildtype TelA required μM amounts of protein and extended incubation times to visualize product formation, *in vitro* (Shi et al., 2013). Truncation of the N-terminal domain of TelA unexpectedly relieved the enzyme of its divalent metal dependent phenotype. In previous studies, ResT was shown to be subject to autoinhibition by its N-terminal domain (Tourand et al., 2007). Perhaps TelA possesses a similar type of regulatory mechanism that can be overcome by either removal of the regulatory N-terminal domain or by the addition of a divalent metal ion. Mutation of the D202 residue in TelA also allowed a partial independence from a divalent metal ion requirement, as well as a broadly hyperactivated telomere resolution activity suggesting this residue may be involved in autoinhibition as well.

In addition to TelA (D202A), the phenotype of the TelA mutant, R205A was characterized. Previous studies suggested this mutant was deficient for telomere resolution (Shi et al., 2013), but our recent identification of the divalent metal ion stimulation of telomere resolution suggested the mutant was worth revisiting. TelA (R205A) displayed significantly hypoactive telomere resolution activity that could be partially rescued in the presence of calcium; although, wildtype levels of activity could not be reached (Figure 4.5b). Previous studies suggested this mutant was cleavage competent, but was defective in hairpin formation, and its positioning within a TelA-mutant DNA complexed crystal structure suggested the residue was involved with enforcing a strand trajectory change to promote hairpin formation (Shi et al., 2013). It is possible that the positive charge contacts lost by mutation of this arginine residue could be partially filled by calcium, *in vitro*, allowing the reaction to proceed and form hairpin products. However, it is unclear why these effects were specific to calcium for this mutant; magnesium did not rescue the defect. Perhaps, TelA possesses separate calcium and magnesium binding sites and the R205A mutant is alternatively rescued through allosteric stimulation of TelA's activity by calcium binding.

5.2 "ATP interference" of telomere resolution and *rTel* recognition, intertwined

In investigating the optimum conditions under which TelA performed telomere resolution, *in vitro*, we also tested high energy cofactors such as ATP. In the presence of

calcium, ATP appeared to interfere with wildtype TelA's ability to perform telomere resolution (Figure 4.7, 4.8a), and diminished TelA's affinity for its *rTel* sequence (Figure 4.14). Mutation of both the D202 and R205 residues of TelA appeared to relieve this apparent "ATP interference" of telomere resolution (Figure 4.7, 4.8). However, ATP photoaffinity crosslinking experiments revealed wildtype TelA, TelA (D202A), and TelA (R205A) possessed similar ATP binding capacities; ATP binding was only significantly diminished by removal of the N-terminal domain of TelA (Figure 4.10). Similarly, ResT only displayed the ability to bind ATP in the context of the entire enzyme (Huang et al., 2017). While ATP clearly played a role in modulating TelA's activity, this contrast in "ATP interference" between the wildtype enzyme, and TelA (D202A) and (R205A) could not be accounted for through ATP binding alone. A series of *rTel* binding experiments using a titration of non-target DNA revealed TelA displayed a low differential between its affinity for its *rTel* sequence and bulk DNA. In the presence of ATP, this differential is even lower than without ATP present and when provided with many alternative binding sites (as is the case with the plasmid substrate used for *in vitro* telomere resolution assays) TelA struggled to identify its *rTel*, giving ATP the appearance of being a potent inhibitor of telomere resolution, *in vitro*. It is likely that TelA (D202A)'s elevated affinity for its *rTel* (Figure 4.15) in combination with its metal independent phenotype are enough to overcome the mild inhibitory effect of ATP, *in vitro*.

As TelA lacks a strong affinity for its own *rTel* sequence above non-target DNA, it becomes unclear how TelA identifies its target, *in vivo*. The klebsiellal telomere resolvase, TelK, has been shown to survey the DNA as a monomer, becoming immobilized upon dimerization or when it encounters its target sequence. Immobilized dimers have been hypothesized to be able to induce bends on non-target DNA, as is required at the target site during TelK promoted telomere resolution, to test substrate compatibility and aid in target identification (Landry et al., 2013). However, TelA does not induce such a significant bend in its target DNA (Figure 1.7) and would require an alternative mechanism for rapid target identification. It is possible that a divalent metal ion or some other factor guides TelA to its target sequence, *in vivo*. Moreover, TelA's low affinity for its *rTel* provides a potential explanation for the high abundance of ResT observed in *B. burgdorferi*, at about 15 000 monomers per cell. This is significant overexpression for a protein with defined sites of action (Bandy et al., 2014). In contrast, the abundance of TelK is much lower, maintaining a cellular copy number of approximately <20 (Landry et al., 2013).

Notably, ResT's C-terminal end alone, ResT (163-449), displays increased affinity for its *rTel* above the full-length protein (Bankhead et al., 2006; Tourand et al., 2007) due to the autoinhibitory nature of the N-terminal domain. Our data suggested TelA could be subject to a similar regulatory mechanism by its N-terminal end and it would be interesting to see whether we observe an increase in *rTel* affinity with the N-terminal truncation mutant, TelA (107-442).

5.3 Separation-of-function between TelA's annealing activity and telomere resolution

In examining TelA for the unexpected activities of ssDNA annealing and ATP-dependent unwinding observed in ResT, we found that TelA was also able to promote the annealing of complementary ssDNA. However, TelA required a 10-fold higher concentration of protein than ResT to reach a half maximal annealing rate (Figure 4.16c, (Mir et al., 2013)). The N-terminal truncation mutant of TelA was unable to anneal ssDNA above the spontaneous rate suggesting TelA's annealing activity stems from its N-terminal domain. Similarly, ResT's N-terminal domain was shown to display a non-specific DNA binding activity (Tourand et al., 2007) and was later shown to be able to act as an annealing protein independently of the rest of the protein (Mir et al., 2013). While the TelA N-terminal truncation mutant displayed a loss of annealing activity, it was still active for telomere resolution, representing a separation-of-function between annealing activity and telomere resolution previously unobserved in the telomere resolvase family. An N-terminal truncation of ResT, ResT (163-449), displayed a similar annealing incompetency, but the mutant was also inactive for telomere resolution (Tourand et al., 2007). This was unsurprising as the N-terminal domain of ResT contains a unique hairpin-binding module essential for telomere resolution activity (Kobryn et al., 2005). Additionally, although there is no evidence of annealing activity to date in the klebsiellal telomere resolvase, TelK, removal of its N-terminal domain leaves a similarly telomere resolution incompetent mutant (Aihara et al., 2007). Our biochemical analysis of TelA included a mutant of TelA's active site nucleophile, TelA (Y405F); aside from its expected telomere resolution incompetency, the mutant was still a proficient annealing protein. In combination, TelA (Y405F) and the N-terminal truncation mutant of TelA demonstrate clean separation-of-function phenotypes between TelA's telomere resolution and annealing activities, and provide potential tools for investigating the functional role of TelA's annealing activity, *in vivo*, and perhaps, for telomere resolvases in general.

5.4 Divergent properties among telomere resolvases

In addition to annealing activity, ResT was shown to possess a ssDNA-dependent ATPase activity as well as a 3'-5', ATP-dependent unwinding activity, *in vitro*. Despite preliminary results that TelA appeared to also possess these ATPase and unwinding activities, they were eventually determined to stem from an *E. coli* contaminant in our protein preparation, HelD (Figure 4.27). This conclusion was supported through the many unwinding-centric properties of ResT that TelA appeared to lack. ResT displayed both ATP-mediated dimerization as well as the ability to transfer the gamma phosphate group from ATP to itself, both of which were absent in TelA (unpublished data). TelA was also incapable of performing fork regression, an activity that requires concerted unwinding and annealing, and was observed in ResT. In the original report of ResT's fork regression activity, it was hypothesized that this activity may allow for template switching during DNA replication near the hairpin telomere ends to allow for complete replication if the hairpin structure prompted stalling of the replication machinery (Huang et al., 2017). In support of this hypothesis, ResT's annealing activity was stimulated by ATP (Huang et al., 2017), while TelA's annealing activity was inhibited in the presence of ATP (unpublished data). This suggests a possible functional difference between ResT and TelA's annealing activities. Conversely, while ResT may be able to perform fork regression independently, similar to some RecQ family helicase members (Croteau et al., 2014), TelA may require additional proteins to contribute towards completing replication around the hairpin telomeres – providing cleavage or annealing activity while still requiring the additional activity of a DNA helicase.

However, without possession of an ATPase or unwinding activity, the purpose ATP binding plays in TelA's function remains unclear. There are some examples of a role for NTP binding in the modulation of enzymatic activity alone. GTP acts as an allosteric effector of P element transposition in *Drosophila*, as it promotes the formation of a specific DNA-protein pre-synaptic complex between the transposase and P-DNA (Tang et al., 2005). Additionally, some pseudokinases have been shown to still bind ATP despite lacking catalytic activity (Min et al., 2015; Toms et al., 2013; Zeqiraj et al., 2009). As previously discussed, ATP does seem to inhibit TelA's ssDNA annealing activity (unpublished data), impede *rTel* recognition (Figure 4.14) and under certain conditions, modulate telomere resolution activity (Figure 4.7) suggesting a potential regulatory role in which enzymatic function is repressed in ATP-rich environments.

When considering the N- and C- terminal extension diversity among the telomere resolvase enzyme family, the emergence of divergent properties is not entirely surprising. Specifically, ResT possesses a sequence insert within its catalytic domain that does not share homology with other telomere resolvases (Figure 1.3b). This insert houses many of the residues whose characterized mutants displayed significantly hypoactive unwinding activity, *in vitro* (Huang et al., 2017), and provides a possible explanation for the absence of unwinding activity in TelA. Additionally, TelN and TelK display a weak homology to UrvD helicase and P-loop NTPase domains, respectively that has yet to be explored (Figure 1.3, (Kelley et al., 2015)). Although telomere resolvases possess the common core function of telomere resolution, evidence of additional, distinct functions from one another continue to accumulate and highlight the importance of continued characterization of this diverse enzyme family.

6. Conclusions and Future Directions

The work presented here furthers our understanding of both the mechanistic details of TelA promoted telomere resolution, and the role domain structure plays in both the analogous and contrasting properties among the telomere resolvase enzyme family. One intriguing aspect of our biochemical characterization of TelA was the unexpected stimulation of telomere resolution by a divalent metal ion; specifically, the reaction's preference for calcium over magnesium. This is intriguing from a physiological perspective as calcium is present at much lower levels than magnesium in prokaryotes, in about the low hundred nM range (Dominguez, 2004). Additionally, calcium appeared to be able to partially rescue the hypoactive telomere resolution phenotype of TelA (R205A), with increased stimulation of the reaction being correlated to increasing calcium levels up to 8 mM (the highest amount of calcium tested). It would be interesting to explore the step during telomere resolution at which the metal ion participates, and if there are any observable variations between magnesium and calcium, or among our multiple TelA mutants. We already have evidence that the metal ion does not stimulate at the point of telomere recognition (unpublished data); to test other steps of the reaction would be relatively straightforward. Using modified *rTel* half-sites we could elucidate the step at which divalent metal ion stimulation occurs. The cleavage step of telomere resolution can be examined through use of an *rTel* half-site that's 5' overhang has been truncated by 1 nucleotide (leaving a 5-nucleotide overhang). The substrate can be cleaved, but the resulting overhang cannot form a hairpin and the enzyme is left tethered to the DNA. To study hairpin formation, an *rTel* half-site with the correct length of overhang would be used (6 nucleotides) to allow formation of the hairpin. The resulting products would then need to be analysed using a denaturing gel to distinguish between the annealed substrate composed of two single-stranded oligonucleotides and a product where the two strands are linked by the formed hairpin. These substrates could also be used to analyze potential "ATP interference" of these individual steps of telomere resolution. Our current data indicates variant "ATP interference" of telomere resolution across our multiple TelA mutants and the wildtype enzyme, as well as differing levels of "ATP interference" depending on whether calcium or magnesium ions were present.

We have shown that in addition to telomere resolution, the agrobacterial telomere resolvase, TelA, also displays an annealing activity stemming from its N-terminal domain, similar to that observed in the borrelial telomere resolvase, ResT. It would be intriguing to see

whether TelA's N-terminal domain alone could function as an annealing protein, as observed in ResT (Mir et al., 2013). Moreover, TelA's annealing activity can be separated from its telomere resolution activity and vice versa through mutation, represented by the N-terminal truncation mutant of TelA, TelA (107-442), and the active site nucleophile mutant, TelA (Y405F). As these mutants represent the first successful separation-of-function among telomere resolvases, they provide a platform for future *in vivo* functional studies not previously possible. Construction of these mutants for expression in *Agrobacterium tumefaciens* could help elucidate the functional role this annealing activity plays within the bacterial cell.

In contrast to our hypothesis, TelA did not possess the *in vitro* unwinding activity observed in the borrelial telomere resolvase, ResT. This highlights the potential functional diversity within this enzyme family, and consequently how domain diversity may be tied to these observable functional differences. An excellent example comes from the multiple mutants of ResT that display hypoactive unwinding activity residing in a non-homologous sequence insert of ResT's catalytic domain (Figure 1.3b, (Huang et al., 2017)). At present, an ATPase/unwinding separation-of-function mutant for ResT has yet to be identified and this non-homologous insert represents a promising target area for future screening of potential ATPase/unwinding separation-of-function mutants for ResT.

In part, the emergence of these contrasting properties among telomere resolvases could be linked to a finding by the Domain Architectural Retrieval Tool (DART) of the CDD that telomere resolvases domains can be found as part of the domain architecture of multiple ancient cyanobacterial species (Marchler-Bauer et al., 2015). More intriguingly, these species do not contain linear genetic elements and linear genetic elements are decidedly rare among cyanobacteria, in general (Gagunashvili and Andrésson, 2018; Welsh et al., 2008). Furthermore, some of these proteins, in addition to their telomere resolvase domains, possess domains in common with ATPases (Figure 6.1) providing a potential evolutionary link between telomere resolvases and their seemingly diverse secondary functions. It would be interesting to identify whether these cyanobacterial proteins have topoisomerase IB-like cleavage and rejoining activity or an ATPase/unwinding activity similar to that observed in ResT; similarly exploring whether additional telomere resolvase family members such as TelN and TelK that display weak homology to UrvD helicase and NTPase domains, respectively, possess secondary ATPase or unwinding functions would also be enlightening.

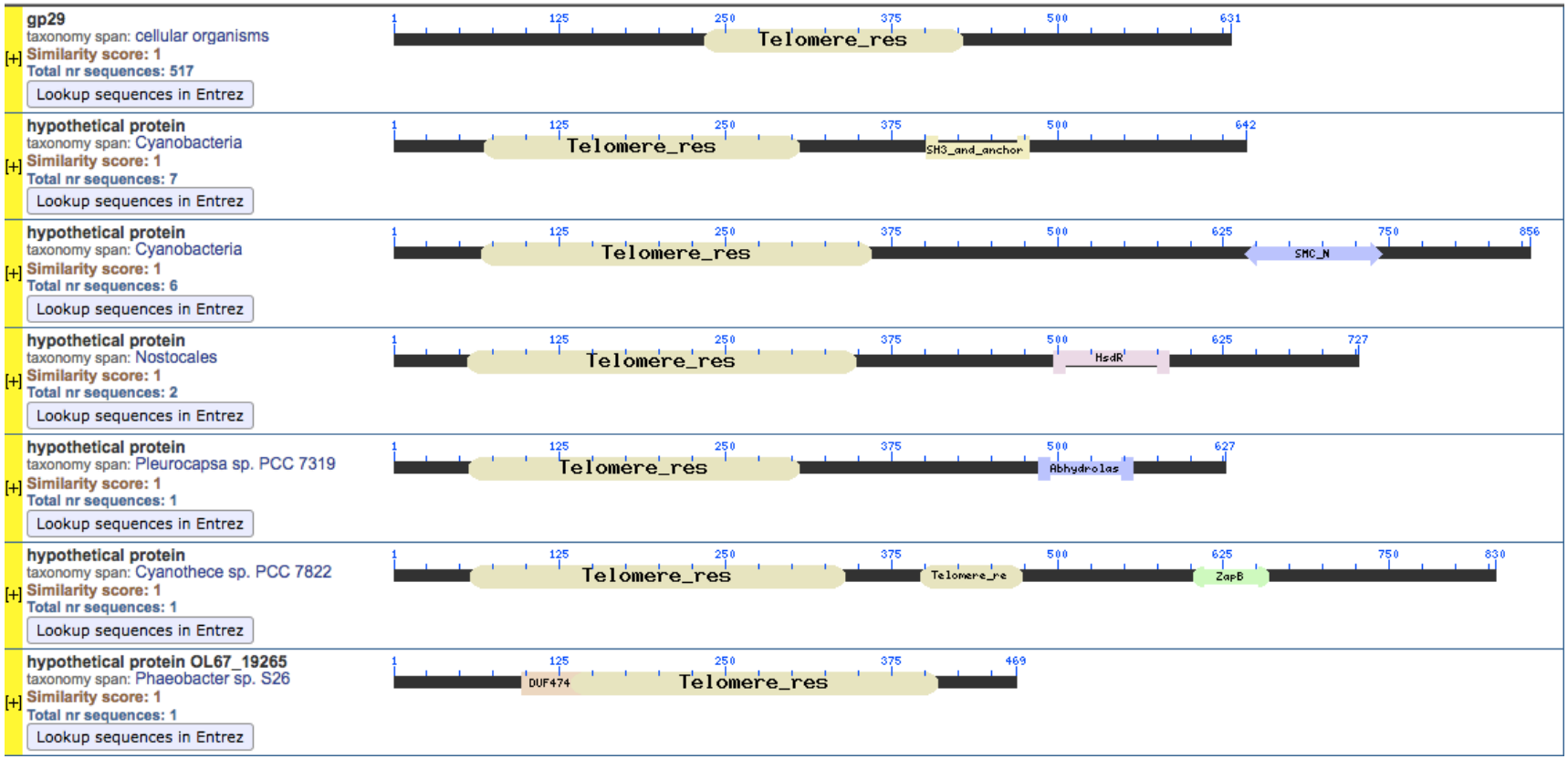

Figure 6.1. The conserved telomere resolvase domain is present in proteins from multiple cyanobacterial species. A group of cyanobacterial proteins containing the conserved telomere resolvase domain typified from TelN, the telomere resolvase of the *E. coli* phage N15 (gp29). In addition to the telomere resolvase domain, other conserved domains have been identified in the multi domain proteins of these cyanobacterial species including some involved with ATPase or unwinding activities. SH3 domains are involved in the recognition of proline rich ligands; SMC_N domains participate in ATP binding (in combination with SMC_C domains) of RecF, RecN, and SMC recombination/repair proteins; HsdR possesses helicase and endonuclease activity; Abhydrolase domains contain alpha and beta elements and promote nucleophilic attack on a carbonyl carbon atom; ZapB is a cell division protein that aids in septal Z-ring formation; and DUF474 is a domain with currently unknown functions.

7. References

Aihara, H., Huang, W.M., and Ellenberger, T. (2007). An Interlocked Dimer of the Protelomerase TelK Distorts DNA Structure for the Formation of Hairpin Telomeres. Mol. Cell *27*, 901–913.

Arnold, D.A., Handa, N., Kobayashi, I., and Kowalczykowski, S.C. (2000). A novel, 11 nucleotide variant of χ, χ*: One of a class of sequences defining the Escherichia coli recombination hotspot χ. J. Mol. Biol. *300*, 469–479.

Aroyo, M., Colloms, S.D., Helfrich, A., and Sherratt, D.J. (2000). FtsK functions in the processing of a Holliday junction intermediate Franc. Genes Dev. *14*, 2976–2988.

Arthur, H.M., and Lloyd, R.G. (1980). Hyper-recombination in uvrD mutants of Escherichia coli K-12. MGG Mol. Gen. Genet. *180*, 185–191.

Bachrati, C.Z., and Hickson, I.D. (2008). RecQ helicases: Guardian angels of the DNA replication fork. Chromosoma *117*, 219–233.

Bailey, S., Eliason, W.K., and Steitz, T.A. (2007). Structure of hexameric DnaB helicase and its complex with a domain of DnaG primase. Science (80-.). *318*, 459–463.

Bandy, N.J., Salman-Dilgimen, A., and Chaconas, G. (2014). Construction and characterization of a Borrelia burgdorferi strain with conditional expression of the essential telomere resolvase, ResT. J. Bacteriol. *196*, 2396–2404.

Bankhead, T., and Chaconas, G. (2004). Mixing active-site components: A recipe for the unique enzymatic activity of a telomere resolvase. Proc. Natl. Acad. Sci. *101*, 13768–13773.

Bankhead, T., Kobryn, K., and Chaconas, G. (2006). Unexpected twist: Harnessing the energy in positive supercoils to control telomere resolution. Mol. Microbiol. *62*, 895–905.

Bao, K., and Cohen, S.N. (2003). Recruitment of terminal protein to the ends of Streptomyces linear plasmids and chromosomes by a novel telomere-binding protein essential for linear DNA replication. Genes Dev. *17*, 774–785.

Barbour, A.G., and Garon, C.F. (1987). Linear plasmids of the bacterium Borrelia burgdorferi have covalently closed ends. Science (80-.). *237*, 409–411.

Blanco, L., Bernad, A., Esteban, J.A., and Salas, M. (1992). DNA-independent deoxynucleotidylation of the φ29 terminal protein by the φ29 DNA polymerase. J. Biol. Chem. *267*, 1225–1230.

Boratyn, G.M., Schäffer, A.A., Agarwala, R., Altschul, S.F., Lipman, D.J., and Madden, T.L. (2012). Domain enhanced lookup time accelerated BLAST. Biol. Direct *7*, 1–14.

Bradford, M.M. (1976). A rapid and sensitive method for the quantitation of microgram quantities of protein utilizing the principle of protein-dye binding. Anal. Biochem. 248–254.

Brendel, V., Brocchieri, L., Sandler, S.J., Clark, A.J., and Karlin, S. (1997). Evolutionary comparisons of RecA-like proteins across all major kingdoms of living organisms. J. Mol. Evol. *44*, 528–541.

Briffotaux, J., and Kobryn, K. (2010). Preventing broken Borrelia telomeres: ResT couples dual hairpin telomere formation with product release. J. Biol. Chem. *285*, 41010–41018.

Byram, R., Stewart, P.E., and Rosa, P. (2004). The essential nature of the ubiquitous 26-kilobase circular replicon of Borrelia burgdorferi. J. Bacteriol. *186*, 3561–3569.

Carles-Kinch, K., George, J.W., and Kreuzer, K.N. (1997). Bacteriophage T4 UvsW protein is a helicase involved in recombination, repair and the regulation of DNA replication origins. EMBO J. *16*, 4142–4151.

Casjens, S. (1999). Evolution of the linear DNA replicons of the Borrelia spirochetes. Curr. Opin. Microbiol. 2: 529-534.

Casjens, S., Murphy, M., DeLange, M., Sampson, L., Van Vugt, R., and Huang, W.M. (1997). Telomeres of the linear chromosomes of Lyme disease spirochaetes: Nucleotide sequence and possible exchange with linear plasmid telomeres. Mol. Microbiol. *26*, 581–596.

Casjens, S., Palmer, N., Van Vugt, R., Huang, W.M., Stevenson, B., Rosa, P., Lathigra, R., Sutton, G., Peterson, J., Dodson, R.J., et al. (2000). A bacterial genome in flux: The twelve linear and nine circular extrachromosomal DNAs in an infectious isolate of the Lyme disease spirochete Borrelia burgdorferi. Mol. Microbiol. *35*, 490–516.

Casjens, S.R., Gilcrease, E.B., Huang, W.M., Bunny, K.L., Pedulla, M.L., Ford, M.E., Houtz, J.M., Hatfull, G.F., and Hendrix, R.W. (2004). The pKO2 Linear Plasmid Prophage of Klebsiella oxytoca. J. Bacteriol. *186*, 1818–1832.

Chaconas, G. (2005). Hairpin telomeres and genome plasticity in Borrelia: All mixed up in the end. Mol. Microbiol. *58*, 625–635.

Chaconas, G., and Kobryn, K. (2010). Structure, Function, and Evolution of Linear Replicons in Borrelia. Annu. Rev. Microbiol. *64*, 185–202.

Chaconas, G., Stewart, P.E., Tilly, K., Bono, J.L., and Rosa, P. (2001). Telomere resolution in the Lyme disease spirochete. EMBO J. *20*, 3229–3237.

Chang, P.C., and Cohen, S.N. (1994). Bidirectional replication from an internal origin in a linear streptomyces plasmid. Science (80-.). 952–954.

Chen, Y., and Rice, P.A. (2003). The role of the conserved Trp330 in Flp-mediated recombination: Functional and structural analysis. J. Biol. Chem. *278*, 24800–24807.

Chow, K.H., and Courcelle, J. (2004). RecO Acts with RecF and RecR to Protect and Maintain Replication Forks Blocked by UV-induced DNA Damage in Escherichia coli. J. Biol. Chem. *279*, 3492–3496.

Clark, A.J., and Margulies, A.D. (1965). Isolation and Characterization of Recombination-Deficient Mutants of. Proc. Natl. Acad. Sci. United States *53*, 451–459.

Courcelle, J., and Hanawalt, P.C. (2003). RecA-Dependent Recovery of Arrested DNA Replication Forks. Annu. Rev. Genet. *37*, 611–646.

Courcelle, C.T., Chow, K.H., Casey, A., and Courcelle, J. (2006). Nascent DNA processing by RecJ favors lesion repair over translesion synthesis at arrested replication forks in Escherichia coli. Proc. Natl. Acad. Sci. U. S. A. *103*, 9154–9159.

Croteau, D.L., Popuri, V., Opresko, P.L., and Bohr, V.A. (2014). Human RecQ Helicases in DNA Repair, Recombination, and Replication. Annu. Rev. Biochem. *83*, 519–552.

Deneke, J., Ziegelin, G., Lurz, R., and Lanka, E. (2000). The protelomerase of temperate

Escherichia coli phage N15 has cleaving-joining activity. Proc. Natl. Acad. Sci. U. S. A. *97*, 7721–7726.

Deneke, J., Burgin, A.B., Wilson, S.L., and Chaconas, G. (2004). Catalytic residues of the telomere resolvase ResT: A pattern similar to, but distinct from, tyrosine recombinases and type IB topoisomerases. J. Biol. Chem. *279*, 53699–53706.

Dillingham, M.S., and Kowalczykowski, S.C. (2008). RecBCD Enzyme and the Repair of Double-Stranded DNA Breaks. Microbiol. Mol. Biol. Rev. *72*, 642–671.

Dillingham, M.S., Spies, M., and Kowalczykowski, S.C. (2003). RecBCD enzyme is a bipolar DNA helicase. Nature *423*, 893–897.

Dominguez, D.C. (2004). Calcium signalling in bacteria. Mol. Microbiol. *54*, 291–297.

Draper, G.C., McLennan, N., Begg, K., Masters, M., and Donachie, W.D. (1998). Only the N-terminal domain of FtsK functions in cell division. J. Bacteriol. *180*, 4621–4627.

Fraser, C.M., Casjens, S., Huang, W.M., Sutton, G.G., Clayton, R., Lathigra, R., White, O., Ketchum, K.A., Dodson, R., Hickey, E.K., et al. (1997). Genomic sequence of a Lyme disease spirochaete, Borrelia burgdorferi. Nature *390*, 580–586.

Gagunashvili, A.N., and Andrésson, Ó.S. (2018). Distinctive characters of Nostoc genomes in cyanolichens. BMC Genomics *19*, 1–18.

Goodner, B., Hinkle, G., Gattung, S., Miller, N., Blanchard, M., Qurollo, B., Goldman, B.S., Cao, Y., Askenazi, M., Halling, C., et al. (2001). Genome sequence of the plant pathogen and biotechnology agent Agrobacterium tumefaciens C58. Science (80-.). *294*, 2323–2328.

Goodner, B.W., Markelz, B.P., Flanagan, M.C., Crowell, C.B., Racette, J.L., Schilling, B.A., Halfon, L.M., Mellors, J.S., and Grabowski, G. (1999). Combined genetic and physical map of the complex genome of Agrobacterium tumefaciens. J. Bacteriol. *181*, 5160–5166.

Grindley, N.D.F., Whiteson, K.L., and Rice, P.A. (2006). Mechanisms of Site-Specific Recombination. Annu. Rev. Biochem. *75*, 567–605.

Gupta, R., Shuman, S., and Glickman, M.S. (2015). RecF and RecR play critical roles in the homologous recombination and single-strand annealing pathways of mycobacteria. J. Bacteriol. *197*, 3121–3132.

Hager, D.A., and Burgess, R.R. (1980). Elution of proteins from sodium dodecyl sulfate-polyacrylamide gels, removal of sodium dodecyl sulfate, and renaturation of enzymatic activity: Results with sigma subunit of Escherichia coli RNA polymerase, wheat germ DNA topoisomerase, and other enzymes. Anal. Biochem.

Hermoso, J.M., Méndez, E., Soriano, F., and Salas, M. (1985). Location of the serine residue involved in the linkage between the terminal protein and the DNA of phage φ29. Nucleic Acids Res. *13*, 7715–7728.

Hertwig, S., Klein, I., Lurz, R., Lanka, E., and Appel, B. (2003). PY54, a linear plasmid prophage of Yersinia enterocolitica with covalently closed ends. Mol. Microbiol. *48*, 989–1003.

Hirata, Y., Funato, Y., Takano, Y., and Miki, H. (2014). Mg2+-dependent interactions of ATP with the cystathionine-beta-synthase (CBS) domains of a magnesium transporter. J. Biol. Chem. *289*, 14731–14739.

Huang, S.H., and Kobryn, K. (2016). The Borrelia burgdorferi telomere resolvase, ResT, anneals ssDNA complexed with its cognate ssDNA-binding protein. Nucleic Acids Res. *44*, 5288–5298.

Huang, C.H., Lin, Y.S., Yang, Y.L., Huang, S.W., and Chen, C.W. (1998). The telomeres of Streptomyces chromosomes contain conserved palindromic sequences with potential to form complex secondary structures. Mol. Microbiol. *28*, 905–916.

Huang, S.H., Cozart, M.R., Hart, M.A., and Kobryn, K. (2017). The Borrelia burgdorferitelomere resolvase, ResT, possesses ATP-dependent DNA unwinding activity. Nucleic Acids Res. *45*, 1319–1329.

Huang, W.M., Joss, L., Hsieh, T., and Casjens, S. (2004a). Protelomerase Uses a Topoisomerase IB/Y-Recombinase Type Mechanism to Generate DNA Hairpin Ends. J. Mol. Biol. *337*, 77–92.

Huang, W.M., Robertson, M., Aron, J., and Casjens, S. (2004b). Telomere exchange between linear replicons of Borrelia burgdorferi. J. Bacteriol. *186*, 4134–4141.

Huang, W.M., DaGloria, J., Fox, H., Ruan, Q., Tillou, J., Shi, K., Aihara, H., Aron, J., and Casjens, S. (2012). Linear chromosome-generating system of agrobacterium tumefaciens C58: Protelomerase generates and protects hairpin ends. J. Biol. Chem. *287*, 25551–25563.

Kantake, N., Madiraju, M.V.V.M., Sugiyama, T., and Kowalczykowski, S.C. (2002a). Escherichia coli RecO protein anneals ssDNA complexed with its cognate ssDNA-binding protein: A common step in genetic recombination. Proc. Natl. Acad. Sci. U. S. A. *99*, 15327–15332.

Kantake, N., Madiraju, M.V.V.M., Sugiyama, T., and Kowalczykowski, S.C. (2002b). Escherichia coli RecO protein anneals ssDNA complexed with its cognate ssDNA-binding protein: A common step in genetic recombination. Proc. Natl. Acad. Sci. U. S. A. *99*, 15327–15332.

Karakousis, G., Ye, N., Li, Z., Chiu, S.K., Reddy, G., and Radding, C.M. (1998). The beta protein of phage λ binds preferentially to an intermediate in DNA renaturation. J. Mol. Biol. *276*, 721–731.

Kelley, L.A., Mezulis, S., Yates, C.M., Wass, M.N., and Sternberg, M.J.E. (2015). The Phyre2 web portal for protein modeling, prediction and analysis. Nat. Protoc. *10*, 845–858.

Kobryn, K., and Chaconas, G. (2002). ResT, a telomere resolvase encoded by the Lyme disease spirochete. Mol. Cell *9*, 195–201.

Kobryn, K., and Chaconas, G. (2005). Fusion of hairpin telomeres by the B. burgdorferi telomere resolvase ResT: Implications for shaping a genome in flux. Mol. Cell *17*, 783–791.

Kobryn, K., and Chaconas, G. (2014). Hairpin Telomere Resolvases. Microbiol. Spectr. *2*.

Kobryn, K., Naigamwalla, D.Z., and Chaconas, G. (2000). Site-specific DNA binding and bending by the Borrelia burgdorferi Hbb protein. Mol. Microbiol. *37*, 145–155.

Kobryn, K., Burgin, A.B., and Chaconas, G. (2005). Uncoupling the chemical steps of telomere resolution by ResT. J. Biol. Chem. *280*, 26788–26795.

Landry, M.P., Zou, X., Wang, L., Huang, W.M., Schulten, K., and Chemla, Y.R. (2013). DNA target sequence identification mechanism for dimer-Active protein complexes. Nucleic Acids Res. *41*, 2416–2427.

De Lange, T. (2005). Shelterin: The protein complex that shapes and safeguards human telomeres. Genes Dev. *19*, 2100–2110.

LeBel, C., and Wellinger, R.J. (2005). Telomeres: What's new at your end? J. Cell Sci. *118*, 2785–2788.

Lenhart, J.S., Brandes, E.R., Schroeder, J.W., Sorenson, R.J., Showalter, H.D., and Simmons, L.A. (2014). RecO and RecR are necessary for RecA loading in response to DNA damage and replication fork stress. J. Bacteriol. *196*, 2851–2860.

Lingner, J., Cooper, J.P., and Cech, T.R. (1995). Telomerase and DNA end replication: No longer a lagging strand problem? Science (80-.). 269: 1533-1534.

Lucyshyn, D., Huang, S.H., and Kobryn, K. (2015). Spring loading a pre-cleavage intermediate for hairpin telomere formation. Nucleic Acids Res. *43*, 6062–6074.

Luisi-Deluca, C., and Kolodner, R. (1994). Purification and characterization of the Escherichia coli RecO protein. Renaturation of complementary single-stranded DNA molecules catalyzed by the RecO protein. J. Mol. Biol. *236*, 124–138.

Maher, R.L., Branagan, A.M., and Morrical, S.W. (2011). Coordination of DNA replication and recombination activities in the maintenance of genome stability. J. Cell. Biochem. *112*, 2672–2682.

Manosas, M., Perumal, S.K., Bianco, P., Ritort, F., Benkovic, S.J., and Croquette, V. (2013). RecG and UvsW catalyse robust DNA rewinding critical for stalled DNA replication fork rescue. Nat. Commun. *4*, 2368.

Marchler-Bauer, A., Derbyshire, M.K., Gonzales, N.R., Lu, S., Chitsaz, F., Geer, L.Y., Geer, R.C., He, J., Gwadz, M., Hurwitz, D.I., et al. (2015). CDD: NCBI's conserved domain database. Nucleic Acids Res. *43*, D222–D226.

Mardanov, A. V., and Ravin, N. V. (2006). Functional characterization of the repA replication gene of linear plasmid prophage N15. Res. Microbiol. *157*, 176–183.

Mardanov, A. V., and Ravin, N. V. (2009). Conversion of Linear DNA with Hairpin Telomeres into a Circular Molecule in the Course of Phage N15 Lytic Replication. J. Mol. Biol. *391*, 261–268.

Mehta, A., and Haber, J.E. (2014). Sources of DNA double-strand breaks and models of recombinational DNA repair. Cold Spring Harb. Perspect. Biol. *6*, a016428.

Mendez, J., Blanco, L., Esteban, J.A., Bernad, A., and Salas, M. (1992). Initiation of φ29 DNA replication occurs at the second 3' nucleotide of the linear template: A sliding-back mechanism for protein-primed DNA replication. Proc. Natl. Acad. Sci. U. S. A. *89*, 9579–9583.

Min, X., Ungureanu, D., Maxwell, S., Hammarén, H., Thibault, S., Hillert, E.K., Ayres, M., Greenfield, B., Eksterowicz, J., Gabel, C., et al. (2015). Structural and functional characterization of the JH2 pseudokinase domain of JAK family tyrosine kinase 2 (TYK2). J. Biol. Chem. *290*, 27261–27270.

Mir, T., Huang, S.H., and Kobryn, K. (2013). The telomere resolvase of the Lyme disease spirochete, Borrelia burgdorferi, promotes DNA single-strand annealing and strand exchange. Nucleic Acids Res. *41*, 10438–10448.

Moriarty, T.J., and Chaconas, G. (2009). Identification of the determinant conferring permissive substrate usage in the telomere resolvase, ResT. J. Biol. Chem. *284*, 23293–23301.

Morrical, S.W. (2016). DNA-Pairing and Annealing Processes HR HDR. Cold Spring Harb Perspect Biol *7*, 1–20.

Mouw, K.W., and Rice, P.A. (2007). Shaping the Borrelia burgdorferi genome: Crystal structure and binding properties of the DNA-bending protein Hbb. Mol. Microbiol. *63*, 1319–1330.

Muyrers, J.P.P., Zhang, Y., Buchholz, F., and Stewart, A.F. (2000). RecE/RecT and Redα/Redβ initiate double-stranded break repair by specifically interacting with their respective partners. Genes Dev. *14*, 1971–1982.

Nelson, S.W., and Benkovic, S.J. (2007). The T4 phage UvsW protein contains both DNA unwinding and strand annealing activities. J. Biol. Chem. *282*, 407–416.

New, J.H., Sugiyama, T., Zaitseva, E., and Kowalczykowski, S.C. (1998). Rad52 protein stimulates DNA strand exchange by Rad51 and replication protein A. Nature *391*, 407–410.

Newell, C.A. (2000). Plant transformation technology: Developments and applications. Appl. Biochem. Biotechnol. - Part B Mol. Biotechnol. 16, 53.

Nimonkar, A. V., Sica, R.A., and Kowalczykowski, S.C. (2009). Rad52 promotes second-end DNA capture in double-stranded break repair to form complement-stabilized joint molecules. Proc. Natl. Acad. Sci. U. S. A. *106*, 3077–3082.

Nunes-Düby, S.E., Kwon, H.J., Tirumalai, R.S., Ellenberger, T., and Landy, A. (1998). Similarities and differences among 105 members of the Int family of site-specific recombinases. Nucleic Acids Res. *26*, 391–406.

Ohki, R., Tsurimoto, T., and Ishikawa, F. (2001). In Vitro Reconstitution of the End Replication Problem. Mol. Cell. Biol. *21*, 5753–5766.

Olovnikov, A.M. (1973). A theory of marginotomy. The incomplete copying of template margin in enzymic synthesis of polynucleotides and biological significance of the phenomenon. J. Theor. Biol. *41*, 181–190.

Picardeau, M., Lobry, J.R., and Hinnebusch, B.J. (1999). Physical mapping of an origin of bidirectional replication at the centre of the Borrelia burgdorferi linear chromosome. Mol. Microbiol. *32*, 437–445.

Radzimanowski, J., Dehez, F., Round, A., Bidon-Chanal, A., McSweeney, S., and Timmins, J. (2013). An "open" structure of the RecOR complex supports ssDNA binding within the core of the complex. Nucleic Acids Res. *41*, 7972–7986.

Ralf, C., Hickson, I.D., and Wu, L. (2006). The Bloom's syndrome helicase can promote the regression of a model replication fork. J. Biol. Chem. *281*, 22839–22846.

Ravin, N. V. (2015). Replication and Maintenance of Linear Phage-Plasmid N15. Microbiol. Spectr. *3*, 1–12.

Ravin, N. V., Kuprianov, V. V., Gilcrease, E.B., and Casjens, S.R. (2003). Bidirectional replication from an internal ori site of the linear N15 plasmid prophage. Nucleic Acids Res. *31*, 6552–6560.

Ravin, V., Ravin, N., Casjens, S., Ford, M.E., Hatfull, G.F., and Hendrix, R.W. (2000). Genomic

sequence and analysis of the atypical temperate bacteriophage N15. J. Mol. Biol. *299*, 53–73.

Rice, P.A., and Baker, T.A. (2001). Comparative architecture of transposase and integrase complexes. Nat. Struct. Biol. *8*, 302–307.

Rybchin, V.N., and Svarchevsky, A.N. (1999). The plasmid prophage N15: A linear DNA with covalently closed ends. Mol. Microbiol. *33*, 895–903.

Salman-Dilgimen, A., Hardy, P.O., Radolf, J.D., Caimano, M.J., and Chaconas, G. (2013). HrpA, an RNA Helicase Involved in RNA Processing, Is Required for Mouse Infectivity and Tick Transmission of the Lyme Disease Spirochete. PLoS Pathog. e1003841.

Shi, K., Huang, W.M., and Aihara, H. (2013). An Enzyme-Catalyzed Multistep DNA Refolding Mechanism in Hairpin Telomere Formation. PLoS Biol. *11*.

Shinohara, A., Shinohara, M., Ohta, T., Matsuda, S., and Ogawa, T. (1998). Rad52 forms ring structures and co-operates with RPA in single-strand DNA annealing. Genes to Cells *3*, 145–156.

Shuman, S. (1998). Vaccinia virus DNA topoisomerase: A model eukaryotic type IB enzyme. Biochim. Biophys. Acta - Gene Struct. Expr. 1400: 321-337.

Singleton, M.R., Dillingham, M.S., and Wigley, D.B. (2007). Structure and Mechanism of Helicases and Nucleic Acid Translocases. Annu. Rev. Biochem. *76*, 23–50.

Smith, E.F., and Townsend, C.O. (1907). A Plant-Tumor of Bacterial Origin. Science (80-.). *25*, 671–673.

Soudet, J., Jolivet, P., and Teixeira, M.T. (2014). Elucidation of the DNA end-replication problem in saccharomyces cerevisiae. Mol. Cell *53*, 954–964.

Stoppel, R.D., Meyer, M., and Schlegel, H.G. (1995). The nickel resistance determinant cloned from the enterobacterium Klebsiella oxytoca: conjugational transfer, expression, regulation and DNA homologies to various nickel-resistant bacteria. Biometals *8*, 70–79.

Sugiyama, T., New, J.H., and Kowalczykowski, S.C. (1998). DNA annealing by Rad52 protein is stimulated by specific interaction with the complex of replication protein A and single-stranded DNA. Proc. Natl. Acad. Sci. U. S. A. *95*, 6049–6054.

Tang, M., Cecconi, C., Kim, H., Bustamante, C., and Rio, D.C. (2005). Guanosine triphosphate acts as a cofactor to promote assembly of initial P-element transposase-DNA synaptic complexes. Genes Dev. *19*, 1422–1425.

Tilly, K., Fuhrman, J., Campbell, J., and Samuels, D.S. (1996). Isolation of Borvelia burgdorferi genes encoding homologues of DNA-binding protein HU and ribosomal protein S20. Microbiology *142*, 2471–2479.

Toms, A. V., Deshpande, A., McNally, R., Jeong, Y., Rogers, J.M., Kim, C.U., Gruner, S.M., Ficarro, S.B., Marto, J.A., Sattler, M., et al. (2013). Structure of a pseudokinase-domain switch that controls oncogenic activation of Jak kinases. Nat. Struct. Mol. Biol. *20*, 1221–1223.

Tourand, Y., Kobryn, K., and Chaconas, G. (2003). Sequence-specific recognition but position-dependent cleavage of two distinct telomeres by the Borrelia burgdorferi telomere resolvase, ResT. Mol. Microbiol. *48*, 901–911.

Tourand, Y., Lee, L., and Chaconas, G. (2007). Telomere resolution by Borrelia burgdorferi ResT through the collaborative efforts of tethered DNA binding domains. Mol. Microbiol. *64*,

580–590.

Tourand, Y., Deneka, J., Moriarty, T.J., and Chaconas, G. (2009). Characterization and in vitro reaction properties of 19 unique hairpin telomeres from the linear plasmids of the lyme disease spirochete. J. Biol. Chem. *284*, 7264–7272.

Umezu, K., Chi, N.W., and Kolodner, R.D. (1993). Biochemical interaction of the Escherichia coli RecF, RecO, and RecR proteins with RecA protein and single-stranded DNA binding protein. Proc. Natl. Acad. Sci. U. S. A. *90*, 3875–3879.

Vales, L.D., Rabin, B.A., and Chase, J.W. (1982). Subunit structure of Escherichia coli exonuclease VII. J. Biol. Chem. *257*, 8799–8805.

Veaute, X., Delmas, S., Selva, M., Jeusset, J., Le Cam, E., Matic, I., Fabre, F., and Petit, M.A. (2005). UvrD helicase, unlike Rep helicase, dismantles RecA nucleoprotein filaments in Escherichia coli. EMBO J. *24*, 180–189.

Wang, L., and Lutkenhaus, J. (1998). FtsK is an essential cell division protein that is localized to the septum and induced as part of the SOS response. Mol. Microbiol. *29*, 731–740.

Welsh, E.A., Liberton, M., Stöckel, J., Loh, T., Elvitigala, T., Wang, C., Wollam, A., Fulton, R.S., Clifton, S.W., Jacobs, J.M., et al. (2008). The genome of Cyanothece 51142, a unicellular diazotrophic cyanobacterium important in the marine nitrogen cycle. Proc. Natl. Acad. Sci. U. S. A. *105*, 15094–15099.

Wood, E.R., and Matson, S.W. (1987). Purification and characterization of a new DNA-dependent ATPase with helicase activity from Escherichia coli. J. Biol. Chem. *262*, 15269–15276.

Wu, L., and Hickson, I.D. (2006). DNA Helicases Required for Homologous Recombination and Repair of Damaged Replication Forks. Annu. Rev. Genet. *40*, 279–306.

Yang, C.C., Tseng, S.M., and Chen, C.W. (2015). Telomere-associated proteins add deoxynucleotides to terminal proteins during replication of the telomeres of linear chromosomes and plasmids in Streptomyces. Nucleic Acids Res. *43*, 6373–6383.

Yang, C.C., Tseng, S.M., Pan, H.Y., Huang, C.H., and Chen, C.W. (2017). Telomere associated primase Tap repairs truncated telomeres of Streptomyces. Nucleic Acids Res. *45*, 5838–5849.

Zeqiraj, E., Filippi, B.M., Goldie, S., Navratilova, I., Boudeau, J., Deak, M., Alessi, D.R., and Van Aalten, D.M.F. (2009). ATP and MO25α regulate the conformational state of the STRADα pseudokinase and activation of the LKB1 tumour suppressor. PLoS Biol. *7*, e1000126.